photonics

MDPI

Review

A Comprehensive Review of the Fundamentals, Progress, and Applications of the LIBS Method in Analysis of Plants: Quantitative and Qualitative Analysis

Fatemeh Rezaei [1,*], Alireza Eskandary [1,2], Mobina Zahedi [2], Saleheh Beheshtipour [3] and Vincenzo Palleschi [4,*]

[1] Department of Physics, K. N. Toosi University of Technology, Tehran P.O. Box 158754416, Iran; s.alirezaeskandar@ut.ac.ir
[2] Nanophysics Research Laboratory, Department of Physics, University of Tehran, Tehran P.O. Box 1439955961, Iran; mobinazahedi@ut.ac.ir
[3] Department of Physics, Central Tehran Branch, Islamic Azad University, Tehran P.O. Box 1955847881, Iran; sbeheshtipour@iau.ac.ir
[4] Applied and Laser Spectroscopy Laboratory, Institute of Chemistry of Organometallic Compounds, Research Area of National Research Council, Via G. Moruzzi, 1, I-56124 Pisa, Italy
* Correspondence: fatemehrezaei@kntu.ac.ir (F.R.); vincenzo.palleschi@cnr.it (V.P.)

Abstract

The primary aim of this work is to present, in detail, the recent applications and progress of LIBS in the study of plant samples and related components, highlighting several innovative methods and experimental setups. The latest developments in using LIBS to analyze crop plant leaves, pasture vegetables, grains, seeds, fruits, plant derivatives, and other agricultural products are discussed, with particular emphasis on the analysis of minerals and trace elements in various plant matrices. Trace and metallic minerals are vital for regulating plant growth and development. Understanding how these elements are distributed within plant tissues provides deeper insights into metabolic pathways and processes, as well as potential applications in food technology and agriculture. Advances in quantitative measurements of these elements across different plant sections are examined, with attention given to challenges such as sample preparation, field sampling methods, and calibration techniques. Key features of LIBS, influential parameters, and fundamental instrumentation are also reviewed. Furthermore, this review explores the specific concerns, expectations, and possibilities of using LIBS to assess plant nutritional status and detect toxic elements, while highlighting the distinct advantages and complementary role of LIBS in plant science research.

Keywords: LIBS; plants; spectroscopy; nutrients; agricultural; mapping

check for updates

Received: 5 August 2025
Revised: 4 September 2025
Accepted: 26 September 2025
Published: 27 October 2025

Citation: Rezaei, F.; Eskandary, A.; Zahedi, M.; Beheshtipour, S.; Palleschi, V. A Comprehensive Review of the Fundamentals, Progress, and Applications of the LIBS Method in Analysis of Plants: Quantitative and Qualitative Analysis. *Photonics* **2025**, *12*, 1061. https://doi.org/10.3390/photonics12111061

Copyright: © 2025 by the authors. Licensee MDPI, Basel, Switzerland. This article is an open access article distributed under the terms and conditions of the Creative Commons Attribution (CC BY) license (https://creativecommons.org/licenses/by/4.0/).

1. Introduction

Laser-Induced Breakdown Spectroscopy (LIBS) is an innovative spectroscopic method, particularly suited for the quick chemical processing of a wide range of materials [1]. LIBS is frequently used to analyze and track the spatial distribution of elements in various materials, including biological samples [2], chemical targets [3], and industrial products [4–6].

In LIBS analysis, information is obtained by focusing a laser pulse onto a small area of the sample surface using an optical lens [7]. The high laser power ablates a small amount of material from the surface, generating an excited and ionized plasma [8,9]. The light emitted by this plasma is collected using an optical fiber and analyzed by a spectrometer connected to a detector [10]. The spectral lines emitted by the sample are identified using

databases like NIST [11]. A significant relationship exists between plasma characteristics and the resulting LIBS spectra, which are influenced by (i) the physical properties of the target (e.g., hardness, porosity, roughness) and (ii) experimental parameters such as the lens-to-sample distance, laser energy, and spectrometer calibration [12].

In recent years, LIBS has garnered significant interest within the scientific community as a promising tool for studying plants, offering insights otherwise difficult to obtain [13,14]. One of the most important applications of LIBS in this field is the determination of the nutrient elements in the plant.

Plants rely on various elements for growth, development, and completing their life cycle [15]. These elements are essential for fundamental processes such as photosynthesis, respiration, metabolism, and reproduction [16,17]. Seventeen essential elements are required for plant growth, categorized into macronutrients and micronutrients [18]. Macronutrients, needed in larger quantities, include carbon, hydrogen, oxygen, calcium, potassium, magnesium, nitrogen, sulfur, and phosphorus. Micronutrients, needed in trace elements, contain chlorine, manganese, molybdenum, boron, copper, iron, nickel, and zinc [18]. Also, depending on environmental conditions, some non-essential elements (cobalt, sodium, aluminum, selenium, silicon) may be beneficial. These factors have a favorable impact on numerous physiological processes, like nutrient assimilation, stress tolerance, and enzyme activity [18].

Aluminum, one of the Earth's most abundant metals, significantly impacts plant growth. It is found in various forms in the soil but becomes soluble and toxic in acidic soils with a pH below 5, where it forms Al^{3+} ions [18,19]. These ions damage root tips, water absorption, inhibit nutrient uptake, ultimately hindering or preventing plant growth [20–22].

Phosphorus is another essential macronutrient that is crucial for processes like root development, nucleic acid formation, and energy transfer [23–26], but phosphorus in acidic soils tends to produce insoluble compounds with aluminum and iron, rendering it unavailable to plants. This dual challenge of phosphate deficiency and aluminum toxicity in acidic soils can drastically reduce plant productivity and quality [20,27].

Santos Jr. et al. in 2012 reported the first review paper on the identification of elements in plants using LIBS [28]. Since then, several review articles [29–40], theses [41,42], and a few book chapters [43,44] have reported on specific issues related to the analysis of agricultural products using LIBS. However, a comprehensive review covering the most recent progress in LIBS analysis of plants is missing.

The primary aim of this work is to present, in detail, the new applications and relevant progress of LIBS in the study of plant samples and related components, highlighting several innovative methods and experimental setups. The most recent developments in using LIBS to analyze crop plant leaves, pasture vegetables, grains, seeds, fruits, plant derivatives, and other agricultural products will be discussed. Additionally, the issue of quality control of plant derivatives, detection of potential agricultural adulteration and early diagnosis of plant diseases using LIBS will be covered. The possibility of detection and quantification of plant nutrition, pesticide residues, phytotoxic elements, impurities, and other pollutants will also be discussed.

Lastly, novel LIBS applications, new trends, and viewpoints on the search for vegetable products and plant derivatives, along with solutions to current LIBS challenges, will be proposed.

2. Experimental Set-Up

2.1. Sample Preparation

One of the most emphasized advantages of LIBS is that it requires no or minimal sample preparation [45]. Unfortunately, this is not always true for biological samples [46].

Only a few simple procedures for biological sample preparation have been published so far. The most common, fast, and economical procedure involves drying molded samples by embedding them in epoxy or double-sided adhesive tape on glass slides. Plant leaves can be quickly molded, frozen, and then analyzed. However, the 2D elemental maps acquired during these experiments do not allow for the identification of particles adsorbed on the plant surface, the distribution of elements in plant tissue, or the exact uptake routes [46]. To determine values for these features, measurements must be combined with results from other robust spectral analytical procedures.

2.2. Lasers

The most frequently utilized laser source for researching plant materials is the nanosecond (ns) Q-switched Nd:YAG laser [47], typically operating at the fundamental wavelength (1064 nm); higher harmonics are used less frequently. Ultraviolet (UV) laser irradiation, achievable using Nd:YAG fourth harmonic (266 nm) or ArF excimer (193 nm) [48] lasers, can be advantageous in minimizing matrix effects and improving measurement precision. The benefits of Ti:Sapphire [49] ultra-short pulse durations, such as minimal continuum radiation, low matrix effects, and reduced thermodynamic variations, also suggest the potential use of femtosecond lasers in plant analysis [50]. Femtosecond-LIBS (fs-LIBS) has great potential for depth-resolved analysis, which can also be applied for biological elemental imaging [51]. In contrast to short-pulse LIBS analysis, the longer pulse duration and wavelength of the CO_2 laser [52] can be utilized for the analysis of powder samples without the need for pelletizing [53]. Stand-off [54] and portable LIBS [55] systems are also available for plant analysis, but they are mainly used for environmental studies [31,56], industrial application [5,57], and investigation into hostile media [58,59].

Table 1 presents an overview of different sections of plant samples analyzed using LIBS under various laser conditions.

Table 1. An overview of the studies on plant materials using LIBS. Here t_{delay} is the delay time, and t_{int} is integration time gate.

Samples Name	Test Sample	*Analytes*	Laser(s)	t_{delay} (µs)	t_{int} (µs)	Ref.
Capsicum annuum L., Sophora (*Styphnolobium japonicum*)	Fresh leaves	Mn, Pb, K, Ca	Nd:YAG, 532 nm	1.0	10	[60]
Algal (*Trachydiscus minutus*)		K, Ca, Cu, Mg, Na	Nd:YAG, 1064 nm	-	-	[61]
Sunflower, Zea mays		Pb, Mg	Nd:YAG, 532 nm	1.0	10	[62]
Leaves of soya, lettuce, endive, boldo, grass, jack, brachiaria coffee, mango, maize, and pepper		Mn, Fe, B, Cu, Zn	Nd:YAG, 1064 nm	-	-	[63]
Folium lycii		Cl, Ti, Al, Ca, K, Si, Li, Mg, Na, Sr	Nd:YAG, 1064 nm	0.8	2000	[64]
Leaves and flowers of cannabis		Ca, Br, Al, Ba, Cu, Fe, K, Rb, Sr, Mg, Mn, Na, P	Nd:YAG, 1064 nm	-		[65]
Holly		Fe, K, Al, C, CN, Co, Cr, Cu, Mg, Mn, C_2, V, Zn, Ca, Mo, Na, Ni, O, Pb, Si, Ti,	Nd:YAG, 1064 and 266 nm	0.5	2000	[66]
Lettuce, endive, boldo, brachiaria, coffee, grass, jack, mango, maize, pepper, soya		Fe, B, Zn Cu, Mn,	Nd:YAG, 1064 nm	-	-	[47]
Helianthus annuus	Dried leaves	Pb, K, Mn	Nd:YAG, 532 nm	1.0	10	[67]
Bermuda Grass (*Cynodon dactylon*)		Ca, Al, Mg, Si, C, Sr, Zn	Nd:YAG, 532 nm	-	-	[68]

Table 1. *Cont.*

Samples Name	Test Sample	*Analytes*	Laser(s)	t_{delay} (μs)	t_{int} (μs)	Ref.
Capsicum annuum L.		K, Pb, Mn	Nd:YAG, 532 nm	1.0	10	[60]
Dried maize and fresh *Cornus stolonifera*, Red osier dogwood (*Cornus stolonifera*)		Fe	fs-laser, 795 nm	-	-	[69]
Powdered rice, starch, seaweed (agar)	Powder leaves	Cr, Fe, Al, B, C, Ca, Cu	TEA CO_2, 10.6 μm	10	100	[70]
		Cr, Mg, Ca, CH, Zn	TEA CO_2, 10.6 μm	10	100	[71]
Citrus		Ca, CH	Nd:YAG, 355 nm, Nd:YAG, 1064 nm	1.0	50	
Brassica juncea	Pellets from leaves	Mg, Al, K, Ca, Si, Fe, O	Nd:YAG, 1064 nm	-	-	[72]
Cotton	-	Mg, Sr, Al, Ba, Cu, Cr, Ca, Fe		-	-	[73]
Cabbage, soya flour, rice flour, wheat flour, spinach, brachiaria, banana, coffee, maize, mango, pepper, soya leaves, olive, apple, guava, grass jackfruit leaves	Leaves	Mn, Zn, B, Cu, Fe	Nd:YAG, 532 nm	1.1	9.0	[74]
Longleaf pine tree (*Pinus palustris*)		Fe, Na, Ca, S	Nd:YAG, 532 nm	-	-	[75]
Orange tree, soy, sugarcane		P, K, Ca, Mn, Zn, Mg, B, Fe, Cu	Nd:YAG, 1064 nm	2.0	4.5	[76]
Sugar cane		Hz Ca, Mg, K, P, B, Cu, Fe, Mn, Zn, Al,	Nd:YAG, 1064 nm,	-	-	[77]
Allium cepa L. leaves		Cu	Nd:YAG, 532 nm	-	-	[78]
Scented geranium, *Pelargonium zonale*		Mn, Pb, Al, Ca, Sr	Nd:YAG, 1064 nm	5.0	15	[79]
Poplar tree		K, Ca, N, P, Mn, Na, Fe, Ti,	femtosecond laser, 800 nm	-	-	[80]
Tall fescue seed		Ca, Cu, Ni, Mg, Fe, Mn, Cd, Zn	Nd:YAG, 532 nm	0.5	10	[81]
Sugar cane		B, Ca, P, Mg, Mn, Zn, Cu, Fe, K	Nd:YAG, 1064 nm	2.0	4.5	[82]
Endive (*Cichorium endivia*), Grass (*Axonopus obtusifolius*), Jack (*Artocarpus integrifolia*), Boldo (*Peumus boldus*), Coffee (*Coffea arabica*)		Zn, Fe, Cu, B, Mn	Nd:YAG, 1064 nm	-	-	[47]
Barley, poppy, wheat, rape		Mg, P, Ca, K	Nd:YAG, 1064 nm	7.0	1.0	[83]
Spanish moss, pine needles		K, Mg, Ca, P	Nd:YAG, 1064 nm	2.0	5.0	[63]
Tobacco		Fe, Ca, Mg, Mn, Al, Cu, Ti, K, Li, Na, Sr, Zn		-	-	[84]
Bean (*Phaseolus vulgaris*)		B, Fe, Cu, Mn, Zn	Nd:YAG, 1064 nm	2.0	5.0	[47]
Lactuca sativa L. var. capitata		Pb, Mg	Nd:YAG, 532 nm	1.0	10	[85]
Potato	Vegetables	K, Mg, Mn, Al, C, Ca, Cu, O, Si, Ti, Fe, H, Na, Li, Sr, Ba	Nd:YAG, 1064 nm	1.0:5.01, 0:1.0		[83,85]
Potato		Mg, Mn, Al, Ba, Ca, Cu, Fe, K, Ti, Sr, Li, Na, Si, Zn	Nd:YAG, 266 nm	0.07–3	0.7–1.2	[14]
Three fruits	Fruits	K, Fe, Ca, Na, Al, Mg	Nd:YAG, 1064 nm	1.2	2000	[86]
Mango (*Mangifera indica*)		Fe, Mn, B, Cu, Zn	Nd:YAG,1064 nm	-	-	[47]
Oranges (*Citrus sinensis*)		Ca, C, Mn, Ni, Cl, H, Fe, Mg, Na, Zn, N, O, K, S	Nd:YAG,1064 nm	-	-	[67]

Table 1. *Cont.*

Samples Name	Test Sample	*Analytes*	Laser(s)	t_{delay} (μs)	t_{int} (μs)	Ref.
Rice flour-unpolished powder, Ibaraki Japan), starch, powdered rice, powdered zinc, powdered calcium and mineral health supplements, herb medicine (*Tsumura kackontou*), powdered agar Bludru Ungu, powdered agar *Gracilaria Karawang*	Powder of grains	C, Ca, Al, B, Cr, Cu, Fe	TEA CO_2, 10.6 μm	10	100	[70]
Wood of tree	Wood pieces	Al, C, N, Na, Ca, Mg, Mn, S, Si, Fe, Ti	Nd:YAG, 532 nm	-	-	[75]
Wood		Cr, Cu, As, Ca	Nd:YAG, 1064 nm	-	-	[67,87]
Wood		Hg, K, Mg, Al, As, B, Cd, Cr, Si, Sn, Cu, Na, Pb, Zn	Nd:YAG, 1064 nm	-	-	[88]
Rice flour-unpolished, starch, rice, zinc, calcium and mineral health supplements, herb medicine	Flour powder	C, Ca, Al, B, Fe, Cu, Cr	TEA CO_2, 10.6 μm,	-	-	[70]
Lily pollen	Pollen paste	Na, Si, Al, C_2, Ca, Cr, Fe, CN, Mg	Nd:YAG, 1064 nm	-	-	[89]

2.3. Optics

The optical focusing configuration and laser pulse energy determine the laser fluence and irradiance on the sample surface. They both influence the LIBS capability and detection pattern. For a better understanding of these effects, readers are encouraged to read the extensive review of Aguilera and Aragón [90] and the specialized literature on plant analysis. Typically, plane-convex quartz lenses or mirrors are used to collect the light emitted by the plasma, which is then focused onto the spectrometer's entrance slit or into an optical fiber connected to the spectrometer.

2.4. Spectrometers

A wide range of spectrometers are available for spectral analysis and signal detection, with the most commonly used being Czerny-Turner or Echelle spectrometers equipped with CCD (charge-coupled device) or ICCD (intensified charge-coupled device) detectors [46].

The selection of the spectrometer for plant studies depends on the required spectral selectivity and sensitivity [34]. For example, spectrometers equipped with Echelle optics and ICCD detectors offer high spectral resolution over a wide wavelength range (e.g., 200 to 1000 nm) and high sensitivity, making them ideal for determining micronutrients (such as B, Cu, Fe, Zn, Mn) at mg/kg mass fraction levels [28]. Alternatively, compact spectrometers based on Czerny–Turner optics and CCD detectors, despite their limited spectral resolution and sensitivity, are especially attractive due to their portability, flexibility, and lower cost. These spectrometers can be configured as compact multi-channel systems with a wide wavelength range (e.g., from 200 to 1000 nm) and moderate spectral resolution (on the order of 0.1 nm or more), making them suitable for portable devices [30]. Table 2 summarizes the research published in scientific literature and the relevant instruments used for the analysis of plants.

Table 2. A summary of the experimental condition reported in the literature for plant analysis using LIBS.

Laser	Pulse Duration Range	Spectrometer	Detector	Plant Type	Test Sample	*Analytes*	References
Ti:Sapphire, 800 nm Nd:YAG, 1064, 532, 266 nm	fs	Czerny–Turner	ICCD	31 Plant samples	Leaves of sugar cane, soya, Citrus, coffee, maize, bean, eucalyptus, mango, banana, grape, millet, rubber tree, tomato	Fe, Mn, Ca, P, Cu, Zn, Mg	[91]
Nd:YAG, 266, 355 nm	ns	Echelle	ICCD	Vegetable	typical root, stem, and fruit vegetables	Cr, Mn, Na, Mg, Li, Be, Al, K, S, Cl, Ca, Ti, V, Cu, Rb, Sr, Fe, Co, Ni, Mo, Ba, H, C, N, OF, Si	[92]
Nd:YAG 1064 nm (ns)	ns	-	-	Vegetable	Spinach leaves and unpolished rice	Ca, Na, Mg, K	[93]
Nd:YAG 532 nm (ns)	ns	-	-	Leaves	Leaves of brachiaria, soya, banana, coffee, maize, mango, pepper	Fe, B, Cu, Mn, Zn	[74]
Nd:YAG 266, 532 nm (ns)	ns	Czerny–Turner	ICCD	Plant	annual terminal spruce stems, leaves, sunflower	Ca, Cu	[94]
Nd:YAG 266, 532 nm (ns)	ns	Czerny–Turner	ICCD	Plant	Sunflower	lead (II) ion	[95]
Nd:YAG, 266, 532 nm	ns	Czerny–Turner	ICCD	Plant	lettuce tissues	lead (II) ion	[96]
Nd:YAG, 266, 532 nm	ns	Czerny–Turner	ICCD	Plant	sunflower (*Helianthus annuus* L.)	Mg, Pb, Cu	[97]
Nd:YAG, 266, 532 nm	ns	Czerny–Turner	ICCD	Plant	Sunflower	silver (I) ions	[98]
Nd:YAG, 266, 532 nm	ns	Czerny–Turner	ICCD	Plant	leaf samples	lead (II) ion	[67]
Nd:YAG, 266, 532 nm	ns	Czerny–Turner	ICCD	Plant	*Helianthus Annuus* L.	Ag, Cu	[99]
Nd:YAG, 532 nm	ns	Multi-Channel, Czerny–Turner	ICCD	Plant	wheat seedlings	Cr, Ca, Mg, K, Na	[98,99]
Nd:YAG, 532 nm	ns	-	ICCD	Plant	rice leaves	Cr	[100]
Nd:YAG, 532 nm	ns	Multi-Channel, Czerny–Turner	ICCD	Plant	leaves of *Trigonella foenum* (spinach)	Mg	[101]
Nd:YAG, 532 nm	ns	Multi-Channel, Czerny–Turner	ICCD	Plant	*Psoralea corylifolia* (PC)	Na, K, Ca, Mg, Zn, Si, Cl	[102]
Nd:YAG, 532 nm	ns	Multi-Channel, Czerny–Turner	ICCD	Plant	Saccharum	Mg, Ca, Na, Fe, K	[103]
Nd:YAG, 1064 nm	ns	-	ICCD	Plant	Roots, stem, and leaves of Euphorbia indica	Cr	[104]
Nd:YAG, 532 nm	ns	Multi-Channel, Czerny–Turner	ICCD	Plant	Bermuda grass (*Cynodon dactylon*)	Ca, C, Al, Si, Zn, N, Mg, Sr	[68]
Nd:YAG, 532 nm	ns	Multi-Channel, Czerny–Turner	ICCD	Fruit	*Trichosanthes dioica* fruits	Mg, Ca, Fe	[105]
Nd:YAG, 532 nm	ns	Multi-Channel, Czerny–Turner	ICCD	Fruit	*Withania coagulans*	glucose	[106]
Nd:YAG, 532 nm	ns	Multi-Channel, Czerny–Turner	ICCD	Fruit	*Momordica charantia* (family: Cucurbitaceae)	Mg, Ca, Na, K, Fe, Al	[107]
Nd:YAG, 532 nm	ns	Multi-Channel, Czerny–Turner	ICCD	Fruit	Psidium guajava (*P. guajava*)	Na, N, Mg, K, O, C	[108]
Nd:YAG, 532 nm	ns	Multi-Channel, Czerny–Turner	ICCD	Plant	four turmeric samples	K, Mg, Ca, C, Na, Fe, and molecular bands of CN	[109]
Nd:YAG, 532 nm	ns	Czerny–Turner	ICCD	Vegetable	Vegetable oils	C_2	[110]
Nd:YAG, 532 nm	ns	Czerny–Turner	ICCD	Plant	spinach leaves	P, Fe, B, Ca, Mg, Al, Si, Cu, Mn, Zn	[111]

2.5. Hyphenated LIBS: Combining LIBS with Other Methods

Combining different techniques is a significant advance, providing greater details and results during analyte analysis. The combination of LIBS with Raman spectroscopy [112],

hyperspectral imaging [113,114], near-infrared (NIR) spectroscopy [115], and mid-infrared (MIR) spectroscopy [116,117], as well as the exploration of LIBS applications in spectro-electrochemistry [112], marks a promising direction for future research in the quantitative analysis of plant materials using LIBS. Recently, the combination of LIBS with laser-induced fluorescence (LIF) has emerged as an area of great interest. LIBS-LIF is now employed to analyze various materials, including plant samples, alloys, and soil, for detecting heavy metals in aqueous solutions. For example, Jiang et al. [118] utilized LIBS-LIF as a rapid and sensitive analytical method to detect trace amounts of Pb in medicinal samples of *Rheum officinale*. Similarly, Zhu et al. [119] applied LIBS-LIF to estimate Pb concentrations in natural rhododendron leaf samples.

The literature indicates that combining LIBS with other techniques, such as LIF and Raman spectroscopy, is likely to enhance multi-element imaging of plant tissues with improved sensitivity in the future [119]. Additionally, LIBS, along with inductively coupled plasma mass spectrometry using laser ablation (LA-ICP-MS), has been effectively used for determining the spatial distribution of elements in biological samples [115,120,121]. The ease of combining LIBS with ICP-MS, the ability to analyze many elements in a single run, and the flexibility of testing any type of sample are advantages of both approaches [122]. For instance, Guerra et al. [55] employed LIBS and energy-dispersive X-ray fluorescence spectrometry (EDXRF) to investigate the spatial distribution of mineral elements on the surface of leaf samples.

Combining LIBS with ICP-MS, near-infrared spectroscopy, Raman spectroscopy, and novel detection technologies is expected to increase the analytical capabilities and the interpretation of the results. Kaiser et al. [97] presented LIBS mapping and LA-ICP-MS to visualize heterogeneous structures in leaves, carefully differentiated veins from surrounding tissue. In addition, Krizkova et al. [98] followed the distribution of heavy metals in various plants using LA-ICP-MS and LIBS. Their research highlighted the feasibility of using LIBS to estimate the concentrations and spatial distributions of Ag, Cu, Pb, and Mg in *Helianthus annuus* L. leaf samples.

Additionally, Andrade et al. [123] used LIBS and ICP-OES to evaluate the trace and toxic metal content in medicinal herbs, identifying elements such as Ca, Cd, Cr, Mg, Mn, Fe, Co, Cu, Na, Pb, Ni, and Zn.

Carvalho et al. [34] applied LIBS to analyze nutrient elements like N, P, K, Ca, Mg, and S in rice, sugarcane, cress, maize, soybean, and wheat plants. They recommended combining LIBS with XRF for nutritional diagnostics and routine evaluation of plant products. Table 3 reports the critical threshold concentrations (CTCs) and sufficiency ranges (SRs) of macro- and micronutrients in these selected crops.

Table 3. A summary of the critical threshold concentration (CTC) and sufficiency range (SR) values (in %) of the nutrients present in rice, maize, soybean and wheat. Reproduced from Ref. [34] with permission of the Royal Society of Chemistry.

Nutrient	**S**		**P**		**Ca**		**Mg**	
	CTC	SR	CTC	SR	CTC	SR	CTC	SR
Rice	0.0015	0.003	0.0018	0.003	0.0025	0.01	0.0015	0.005
Maize	0.0014	0.003	0.0018	0.003	0.0025	0.01	0.0015	0.005
Soybean	0.0021	0.004	0.0025	0.005	0.004	0.02	0.003	0.01
Wheat	0.0015	0.003	0.0021	0.0033	0.0025	0.01	0.0015	0.003

Tripathi et al. [124] investigated the distribution of silicon and minerals in various sections of wheat (*Triticum aestivum*) plants using phytolith analysis LIBS. The LIBS analysis detected the presence of elements such as Ca, Mg, Si, Fe, Na, K, C, H, O, and N. In contrast,

the phytolith analysis revealed that the leaves of wheat plants contained the highest silicon accumulation, followed by the awn, leaf sheath, lemma, rachilla, and stem. A strong concordance was observed between the results of the two methods. Figure 1 depicts the intensity ratio distribution versus elements: (a) various elements and (b) Si normalized to C, across different parts of the wheat plant.

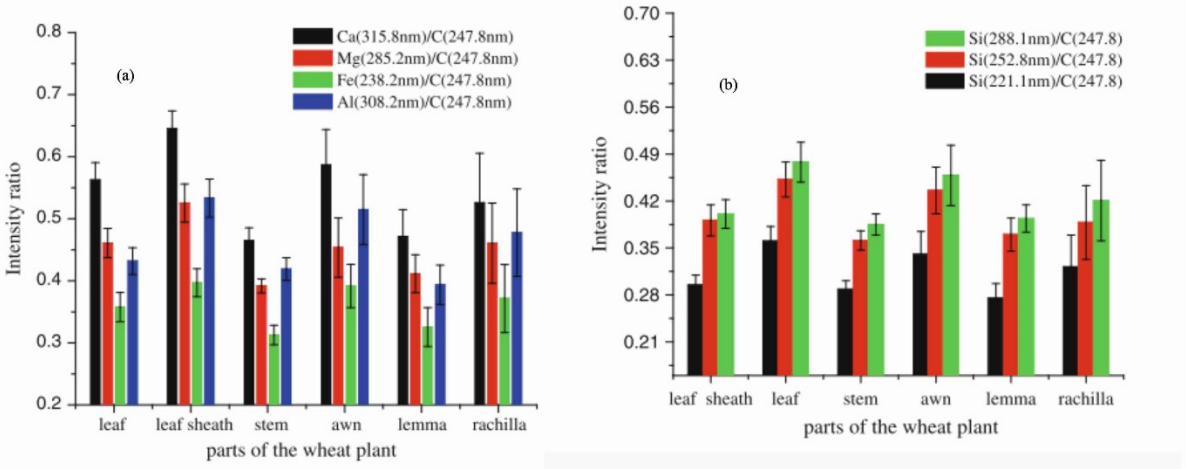

Figure 1. Intensity of (**a**) Mg, Ca, Al, and Fe, and (**b**) Si emission lines at different wavelengths in various sections of the wheat plant. Reproduced from Ref. [124] with the permission of Springer.

Additionally, principal component analysis (PCA), a multivariate statistical technique, was applied to the LIBS spectral data of different wheat sections. The PCA results identified two principal components, PC1 (99%) and PC2 (1%), accounting for 100% of the dataset's variance. The PCA plots effectively distinguished the vegetative and reproductive sections of the wheat plant. The universal presence of silicon across all plant parts highlights its critical role in biocement production.

Table 4 summarizes relevant research on the spatial distribution of various compounds and materials analyzed using LIBS. The table provides comprehensive details about the examined plant sections, identified elements, LIBS experimental setups, complementary techniques, and sample preparation protocols.

Table 4. A summary of research literature employing LIBS instruments, along with the complementary technique, experimental condition, and sample preparation techniques.

Year of Publication	Plant's Section	Identified Element	Experimental Condition	Combined Technique	Sample Preparation	Ref.
2019	*Lemna minor* *Raphanus sativus* leaves, whole plant	Y, Yb, Er	SP-LIBS & NELIBS: Nd:YAG (532 nm), 10 mJ per pulse (*L. minor*), 20 mJ per pulse (*R. sativus*)	Nanoparticles	molded dried leaves glued with epoxide	[125]
2006	*Helianthus annuus* leaves	Pb, Cd, Ca	SP-LIBS; Ti:sapphire (795 nm), 100 μJ per pulse	X-ray Radiography	dried leaves	[126]
2008	CRMs, and leaves of *Brachiaria*, soya, banana, coffee, jack, maize, pepper, guayava	Ca, K, Mg, P	SP-LIBS: Nd:YAG (1064 nm), 10 Hz, 200 mJ/pulse, 23 $J{\cdot}cm^{-2}$, 4.6 $W{\cdot}cm^{-2}$, 8 pulses, 2 μs t_d, 5 μs t_{int}	ICP-OES	drying, cryogenic grinding and pelletizing	[63]
2007	*Helianthus annuus*, part of leaves	Pb, Mn, K	SP-LIBS: Nd:YAG (532 nm), 10 mJ per pulse	Atomic absorption spectrometry (AAS) or atomic emission spectrometry (AES)	molded dried leaves	[67]
2013	Sugar cane leaves	Cu, Mn, P, K, Zn, Ca, Mg	SP-LIBS: Nd:YAG (1064 nm), 10 Hz, 110 mJ/pulse, 25 $J{\cdot}cm^{-2}$, 25 pulses, 2 μs t_d, 5 μs t_i	ICP-OES	drying, cryogenic grinding (95% of particles < 75 μm) and pelletizing	[127]

Table 4. *Cont.*

Year of Publication	Plant's Section	Identified Element	Experimental Condition	Combined Technique	Sample Preparation	Ref.
2008	*Helianthus annuus*, part of leaves	Ag, Cu	SP-LIBS: Nd:YAG (532 nm), 10 mJ per pulse	Laser-Ablation Inductively Coupled Plasma Mass-Spectrometry (LA-ICP-MS)	molded frozen leaves	[99]
2009	*Helianthus annuus*, part of leaves	Pb, Mg, Cu	SP-LIBS: Nd:YAG (532 nm), 10 mJ per pulse	Laser-Ablation Inductively Coupled Plasma Mass Spectrometry (LA-ICP-MS)	dried and partially dried leaves	[97]
2024	CRMs, and leaves of Brachiaria, soya, banana, coffee, maize, mango, pepper	Mn, Zn, B, Cu, Fe	SP-LIBS: Nd:YAG (532 nm), 10 Hz, 70 mJ/pulse, 25 J·cm^{-2}, 2.0 GW·cm^{-2}, 30 pulses, 1.1 µs t_d, 10 µs t_i	chemometric method (PLSR)	drying, cryogenic grinding, mixing with cellulose binder and pelletizing	[7]
2009	Zea mays, *Helianthus annuus*, *Lactuca sativa*, part of leaves	Pb, Mg	SP-LIBS: Nd:YAG (532 nm), 10 mJ per pulse	High performance liquid chromatography with electrochemical (HPLC-ED)	dried and partially dried leaves	[95]
2011	*Capsicum annuum* L., part of leaves	Pb, K, Mn	SP-LIBS: Nd:YAG (532 nm), 10 mJ per pulse	Laser ablation inductively coupled plasma mass spectrometry (LA-ICP-MS)	molded frozen, and dried leaves	[60]
2012	Spinach leaves	Mg, Ca, Na, K	SP-LIBS: Nd:YAG (1064 nm), 10 Hz, 80 and 140 mJ/pulse, 50 laser pulses	Chemometric methods (PLS-DA)	drying, grinding, sieving (50 and 200 mesh) and pelletizing	[93]
2013	*Picea abies* needles	Cu, Ca	DP-LIBS; Nd:YAG (266 nm), 10 mJ per pulse, Nd:YAG (1064 nm), 100 mJ per pulse	Inductively coupled plasma mass spectrometry (ICP-MS)	cross-sections of needles, 1–2 mm in thickness	[94]
2019	*Lactuca sativa* part of leaves and stem *Allium schoenoprasum* part of leaves	P, Cl, Cd	NELIBS: Nd:YAG (1064 nm), 160 mJ per pulse, Ag nanoparticle diameter 80 nm	Ag nanoparticle	dried leaves, fixed to a glass slide with double-sided adhesive tape	[128]
2015	*Saccharum* spp. Leaves	Fe, Mn, B, P, Si, Ca, Mg	SP-LIBS: Nd:YAG (1064 nm), 50 J·cm^{-2}	Energy-dispersive X-ray fluorescence spectrometry (EDXRF)	fragments from dried middle-third leaves	[55]
2016	Maize, holly (*Ilex chinensis Sims*), part of leaves	P, Cl, Mg, K	SP-LIBS: Nd:YAG (1064 nm), 90 mJ per pulse	--	*Zea mays*: stretched fresh plants fixed by adhesive tape onto a platform *Ilex chinensis*: cut fresh leaves fixed to a platform	[129]
2011	Mustard (*Brassica juncea*) leaves	Pb	SP-LIBS: Nd:YAG (1064 nm), 10 Hz, 300 mJ	atomic absorption spectroscopy (AAS)	drying, grinding and Pelletizing	[130]
2017	*Vicia faba* root	Cu, Ag	DP-LIBS & NELIBS: Nd:YAG (266 nm), 5 mJ per pulse, Nd:YAG (1064 nm), 100 mJ per pulse	Ag nanoparticles	cryo-cross-sections of roots, 40 µm in thickness	[131]
2018	*Lemna minor* leaves	Cd, $CdCl_2$	DP-LIBS & NELIBS; Nd:YAG (266 nm), 10 mJ per pulse, Nd:YAG (1064 nm), 100 mJ per pulse	Quantum Dots Nanoparticles	molded dried leaves glued with epoxide	[132]
2009	CRMs and leaves of barley, poppy, wheat and rape	Ca, K, Mg, P	DP-LIBS: Nd:YAG(1064 nm), 20 Hz, double pulse, 65, 68 and 78 mJ/pulse, 30 pulses, 7 µs t_d, 1 µs t_i	ICP-OES	drying, cryogenic grinding and pelletizing	[83]
2018	*Podocarpus macorophyllus* leaves	Li, Ca	SP-LIBS; Nd:YAG (266 nm), 15 mJ per pulse	--	fresh leaves	[133]
2019	Rice (*Oryza sativa* L.) leaves	Mg, Ca, Si, Na, K, CN, N	SP- & DP-LIBS; Nd:YAG (532 nm), 60 mJ per pulse, Nd:YAG (1064 nm), 50 mJ per pulse	chemometric thechniques (PLS, SVM)	dried leaves	[134]

3. Experimental Parameters Affecting LIBS Analysis of Plants

Despite the recent progress, quantitative analysis is a major challenge in LIBS, often called the Achilles' heel of the technique by Hahn and Omenetto [135]. The primary issue lies in the complex laser-sample interaction, which introduces substantial perturbations in matrix and plasma-particle interactions. Reliable quantitative analysis requires an

appropriate calibration strategy, optimization of instrumental parameters (e.g., laser fluence, wavelength, pulse duration), and proper sample preparation (e.g., forming pellets with particle sizes < 100 μm).

Operating parameters, including the space between the lens and the sample, can greatly influence the laser-induced plasma (LIP) parameters [136], the power density of the laser beam [137], and the constitution and pressure of the surrounding atmosphere. Changes in these properties will alter the analyte peaks and the relative intensities of the spectral lines, making the quantitative assessment of elemental ratios more difficult.

Efforts to solve these issues have caused novel instrumentation and excitation sources to enhance LIBS signals. These include using additional lasers, high voltage, and special devices. Double-pulse LIBS (DP-LIBS) is one of the most popular due to its improved analytical performance. In this technique, a second time-resolved laser pulse is introduced, re-stimulating the plasma generated by the first pulse. Various geometric configurations of the two laser pulses, based on propagation directions and temporal sequences, have been proposed to optimize signal amplification [138].

The subsequent sections explore the effects of key parameters on agricultural product analysis using LIBS.

3.1. Influence of Laser Intensity

Laser intensity is an essential factor that impacts sensitivity alongside the detector implementation. Higher laser beam fluences (e.g., 50 J/cm^2 and 750 μm-sized laser spot) produce more ablated mass, and the larger the intense LIP volume, the higher the sensitivity is generally. However, this factor limits the performance of portable instruments equipped with low-energy lasers (e.g., <50 mJ per pulse) in detecting micronutrients in plant materials.

Similar conditions apply to fs-LIBS systems, which produce smaller LIP volumes with less intense spectra but offer improved limits of detection (LODs). Advances in compact high-energy lasers and high-performance spectrometers are anticipated to make more sensitive portable instruments widely available in the near future. A detailed review of the development of portable LIBS devices and their applications can be found in Ref. [139]. Additionally, standard commercial LIBS systems were described by Peng et al. [30,140].

Moreover, A. Alrebdi et al. [141] utilized the Calibration-Free LIBS (CF-LIBS) method to analyze the elemental composition of *Peganum harmala* seed samples without requiring external calibration. This was achieved using a pulsed Nd:YAG laser emitting light at 532 nm. They investigated the effects of laser irradiance and the focal distance of the lens from the sample on plasma parameters, including electron number density and plasma excitation temperature, as illustrated in Figure 2. Their findings indicated that the electron temperature is highest near the target surface and decreases as the distance from the target material increases.

Jabbar et al. [142] investigated the application of LIBS to identify nutrients in the roots, stems, and seeds of rice plants. They studied the evolution of electron number density in relation to variations in laser intensity, detector position, and wavelength. Their experiments conducted using two wavelengths of an Nd:YAG, revealed that the electron number density increased with higher laser energy and closer proximity to the target surface, but decreased exponentially as the distance from the target increased. The authors noted that, keeping the laser beam fluence constant at 5.1 J/cm^2, the electron number density was higher at the fundamental wavelength of the Nd:YAG laser (3.6×10^{17} cm^{-3} at 0.5 mm away from the target) than at 532 nm (2.7×10^{17} cm^{-3} at the same distance). However, the decay length of the electron number density was similar in the two cases

(about 1.4 mm). In addition, they calculated the weight percentage of each element, employing the one-point CF-LIBS approach.

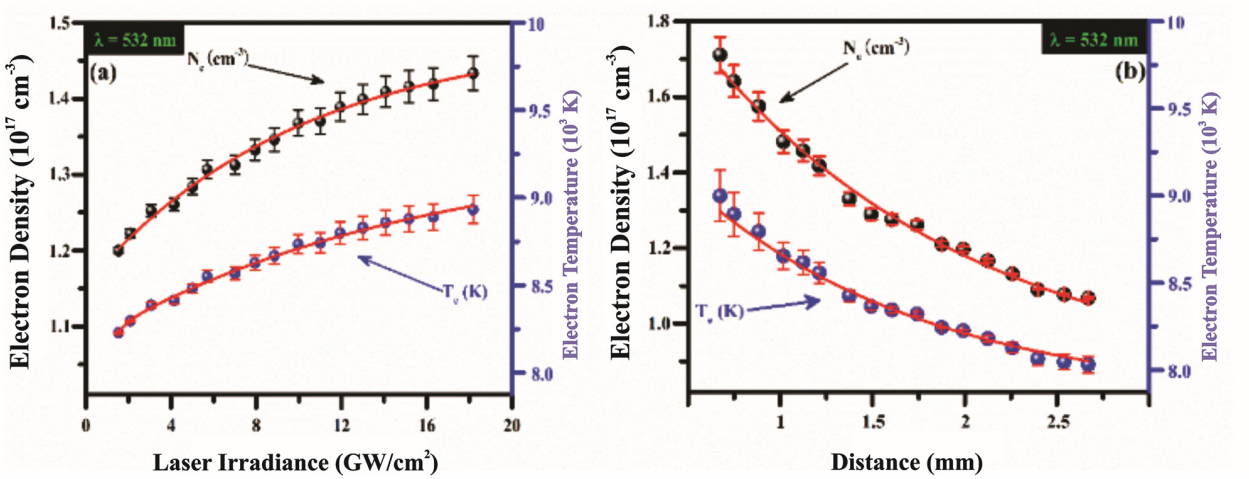

Figure 2. (**a**) The evolution of the electron excitation temperature of the plasma in a target (**a**) as a function of laser intensity ranging from 0 to 20 GW/cm2 at a wavelength of 532 nm; (**b**) The spatial variation in the electron density and excitation plasma temperature inside of a sample. Reproduced from Ref. [141] with permission of Multidisciplinary Digital Publishing Institute.

3.2. Effect of Pulse Duration

The most commonly used laser in plant analysis is the nanosecond (ns) laser, particularly the Nd:YAG, which operates at wavelengths of 266 nm, 532 nm, and 1064 nm with pulse energies ranging from 5 to 160 mJ [46]. Additionally, femtosecond lasers, such as the Ti:sapphire laser operating at a wavelength of 795 nm, including an energy of 0.1 mJ per pulse, have also been employed [143,144].

In the context of biological sample analysis, Assion et al. [51] compared the analytical performance of fs-LIBS and ns-LIBS. They analyzed the limited distribution of calcium ions in the peripheral cell walls of sunflower stems. Their results, shown in Figure 3, demonstrated that femtosecond lasers are superior for achieving high-quality spatial resolution in plant sample analysis using LIBS. The advantages of femtosecond lasers over ns lasers are threefold: (1) femtosecond lasers provide higher spatial resolution; (2) they enable precise ablation conditions; and (3) they generate plasma at a lower energy threshold, requiring less pulse energy than ns lasers.

Arantes de Carvalho et al. [91] conducted a systematic study in 2015 using the fs-LIBS system to quantify macronutrients (Ca, Mg, P) and micronutrients (Cu, Fe, Mn, Zn) in granulated leaves of 31 economically significant crops. Their findings highlighted that fs-LIBS produced accurate results for determining analyte mass fractions, regardless of whether univariate or multivariate modeling approaches were used. However, the predictions from multivariate modeling with ns-LIBS showed slightly better agreement with reference mass fractions. Nevertheless, fs-LIBS was advantageous in nutrient quantification due to its reduced dependence on the chemical composition of the sample matrix.

Ma et al. [80] applied fs-LIBS to analyze the elemental composition of poplar leaves, detecting elements such as Ca, Fe, N, Ti, P, K, Mn, and Na. Similarly, Kunz et al. [145] used fs-LIBS for elemental analysis of grass, wheat, soybean, and dallisgrass plants grown under greenhouse conditions. The literature depicts how fs-LIBS is a promising method for measuring and imaging elemental contents in plant tissues. fs-LIBS has the advantages of topochemical information, spatial resolution, and sensitivity that can further positive outcomes. Samek et al. [69] utilized fs-LIBS to identify and map the spatial distribution of Fe in leaf samples, confirming Fe ion accumulation in all parts of the plants.

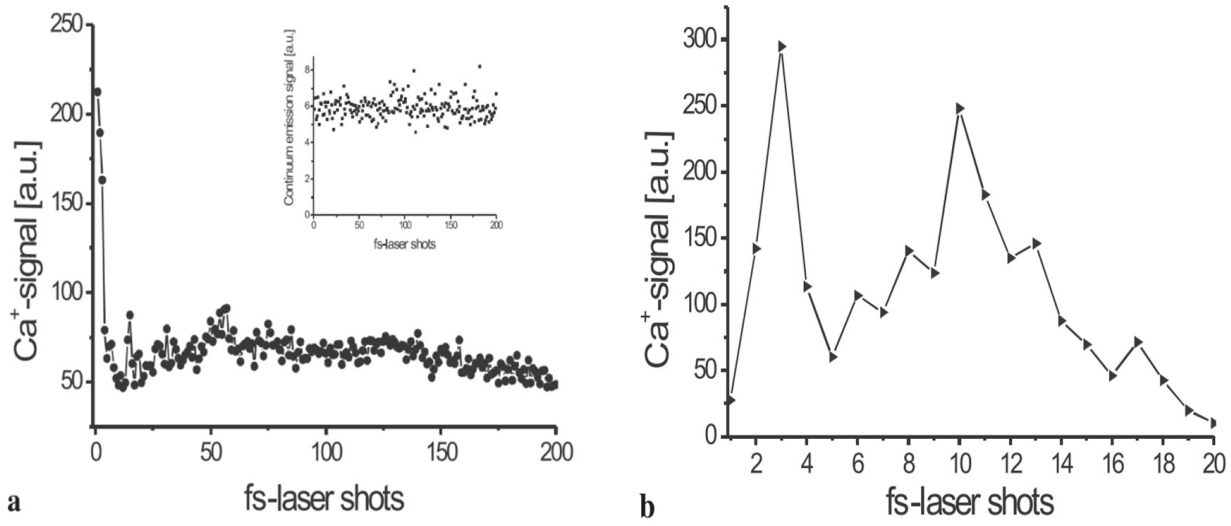

Figure 3. The spread of bound calcium ions (Ca^{2+}) inside a sunflower stem's periphery cell wall. For every femtosecond laser pulse, the plasma radiation was monitored and examined in the spectral interval of 380 nm to 410 nm. The Ca+ signal is obtained by integration over the Ca+ lines at 395 nm. The integrated continuous radiation between 368 nm, and 375 nm is the source of the background emission. (**a**) The Ca^{2+} spread is displayed with the inset, highlighting the continuum radiation signal. The applied fluence laser was 120 J/cm^2. (**b**) The Ca^{2+} spread is shown, including greater resolution, evaluated with a laser pulse fluence of 55 J/cm^2. a.u. = arbitrary units. Reproduced from Ref [51] with the permission of Springer.

A systematic comparison of ns-LIBS (6 ns Nd:YAG laser at 1064, 532, and 266 nm) and fs-LIBS (60 fs Ti:sapphire laser at 880 nm) was conducted by Arantes de Carvalho et al. [91] to analyze a range of heterogeneous composite samples, including pellets from 31 plant species. They demonstrated that the fs-LIBS offered several benefits for quantitative macro- and micronutrient analysis in pelletized leaves from crops such as sugarcane, soy, *Citrus*, maize, and coffee. Their findings emphasized that the validation and calibration processes in fs-LIBS were less affected by the plant material's matrix composition compared to ns-LIBS.

To verify accuracy, five certified reference materials from the National Institute of Standards and Technology (NIST), including SRM 1570a (trace elements in spinach leaves), were tested. Figure 4 illustrates the optical response from nanosecond and femtosecond lasers in two spectral windows for one of these samples. In 2017, another study employed fs-LIBS for analyzing various plants, including dallisgrass, wheat, soybean, and bell pepper leaves [145]. Kunz et al. [145] used LIBS to identify plasma temperatures and to differentiate plant species. Figure 5 depicts the normalized and offset emission spectra of all four samples in order to provide something that allows comparison. They determined LIBS could distinguish crops from weeds due to relatively consistent differences in plasma temperatures among analyzed samples. Further, the authors observed an indirect proportional relationship between plasma temperature and the composition of the plant. Different plants require different energy levels of excitation and ionization depending on their elemental and compound content. Therefore, the plasma temperature and peak ratios produce a distinctive plant signature.

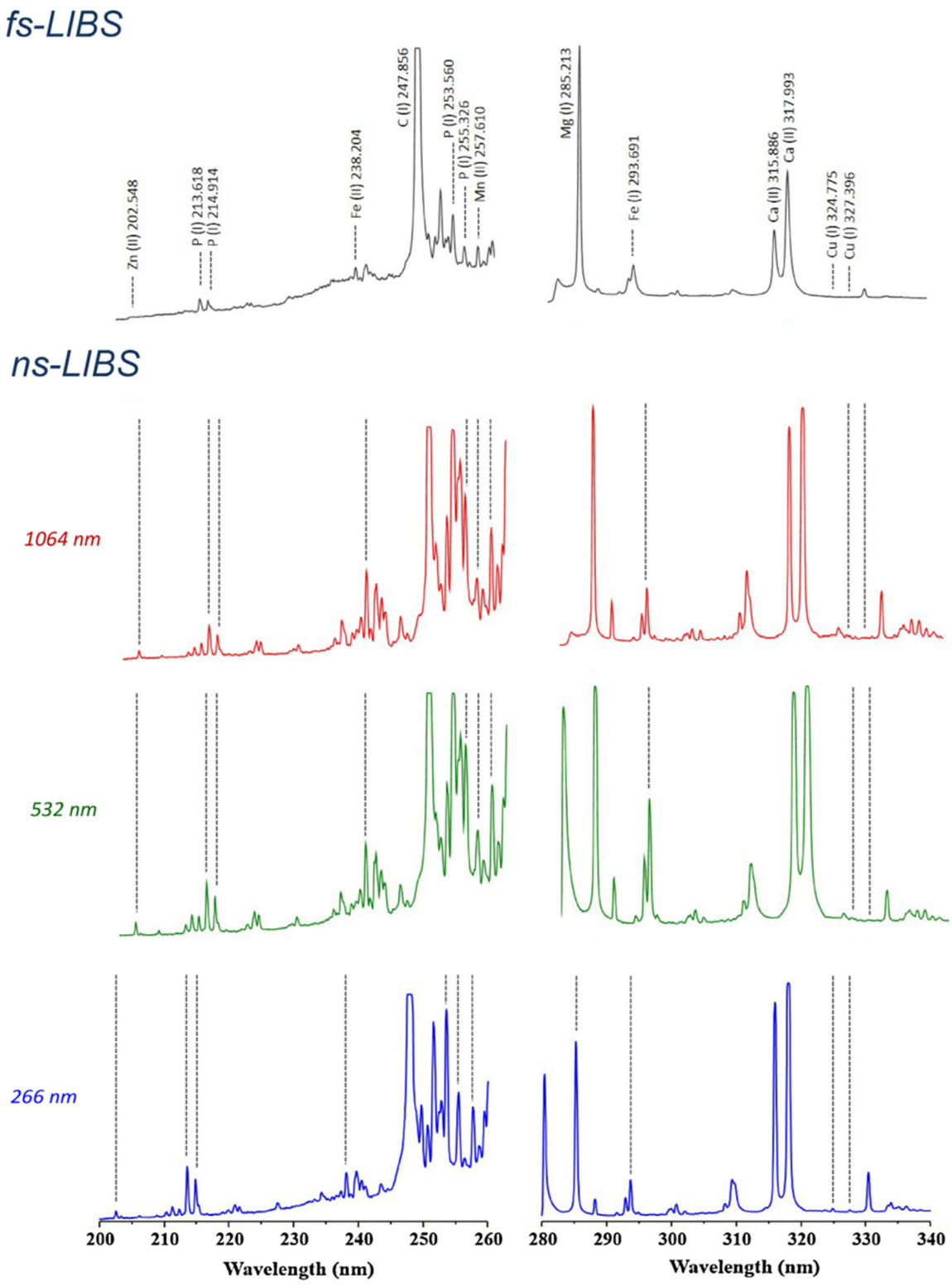

Figure 4. Emission spectra from fs- and ns-LIBS plasmas of a pellet made from NIST SRM 1570a spinach leaves in the specified experimental status. Reproduced from Ref. [91] with permission of Elsevier.

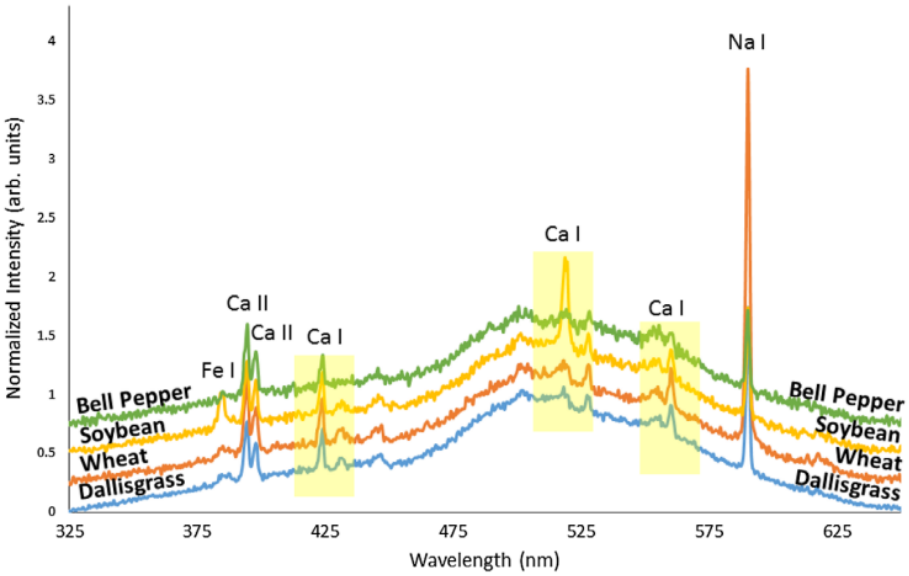

Figure 5. LIBs spectral emission of different plant samples: 3 kinds of crops (wheat, soybean, and bell pepper) and one weed (dallisgrass). The highest peaks are identified with their related elements. Three peaks of calcium are emphasized for the plasma temperature estimation. The spectral signals are normalized to the 500 nm line and vertically displaced for clarity. Reproduced from Ref. [145] with permission of Taylor & Francis.

3.3. Effect of Laser Set-Up Configuration: Single Versus Double Pulse Laser

Over the past decade, substantial efforts have been dedicated to enhancing the sensitivity of LIBS through techniques such as double-pulse LIBS (DP-LIBS) [135–137], spatial-confinement LIBS, and resonance-enhanced LIBS [30,34]. Among these, DP-LIBS has emerged as the predominant configuration for achieving signal enhancement in the analysis of agricultural products 81 [80,127,130,145,146]. By irradiating samples with two or more laser pulses separated by a delay of several microseconds, DP-LIBS can increase signal intensity by up to 100-fold.

DP-LIBS setups are generally classified into three configurations: orthogonal pre-spark, collinear, and orthogonal re-heating. The technique involves using the first laser pulse to ablate the target and generate a LIP, followed by a second laser pulse (applied after a few microseconds delay) to re-excite the pre-formed LIP in either a collinear or orthogonal arrangement [136]. To review DP-LIBS in detail, the reader are referred to the paper by Tognoni and Cristoforetti [136]. It should be noted that this brief discussion does not go into systematic detail about the limit of detection (LOD) as it can vary significantly according to the experimental conditions.

The two-pulse LIBS configuration was employed by Krajcarová et al. [131] to study the root tissues of *Vicia faba* (broad bean). This plant was chosen for its robust primary root structure, which facilitates the preparation of cross-sections and allows for the spatial distribution analysis of Ag nanoparticles in different root sections. Their study suggested that Ag nanoparticles were restricted to the outermost root layers and did not penetrate inner tissues. Figure 6 shows the LIBS spectrum of a root cross-section. In this spectrum, there were two notable observations: when roots were grown in solutions with similar concentrations of silver and copper ions, the peak intensities of copper were much larger than those of silver. This is a crucial consideration for studying silver in plants with LIBS technology since it is especially important for its toxicity to plants and its absorption by the plant depends on its soil concentration. As LIBS allows us to identify silver and other elements in plant tissues positively, it will enable us to understand their ecological and toxicological impact.

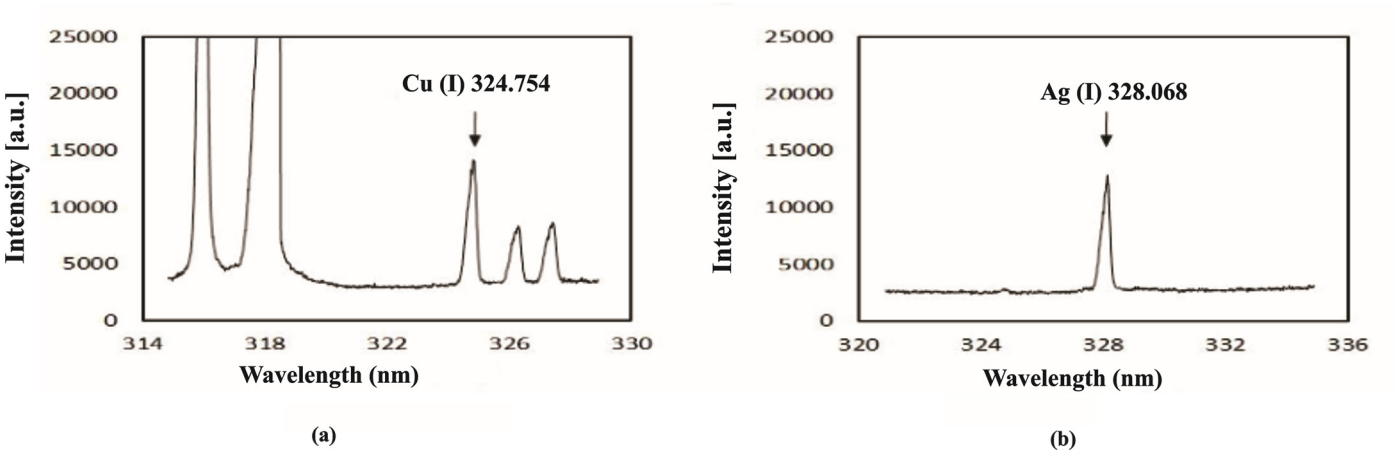

Figure 6. LIBS emission lines evaluated from root cross parts of *Vicia faba*: (**a**) grown in a solution containing 10 µmol L^{-1} Cu^{2+}, (**b**) grown in a solution containing 10 µmol L^{-1} Ag^{+}. Reproduced from Ref. [131] with permission of Elsevier.

Additionally, Peng et al. [140] explored key laser parameters in a collinear DP-LIBS setup to optimize the determination of chromium content in rice leaf pellets. Their research combined DP-LIBS with chemometric methods to identify both toxic and nutrient elements in rice leaves. They demonstrated that the support vector machine (SVM) methodology, based on feature variable selection, yielded the most accurate results. Furthermore, their findings indicated that DP-LIBS presented better modelling accuracy than single-pulse LIBS.

4. LIBS Applications in Plant Analysis

LIBS may be utilized in a variety of applications for elemental analysis of different plant parts, such as roots [147], leaves, and stalks [148].

An example is the work Krizkova et al. [98], who employed the second harmonic of a Nd:YAG laser system with a wavelength of 532 nm. They performed the analysis by placing the samples on a holder inside the ablation chamber, achieving a spatial resolution of 2 µm in all three directions (x, y, and z) using a high-precision motorized translation stage. A CCD camera outside the chamber was used to control the ablation point on the sample, enabling the measurement of the time evolution of the distribution of silver and copper in different parts of the plant stem. The authors demonstrated the possibility of obtaining high-resolution elemental maps of the samples monitored using LIBS. Furthermore, they showed that the total amount of silver and copper accumulated on the plant stem exhibited similar behavior, although their spatial distribution differed (Figure 7). A few days after the treatment, silver accumulated closer to the root of the sample (Figure 7A), while copper accumulated uniformly throughout the stem (Figure 7B). Figure 7C,D represent the relevant maps of gathered silver and copper resulting from the in-depth LIBS analysis of the stem samples.

Similarly, Galiová et al. [99] conducted research on mapping the distribution of silver and copper in *Helianthus annuus* L., with the goal of tracking the potential migration of elements within botanical samples. Their work is significant because the authors demonstrated that the LIBS micro-mapping technique yields results comparable with those obtained through Laser-Ablation Inductively Coupled Plasma Mass Spectrometry (LA-ICP-MS). The scheme of the LIBS experimental setup accompanied by comparison between the Ag and Cu spectra obtained by LIBS and LA-ICP-MS are depicted in Figure 8.

For this study, a Nd:YAG laser emitting at a wavelength of 532 nm was used, with the energy of the laser pulses set at 10 mJ.

Jabbar et al. recently published a study on the application of LIBS in the analysis of plants, agricultural, and herbal products [149]. The samples used in this research were *Aerva javanica*, collected from a salt mine 160 km south of Islamabad in Pakistan. The laser system used in the experiment consisted of a Q-switched Nd:YAG laser with a wavelength of 532 nm, a pulse energy of 120 mJ, a pulse width of 5 nanoseconds, and a repetition rate of 10 Hz. Figure 9a shows the LIBS spectrum of the soil samples selected as targets, in the wavelength range from 300 to 600 nm. Figure 9b represents the emission spectrum of the roots of the *Aerva javanica* plant in two wavelength ranges: from 580 to 675 nm and from 765 to 770 nm. Figure 9c illustrates the spectrum emitted from the shoot of the *Aerva javanica* plant. The wavelength ranges in this case were from 282 to 675 nm and from 766 to 770 nm. The major contribution of this paper was to estimate the percentage of soluble salt metals in all three samples: stem, root, and soil of the Aerva javanica plant. One of the most important results reported in this paper was the demonstration that when LIBS is associated with an electric field, the soluble metal salts signal in soils, water and agricultural samples is enhanced (Figure 10), which yielded a better and more sensitive analysis.

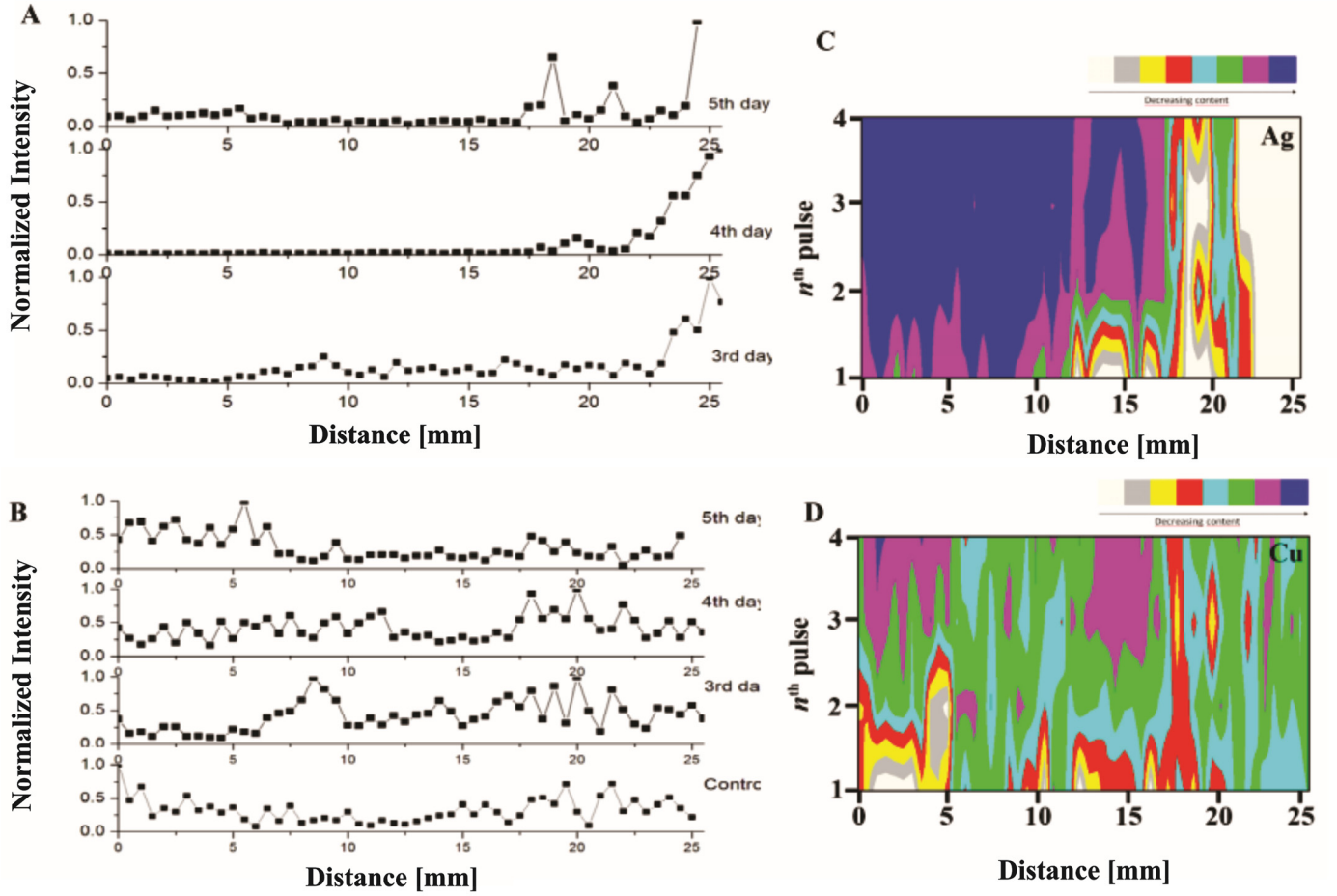

Figure 7. Accumulation of silver (**A**) and copper (**B**) in the stem of the selected species at different times after the treatment. Maps of the accumulated silver (**C**) and copper (**D**) were obtained with a LIBS system for a quasi-3D study of the chosen stem targets. Reproduced from Ref. [98] with permission of Multidisciplinary Digital Publishing Institute.

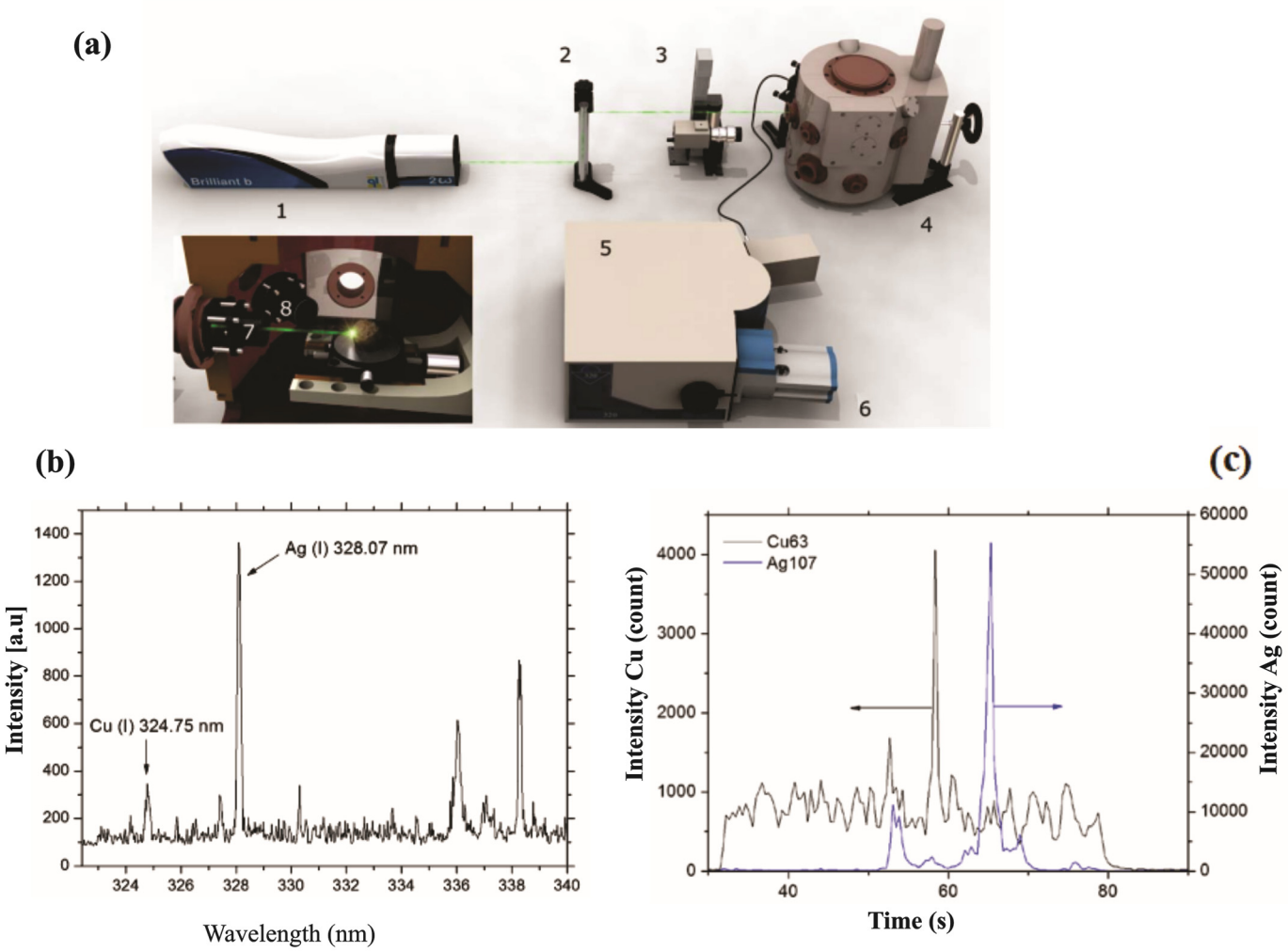

Figure 8. Instrumentation: (**a**) 1—Nd:YAG laser source, 2—periscope, 3—CCD camera to align a target, 4—experimental chamber, 5—monochromator, and 6—ICCD camera. In this set-up, the inner section of the chamber has a stage with micro-displacement: 7—focusing and 8—gathering optics. Experimental results: (**b**) The LIBS spectral emission of Ag(I) at 328.07 nm, and Cu(I) lines at 324.75 nm, and (**c**) the signal of Ag and Cu obtained by LA-ICP-MS technique. Reproduced from ref. [99] with the permission of Springer.

Samek et al. [69] performed elemental analysis on leaves of *Cornus stolonifera* and maize using a femtosecond laser system. Their study focused on Fe due to its biological importance and to explore the possibility of measuring its concentration in crops such as maize, rice, and wheat. The iron concentration in the leaves was determined using Relaxation Weighted Magnetic Resonance Imaging (RWMRI). Their results demonstrated that LIBS analysis can accurately determine the natural abundance of iron in these samples, with a LOD of 5 ppm. Furthermore, the findings confirmed that iron is primarily concentrated in the veins and transported by the xylem, as shown in Figure 10.

They also demonstrated that it is possible to clearly distinguish the leaf veins from other areas of the leaf. As a result, the spatial distribution of the iron element in the leaves was preserved, which is a significant advantage of LIBS analysis compared to other traditional methods. In LIBS, the ablation process is performed without destroying other parts of the plant sample. This makes it possible to survey and analyze any plant parts with low side effects. Additionally, the method has high spatial resolution which can recapture spatial information with regard to where various elements are distributed across plant parts. Other often used methods may lose some of this information with sample preparation.

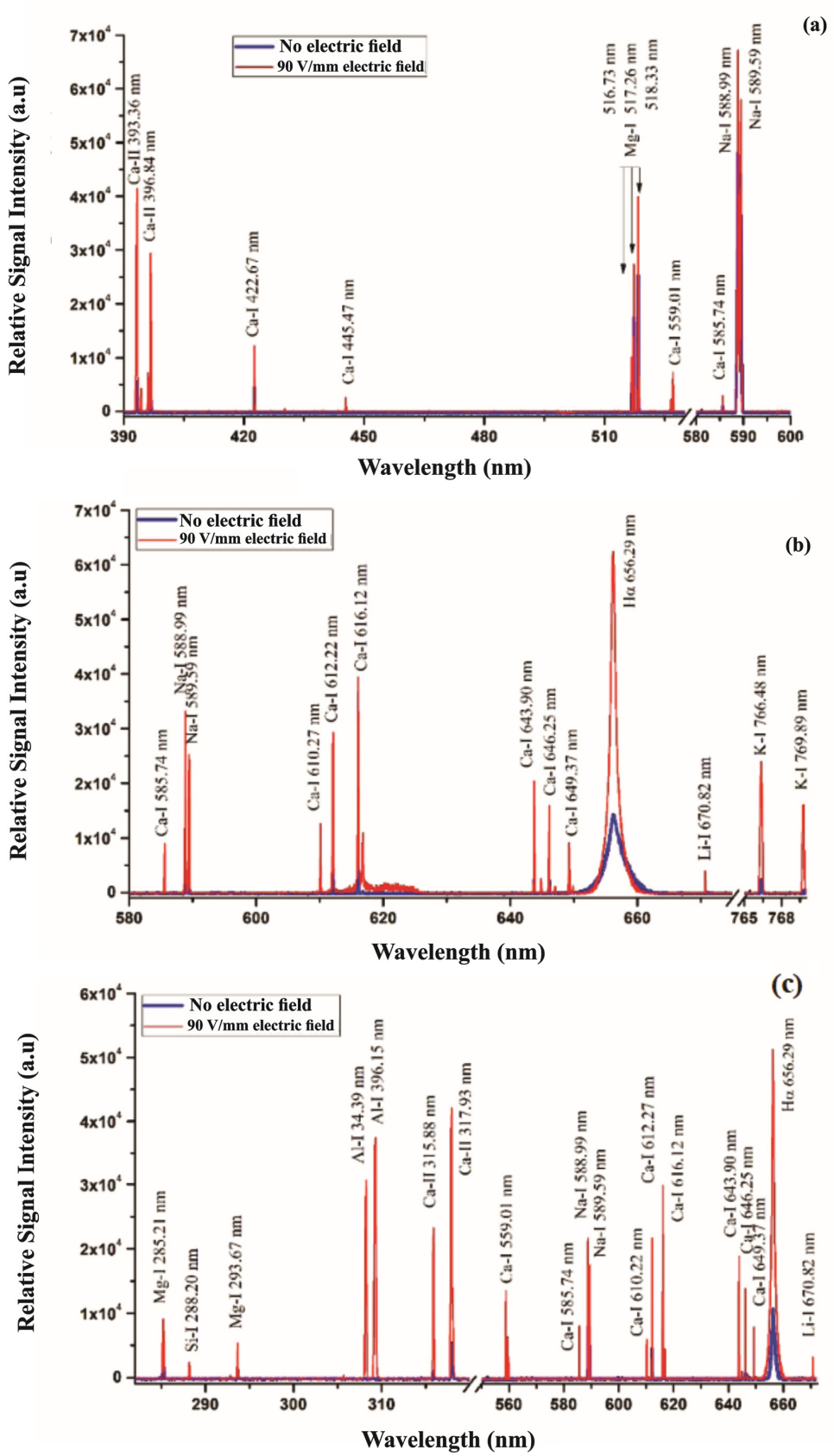

Figure 9. (**a**) LIBS spectrum of the soil targets related to the Khewra Mine, (**b**) LIBS spectrum associated with the *A. javanica* root, and (**c**) LIBS spectra of the *A. javanica* shoot captured in air using a 532 nm laser wavelength, at a 2 µs delay time after the laser pulse, both with and without an external 90 V/mm electric field. Reproduced from Ref. [149] with permission of Taylor & Francis.

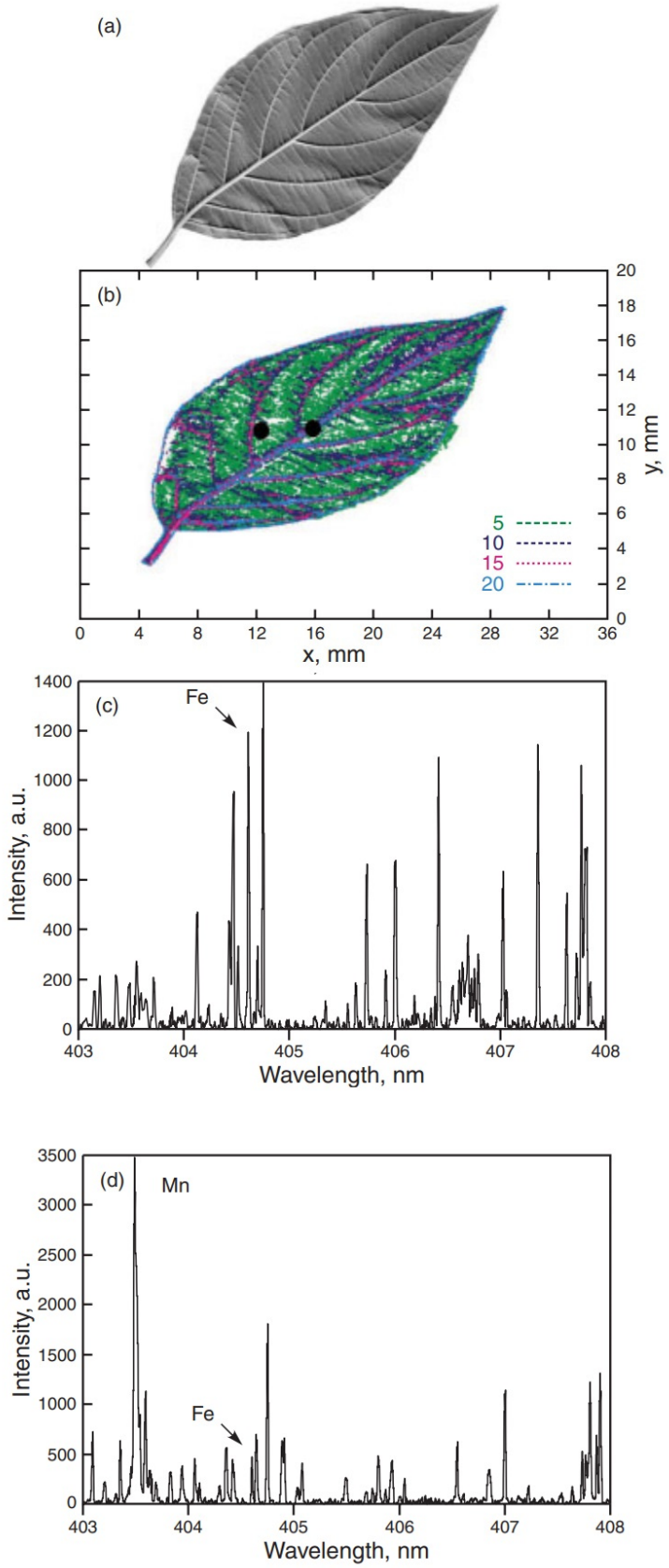

Figure 10. Fe emission from different parts of a leaf of *Cornus stolonifera*. (**a**) Picture of the leaf utilized for the study, (**b**) Distribution of Fe concentration obtained by RWMRI, the two points where LIBS analysis was performed are marked with a dot; (**c**) LIBS spectrum at the vein (Fe concentration of 20 ppm), (**d**) LIBS spectrum taken about 2 mm away from the vein (Fe concentration of 5 ppm). Reproduced from Ref. [69] with permission of WILEY-VCH.

Another study using LIBS on plants was conducted by Bossu et al. [49]. As shown in Figure 11, they used fs-LIBS to detect trace metal elements in *Sophora* leaves.

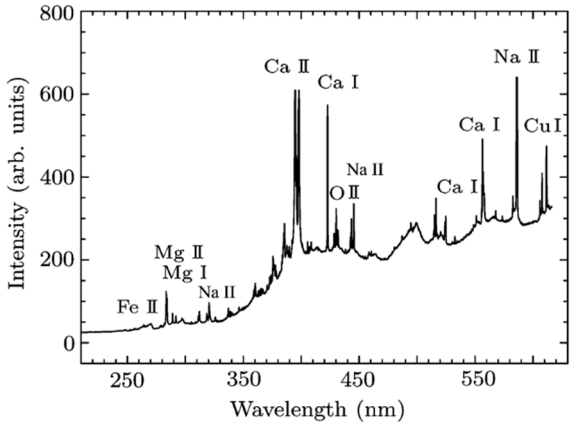

Figure 11. LIBS time-integrated spectral emission of sophora leaves obtained using femtosecond irradiation. Reproduced from Ref. [49] with permission of IOP.

The authors argued that since metals are either deposited on plant tissues or absorbed by plants, fs-LIBS could be applied to plant tissues as an indicator of air pollution. Consequently, they qualitatively ranked the sites of leaf collection from the most polluted (largest concentration of trace metals) to the less polluted (smaller concentration of trace metals). Furthermore, they pointed out that fs-LIBS could be applied to analyze soils from different regions to assess their quality, pollution levels, and elemental composition. It can also be used in botanical research to measure the elemental content in plant tissues and assess environmental stress.

Pouzar et al. [83] used LIBS technology to identify the macronutrient elements Ca, Mg, P, and K in the leaves of plants such as wheat, poppy, barley, and rapeseed. Their aim was to develop a fast and cheap alternative to conventional laboratory instrumentation, with minimal sample preparation, for the analysis of crop plant samples. The amounts of potassium and magnesium were evaluated using LIBS by Silvestre et al. [150]. In this study, the samples were prepared by adding high concentrations of these elements to wood, filter paper, and babassu fruit. The samples used in the research included wood samples (*Pinus*), powdered babassu mesocarp (Esmeraldo Produtos Naturais, Fortaleza, Brazil), filter paper (Whatman 513, 15 mm), and plant samples (apple leaf SRM 1515, peach leaf SRM 1547, and tomato leaf SRM 1573a, NIST, Gaithersburg, MD, USA). These samples were used to determine synthetic calibration standards, considering the large variation in Mg and K concentrations during sample preparation.

The leaves of the yerba mate plant (*Ilex paraguariensis*), which are consumed as tea, contain many nutrients. In research presented by Díaz Pace et al. [29], powder samples of this plant were analyzed using LIBS. The authors' findings confirmed that LIBS is a quick method for studying macronutrients, showing the presence of extractable macronutrients in yerba mate leaves.

Additionally, in the research by Trevizan et al. [47], a fast and practical LIBS methodology was used to analyze sunflower leaves. They determined the presence of magnesium, copper, and lead in these leaves. This research confirmed that LIBS can successfully detect micronutrients such as Cu, Fe, B, Zn, and Mn in pellets of plant material.

In a study by Borduchi et al. [151], some measurements were performed on nutrients in plant leaves using LIBS, highlighting the impact of matrix effects due to variations in fertilizers, water, and atmospheric conditions. The matrix effect is a significant analytical challenge in LIBS and other spectroscopic analyses. It manifests as a dependence of the

LIBS signal intensity on the concentration of the element in the sample, as well as on the sample matrix. The study examined 30 different soybean leaves from various locations with differing nutrient element levels, to evaluate the TiO_2 content in terms of weight. Their findings suggested that the CF-LIBS method with One-Point Calibration (OPC) modification could reduce, and in principle, eliminate the matrix effects in LIBS analysis of samples. In the OPC approach, the intensities of emission lines in the Boltzmann and Saha-Boltzmann plots for each element (atom or ion) were experimentally adjusted to account for spectrometer performance uncertainties and other line-related issues. Additionally, the LIBS instrument was also used to analyze the surface accumulation of metals in *Pakwan* leaves due to environmental air pollution [152]. Elements like aluminum, barium, calcium, chromium, copper, phosphorus, iron, potassium, magnesium, manganese, sodium, sulfur, strontium, and zinc were identified in the leaves, and their abundance was determined.

A study presented by Aldakheel et al. [153] conducted qualitative and quantitative analyses of elements in *Tinnevelly senna* leaf samples using LIBS technology. *Tinnevelly senna* leaves are used for treating various diseases and are commonly found and utilized in sub-desert areas due to their bioactive compounds such as senocides, phenols, and flavonoids. The researchers studied the antibacterial and anticancer properties of these leaves. Their study successfully demonstrated the bactericidal effect of senna leaf extract on *Staphylococcus aureus* (*S. aureus*) and its anticancer activity on cancer cells (HCT-116 and HeLa) as well as normal cells (HEK-293) at varying concentrations of the senna leaf extract. They showed that the bactericidal effect of senna leaf extract significantly inhibited the growth of Gram-positive bacteria. Both MTT and PI analyses revealed that the senna leaf extract hindered the growth of HCT-116 cells, while it had no adverse effect on normal cells (HEK-293), indicating its specificity towards cancer cells. The authors suggested that these extracts could be used for developing antibacterial and anticancer drugs in the future.

Han et al. [84] studied the materials and elements in tobacco and tobacco ash, identifying the presence of elements such as Fe, Ca, K, Li, Mn, Na, Al, Sr, Cu, Mg, Ti, and Zn in these plants.

Furthermore, due to the various properties of the moringa tree, its leaves, flowers, and seeds were utilized in Ref. [154] to identify the nutrients and beneficial substances they contain. Multiple tree samples were analyzed using LIBS, confirming the presence of elements like Ti, Ca, C, Si, Fe, Mg, K, Al, Sr, Na, H, O, and Li. The study revealed that carbon is the main element, with trace elements such as Ca, Mg, K, Fe, Na, Al, Ti, Sr, and Li. Their concentrations were determined, confirming that LIBS technology is well-suited for detecting elements like Li, Al, Si, and Sr in plants.

The study on cotton plants using LIBS was performed by Schenk et al. [73]. The LIBS data indicated the presence of elements such as Al, Ba, Ca, Cr, Cu, Fe, Mg, and Sr in cotton. Additionally, in the research presented by Martelli et al. [155], LIBS was mentioned as an indirect approach to assess the integrity of plant layers. The authors also used wheat leaves and grain layers to prove the same concept. Moreover, a sample of marigold was analyzed using LIBS by Iqbal et al. [156]. The LIBS data revealed spectral lines for Fe, Ca, Ti, Co, Mn, Ni, and Cr in the spectrum of this plant. Investigations into the distribution of minerals and silicon deposition in various parts of wheat (*Triticum aestivum*) plants were performed using LIBS [124]. The authors found that all parts of the wheat plant contained elements such as Ca, Mg, Si, Fe, Na, K, C, H, O, and N. Additionally, Andrews et al. [148] studied the correlation between nutrients in different types of plant tissue and soil depth in *Populus trichocarpa*, following an analysis of its constituent elements. They investigated the use of LIBS for fast, on-site elemental analysis of plant and soil samples. Their work proved that LIBS can identify key nutrients like O, K, C, N, and Ca with little or no sample

preparation. Their approach facilitated the study of plant–soil interactions, selecting optimal bioenergy crops, and estimating carbon sequestration. Their research suggested that LIBS could be an effective instrument for accurate agriculture and ecological evaluation.

In the research conducted by Shukla et al. [157], leaf samples from spinach, chenopodium, pea, mustard, and fenugreek were analyzed using LIBS to determine the distribution of minerals. Their results showed that spinach leaves had the greatest iron content compared to the other leaves. The authors noted that these low-calorie and low-fat plants were rich in protein, iron, fiber, calcium, and phytochemicals. Nunes et al. [111] studied the leaves of spinach (*Spinacia oleracea*) and sugarcane plants using LIBS. Their analysis revealed the presence of macronutrients such as Ca, Mg, and P, and micronutrients such as B, Cu, Fe, Mn, and Zn, as well as Al and Si in the plant leaf samples. Additionally, LIBS can be used to identify elements in living microorganisms, specifically algae [61]. This analysis revealed the presence of biosynthetically unimportant elements such as potassium, magnesium, calcium, sodium, and copper. The authors reported the accumulation of heavy ions in two algae samples, namely *T. minutus* and *Chlamydomonas* sp.

The plant *Aerva javanica*, which grows in saline areas, was analyzed using LIBS by Jabbar et al. [149]. These plants flourish alongside salt mines in Punjab, Pakistan. Through LIBS analysis, the presence of metals from these saline areas was revealed. The concentrations of elements such as sodium, magnesium, and calcium in the samples of the roots and organs of this plant were measured and reported.

Generally, the aqueous extract of ripe and unripe fruit peel of *Psidium guajava* (*P. guajava*) has glycemic potential. For this reason, in a study presented by Rai et al. [105], such extracts were analyzed using LIBS. The LIBS data showed that the concentration of Mg in the aqueous extract of unripe fruit peel was higher than in the aqueous extract of ripe fruit peel. However, the concentration of K in the unripe fruit peel extract was lower than in the ripe fruit peel extract. Meanwhile, it was noted that the concentration of other elements, such as Na, N, O, and C, remained almost the same in both extracts.

A review of the literature revealed that the highest silicon accumulation was found in the leaves of wheat plants, followed by grasses, leaves, lima, raicilla, and stems. Devipriya et al. [158], in reviewing the results of 37 scientific papers, emphasized that the rapid identification capability of LIBS makes it an effective technique for determining the elemental composition of plants. They further explained that therapeutic efficacy and drug development could be enhanced by focusing on Ayurvedic pharmacology and advancements in phytopharmacology.

Furthermore, soybean leaves were analyzed in two forms, with and without petioles, by Assis et al. [159] using LIBS. The macronutrients present, including elements like calcium, potassium, and magnesium, as well as micronutrients like phosphorus and sulfur, were identified in the LIBS spectra.

Tripathi et al. [160] examined the leaves of four *Ocimum* species: *Ocimum basilicum*, *Ocimum sanctum*, *Ocimum gratissimum*, and *Ocimum americanum* using a LIBS setup. The LIBS results revealed the presence of elements such as calcium, potassium, sodium, and magnesium, as well as lighter elements like hydrogen, nitrogen, silicon, carbon, and oxygen. Calcium was the most abundant element in all species, followed by potassium, magnesium, and sodium. Additionally, it was demonstrated that *O. sanctum* was the richest in minerals, followed by *O. gratissimum*, *O. basilicum*, and *O. americanum*.

Kim et al. [93] also introduced LIBS to test spinach and rice samples, analyzing essential elements such as Mg, Ca, Na, and K to distinguish pesticide-contaminated samples from healthy or reference samples. They explored the potential application of LIBS for measuring agricultural pesticide residues.

In a study presented by Liang et al. [161], 15 *Salvia miltiorrhiza* samples were analyzed and classified using a LIBS experimental setup. The study also introduced a classification model based on the particle swarm optimization-kernel extreme learning machine (PSO-KELM) method for identifying *Salvia miltiorrhiza* samples from various regions.

In Ref. [100], a method for further investigating most plant materials using LIBS was presented. It was noted that a decrease in moisture content during analysis allowed for easier detection of heavy metals using LIBS.

Trevizan et al. [63] studied Spanish moss to identify its constituent elements, such as manganese and zinc, using LIBS. Additionally, pine needles were analyzed by the same group to detect elements such as P, Fe, Cu, and Al. Previous research in this field by Cho et al. [143] in 2001 referenced a method for determining potassium and magnesium in starch powders using LIBS. The analysis of calcium in sunflower seedlings was also performed.

Furthermore, the applications of LIBS between 2010 and 2019 in the study of plants, crops, plant products, and food products were discussed in a review paper by Senesi et al. [39]. The authors focused on using LIBS to analyze plant leaves, vegetables, tubers, roots, seeds, grains, and fruits. In addition, they investigated fruits and processed plant products such as commercial coffee, flour, and wine. They highlighted the effectiveness of LIBS in analyzing products such as sugarcane, tobacco, peppermint, and saffron. They also pointed out the suitability of LIBS for diagnosing citrus, soybean, and tobacco diseases.

Martin et al. [81] used LIBS to analyze four samples of tall fescue (*Festuca arundinacea*) leaf tissues collected from the laboratory station of the University of Tennessee, Knoxville. They initially identified the presence of Fe, Mn, Mg, Pb, Ca, Zn, and Cd in the leaf tissue of the plant samples. Figure 12 illustrates the emitted peaks of Cd, Zn, and Mg elements in Tall Fescue. Other metal elements revealed by LIBS fall outside the 252–286 nm window. The authors pointed out that copper was not detected using LIBS. However, they were able to detect and quantify cadmium in the leaves, using the method of standard addition. According to this method, known quantities of the analytes are added to the sample (grinded and pressed to form a pellet); the intercept of the curve at zero added Cd concentration is due to the original Cd content, that in this way can be quantified (Figure 13). Another finding was that the presence of endophytes in the analysis as a treatment could alter the concentration of elements like Mg, Ca, Fe, and Mn. However, due to the limited number of samples, the impact of endophytes could not be conclusively determined, and the effect was not fully transparent across all the samples.

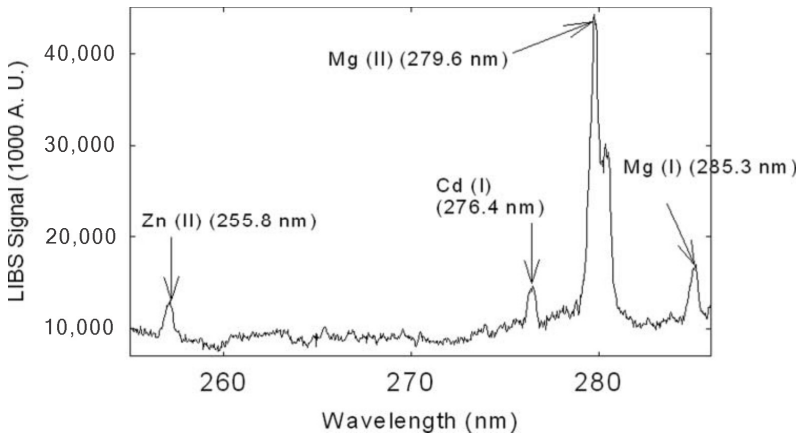

Figure 12. Portion of the LIBS spectrum of dried, grinded tall fescue leaf targets. Zn, Cd, and Mg are identified in this spectrum. Reproduced from Ref. [81] with permission of Optica Publishing Group.

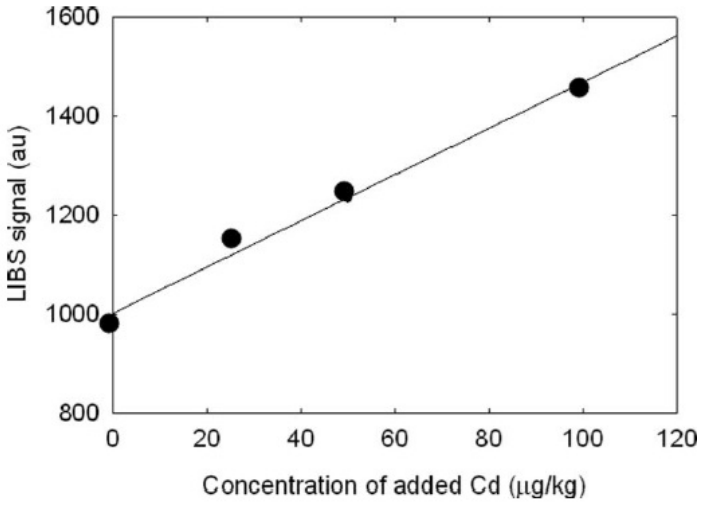

Figure 13. LIBS signal increase with the increase in the Cd content in grinded species of tall fescue leaves, showing a correlation coefficient of 0.994. Reproduced from Ref. [81] with permission of Optica Publishing Group.

In addition, the use of LIBS in soil determination to track heavy metal pollution, which impacts human health as well as agricultural harvests, was discussed by Mahmood et al. [162]. The authors provided the background principles of LIBS, highlighting that it employs spectroscopic fingerprints to identify elements such as Pb, Zn, Cd, and Cu with precision. To enhance research, they implemented improvements to signal quality, optimized analysis conditions, and provided noise reduction strategies. Along with the development of LIBS's use in environmental monitoring, their research also investigated its use for direct soils analysis with minimal preparation. LIBS was proposed as a new method for elemental profiling filamentous fungal species by Rush et al. [163] LIBS presented a fast and inexpensive alternative to fungal analysis, in contrast to traditional techniques such as ICP-OES and ICP-MS, which require time-consuming sample preparation and expensive equipment. Their findings demonstrated that LIBS could accurately determine the elemental profiles of fungi grown on different substrates, with species-dependent patterns of element incorporation, including C, Zn, P, Mn, and Mg. The results demonstrated the application of LIBS as a high-speed phenotyping approach to analyzing fungal behavior and environmental interactions.

4.1. Spatial Distribution of Elements by LIBS Mapping

Realizing the uptake, transport, and accumulation of nutrients as well as hazardous elements, in plants, and recognizing interactions between plants and their environment, critically depends on mapping and sensing how these elements spread within plant structures and their growth environment [33]. Additionally, elemental maps are essential in materials science, where they are used in studying processes such as deposition, coating, combustion, diffusion, segregation, and other manufacturing and processing techniques [164]. LIBS has gained increasing attention in the field of imaging [165] due to high-speed imaging instruments with pixel acquisition rates in the kHz range [166] and spatial resolutions down to a few μm [164,167]. The Vincent Motto-Ros group has published numerous works on the application of LIBS in mapping processes [168]. Another significant advantage of elemental imaging with LIBS is its ability to analyze nearly all elements of the periodic table, including H, C, N, O, and F, which are not easily detectable by ICP-MS. Over the past 20 years, LIBS has proven itself as a reliable analytical method for plant bioimaging, with numerous studies and review articles documenting its applications [34,39,143,166]. The absence of the need to transport ablated material eliminates concerns about carry-over

and wash-out effects, and transport efficiency is no longer a significant issue [167]. Alkali and alkaline earth elements provide the best detection limits, though the sensitivity for nonmetals is lower. However, this is not a limiting factor, as these elements are typically major components in the samples. Unlike mass spectrometers that operate sequentially, LIBS enables the simultaneous detection of a selected wavelength range. This capability allows for the collection of broad spectra without requiring prior analyte selection, enabling the identification of major elements during post-measurement analysis.

LIBS has now matured as a technique in plant bioimaging [46] and is emerging as a promising tool in biomedical applications [2]. Several reviews focusing on the application of LIBS for biological samples, particularly in bioimaging, have been published. These include studies on plant materials [28,168] and plant bioimaging [46].

LIBS has been successfully applied to the elemental scanning of terminal annual stems of spruce (*Picea abies* (L.) Karsten), followed by mass spectrometry to analyze calcium and copper content [94]. This method can also be used for quantitative measurements of copper ion transfer in various plant regions.

For instance, Lu et al. [169] evaluated the existence of heavy metals of Cd and Zn in *S. alfredii* plant by LIBS mapping method employing convolutional neural network techniques. Moreover, Babos et al. [170] conducted a study using LIBS in conjunction with multivariate calibration models to rapidly and precisely evaluate soil fertility. Their analysis of soil samples from diverse agricultural systems identified distinct fertility clusters using principal component analysis. The authors demonstrated that LIBS effectively tested soil variability without extraction, which is applicable to precision and digital agriculture. In addition, their soil chemical property mapping project elucidated the potential of the method in monitoring and enhancing soil fertility.

Investigations into the distribution of minerals and silicon deposition in different parts of *Gondom* plants have also been conducted using LIBS [124]. These studies revealed that all components of the *Gondom* plant contain Ca, Mg, Si, Fe, Na, K, C, H, O, and N.

A study by Shuang et al. [80] analyzed poplar tree (*Populus* sp.) leaves using LIBS. Leaves were collected from four different locations in Changchun City: Jingyue National Forest Park (JYP), Changchun University of Science and Technology (CUST), Casting Factory (CF), and Forging Factory (FF). Spectral mapping showed that the leaves from all four locations contained elements such as N, P, K, Ca, Fe, Ti, Mn, and Na. These findings were obtained using a calibration-free method, as illustrated in Figure 14a. Additionally, Figure 14b presents the emission spectra of the four poplar leaf samples within the wavelength range of 250–600 nm, confirming the presence of N, P, Ca, Fe, Ti, Mn, and Na. A summary of the concentrations of Ca, Fe, N, and P in the leaves from the four regions is provided in Table 5 [80].

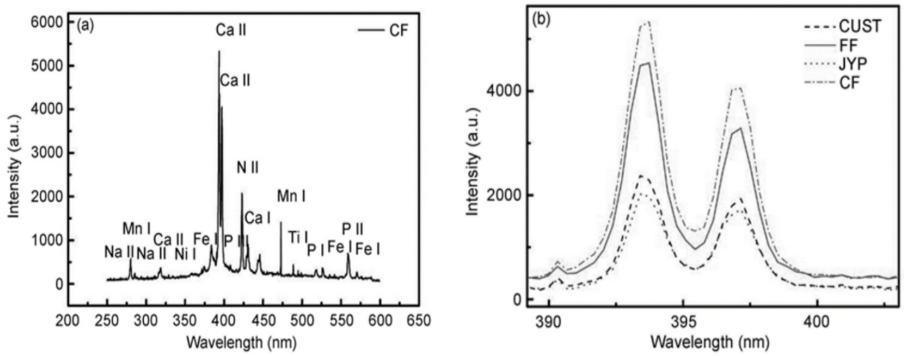

Figure 14. (**a**) Emission lines of leaves from poplar trees in the CF of First Automobile Works (FAW); (**b**) a relative spectral intensity comparison of the Ca II across four sections. Reproduced from Ref. [80] with the permission of Springer.

Table 5. Ca, Fe, N, and P concentrations in poplar leaves from four positions. Reproduced from Ref. [80] with the permission of Springer.

	JYP(C_J)	**CUST**(C_C)	**FF**(C_F)	**CF**(C_{CF})
Ca	0.01556456	0.018851377	0.020282802	0.03194
Fe	0.07650221	0.086808511	0.115235948	0.1271288
N	0.03882128	0.036399361	0.024551016	0.0274323
P	0.03984836	0.038226791	0.035729464	0.0345009

Zhao et al. [129] exploited this adaptability by transitioning a LIBS setup to a maize field (as shown in Figure 15) to conduct a groundbreaking investigation that combined in situ and in vivo 3D elemental mapping. An organophosphorus insecticide (chlorpyrifos, $C_9H_{11}C_{l3}NO_3PS$) was sprayed onto a maize leaf, and after ten hours, the vegetative tissue was analyzed.

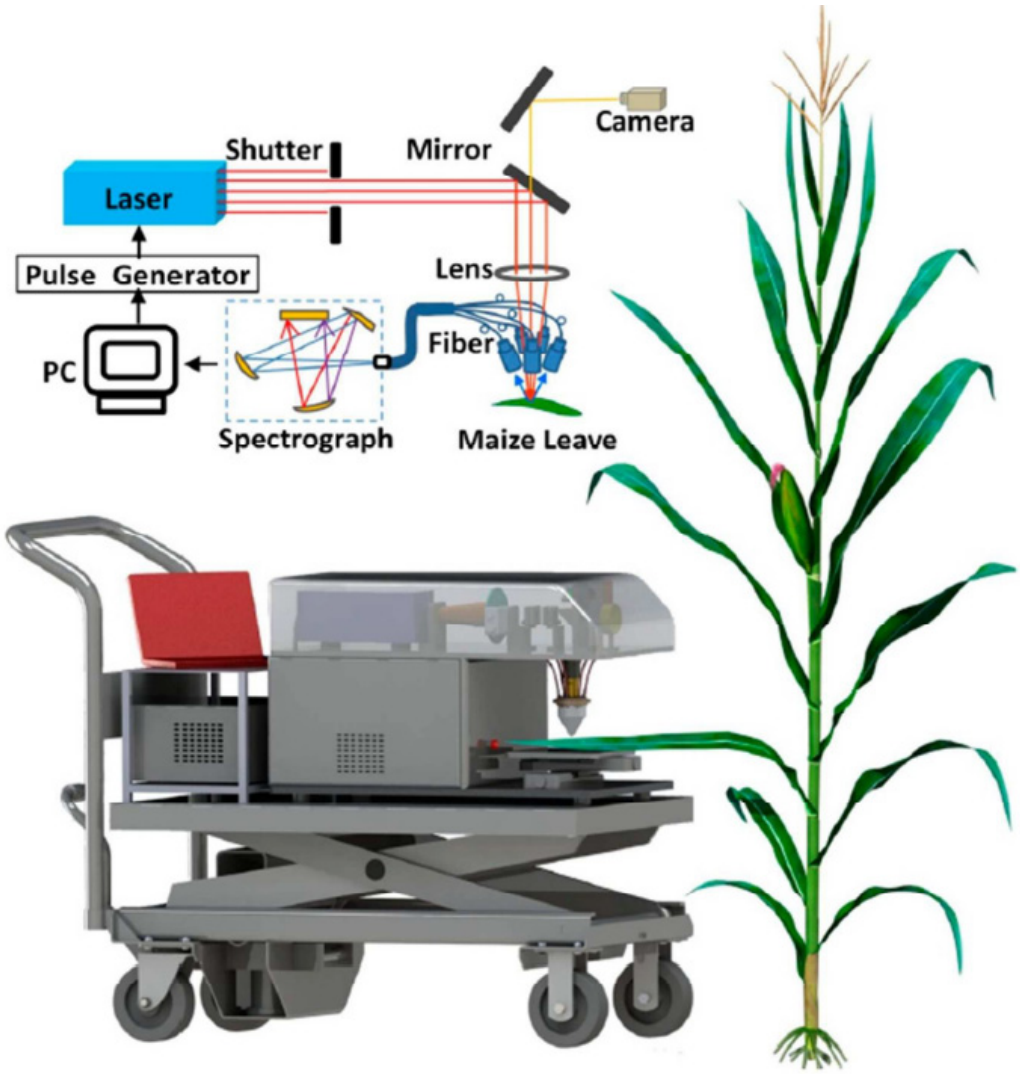

Figure 15. A graphic representation of the LIBS system to map the elements in maize leaves, in situ and in vivo after being sprayed with an organophosphorus pesticide (chlorpyrifos, $C_9H_{11}Cl_3NO_3PS$). Reproduced from Ref. [129] with permission of Multidisciplinary Digital Publishing Institute.

Multivariate regression models were constructed using selected P and Cl emission lines as response variables, with samples of known pesticide concentrations forming the calibration set. This approach enabled precise assessment of pesticide residues.

The resulting maps, generated with a 12 µm step in the *z*-axis, clearly demonstrated that pesticide residue levels decreased significantly with leaf depth, with only trace amounts detected in the fifth layer.

Due to the simplicity of LIBS systems, this type of in situ analysis shows great potential. Additionally, Table 6 highlights the application of LIBS in analyzing agricultural food plants.

Table 6. Usage of LIBS method for detection of different elements in plant species. Reproduced from Ref. [33] with permission of Atomic Spectroscopy Press Limited(Hong Kong, China).

Agricultural Plant Products	Elements Analyzed	Ref.
Bean (Pulses)	Ca	[47]
Pepper (*Capsicum annum* L.)	Pb, Mn, K	[60]
Chickpea	Si, Mg, Ti, Fe, Ca, C, Al	[157]
Fenugreek seeds	Si, Mg, Ti, Fe, Ca, C, Al	[157]
Folium Lycil	Al, Ca, K, Li, Mg, Na, Si, Sr, Ti	[64]
Leaf mustard	Si, Mg, Ti, Fe, Ca, C, Al	[157]
Lettuce (*Lactuca sativa*)	Fe, Mn, B, Cu, Zn	[47]
Maize (*Zea mays*)	B, Fe, Cu, Zn, Mn	[47]
Pepper (*Piper nigrum*)	B, Cu, Fe, Mn, Zn	[47]
Potato (*Solanum tuberosum*)	Al, Ba, Be, Ca, C, Cl, Cr, Co, Cu, Fe, H, K, Li, Mn, Mg, Mo, N, Na, Ni, V, O, Rb, Si, Sr, S, Ti	[14]
		[47]
Soya (*Glycine max*)	Fe, Cu, Mn, Zn, B	[111]
Spinach (*Spinacia oleracea*)	Ca, Mg, P, B, Cu, Fe, Mn, Zn, Al, Si	[111]
Sugarcane	Mg, B, Cu, Ca, K, Mn, Fe, P, Zn	[84]
Sunflower (*Helianthus annuus*)	Ag, Ca, Cu, K, Mn, Mg, Pb	[51]
Wheat seedling	C, Ca, Fe, H, K, Mg, N, Na, O, Si	[124]

4.2. Beneficial Elements, Including Macro and Micronutrients

Plants need seventeen essential elements for growth and life cycle completion. Among these, three elements—oxygen, carbon, and hydrogen—are extracted from the air or water, while the remaining fourteen are typically sourced from the soil. These fourteen essential nutrients are categorized as macronutrients (nitrogen, phosphorus, potassium, magnesium, sulfur, calcium) or micronutrients (iron, zinc, manganese, boron, copper, nickel, chloride, and molybdenum). Both macronutrients and micronutrients are indispensable for plant health.

Soil analysis is typically performed before sowing or planting to quantify the nutrient content in the soil. However, soil nutrient analysis and the actual availability of nutrients to plants are sometimes not aligned [171]. When the content of essential nutrients in certain plant tissues is low, crop yields decrease, and growth is affected. The mineral nutritional status of plants is often characterized based on foliar analysis, which is used to determine and fix nutrient deficiencies for optimal crop yields, such as vegetables, cereals, and fruit.

Tracking plant nutrient content throughout the growing season is vital for detecting serious deficiency events that require accurately determining a plant's mineral content. Despite some deficiencies being identified via visual inspections, it is crucial to recognize that latent deficiencies will not usually show visible symptomology, particularly early on, making these deficiencies very difficult to diagnose [172].

Plant tissue analysis is a reliable method for assessing levels of nutrients that are typically conducted with atomic spectrometry techniques such as inductively coupled

plasma optical emission spectroscopy (ICP-OES) or inductively coupled plasma mass spectrometry (ICP-MS) [173]. These techniques provide consistently accurate results. However, they require extensive resources and investment and thus are less likely to be utilized in plant science. In addition to atomic spectrometry, faster and non-destructive methods are available [174]. For example, handheld devices that measure chlorophyll *a* fluorescence can provide insights into manganese and phosphorus levels [172,175], although their reliability diminishes under high-light-intensity conditions [176]. Near-infrared spectroscopy (NIRS) has also shown promise for predicting nutrient content in crops, with dried and homogenized leaves yielding more accurate results than fresh leaves [177].

XRF can also be used to measure plant nutrients; it is available in benchtop and portable versions. The XRF technique can detect a number of nutrients, but due to varying detection sensitivity, some elements such as magnesium, copper, zinc, and iron may not be detected in the research [34,178]. Despite the advantages of rapid, nondestructive techniques, reliable methods that enable comprehensive, multi-element analysis of plant tissues are still needed.

LIBS has emerged as a promising technology for multi-element analysis of plant tissues [34]. Unlike inductively coupled plasma optical emission spectroscopy (ICP-OES), which requires liquid samples, LIBS creates plasma using a high-energy laser pulse that can ionize both liquid and solid samples. This versatility makes LIBS suitable for various industries, including agriculture, where it can be effectively applied to analyze soil and crop plants [35,176].

In recent years, the Krug research group [74,77,91,94,111,127,178] has extensively utilized LIBS to study various crop plants, with a particular focus on sugarcane leaves. In an initial study, Braga et al. [74] evaluated the effectiveness of LIBS as an alternative to conventional analytical methods involving wet acid digestion for the elemental analysis of plant components, particularly leaves, from 20 different plant species.

Braga Bueno Guerra et al. [55] developed an innovative micro-sampling technique for the efficient determination of elemental concentrations in dried sugarcane leaves using LIBS, in comparison with energy-dispersive XRF (ED-XRF). The correlation analysis between the mass fractions of elements such as Ca, Fe, P, K, Mn, and Si predicted by LIBS and ED-XRF showed strong linear correlation coefficients (r-values) reaching up to 0.9778. This micro-sampling method demonstrated significant potential for on-site analysis of fresh sugarcane leaves and other economically important crops.

In the same year, Arantes de Carvalho et al. [178] conducted research using LIBS to analyze elements such as Ca, K, Mg, P, B, and Mn in boldo leaves. They found that particle size significantly affected emission line intensity and matrix effects. When particles smaller than 100 μm were analyzed, measurement variability decreased to below 10%.

In a groundbreaking study, Arantes de Carvalho et al. [91] employed a femtosecond LIBS system for the first time to quantitatively determine macronutrients (Ca, Mg, P) and micronutrients (Cu, Fe, Mn, Zn) in pelletized leaves from 31 economically significant crop plants, encompassing a diverse range of matrices.

Kim et al. [93] proposed combining LIBS with partial least squares-discriminant analysis (PLS-DA) to quantify Mg, Ca, Na, and K and to differentiate between pesticide-free and pesticide-contaminated spinach leaves. Calibration curves were established using standard reference materials to correlate LIBS peak intensities with concentrations measured by ICP-OES. The limits of detection (LODs) for Mg, Ca, Na, and K were determined as 29.63, 102.65, 36.36, and 44.46 mg/kg, respectively. Strong agreement was observed between the concentrations of these elements obtained through LIBS and those measured by ICP-OES in spinach samples purchased from a local market. Additionally, PLS-DA applied

to LIBS data achieved a good discrimination between pesticide-free and contaminated samples prepared by introducing 10 ppm of parathion.

Han et al. [84] used the CF-LIBS method to monitor trace elements such as Fe, Ca, Al, Cu, K, Li, Mg, Mn, Na, Sr, Ti, and Zn in cigarette tobacco leaves and ashes. The reduced concentrations of metallic elements in ashes compared to leaves indicated potential transfer to cigarette smoke, posing health risks.

In a more recent study, Kunz et al. [179] used fs-LIBS to monitor daily variations in K, Ca, Na, and Fe levels in wheat leaves over 30 days while measuring the effects of drought stress. These elemental markers could be used to distinguish between mild to severe drought stress levels, measuring different mechanisms for drought resistance. The application of LIBS at a remote field scale also demonstrated its potential for on-site plant stress resistance assessment.

Nicolodelli et al. [138] advanced plant nutrient analysis by using double-pulse (DP)-LIBS on soybean leaves, utilizing orthogonal beam geometry at 532 and 1064 nm wavelengths in a reheating configuration. Bhatt et al. [180] applied LIBS to compare the nutrient compositions of key elements in the tops and stems of organically and conventionally grown cauliflower and broccoli.

Rehan et al. [152] optimized a LIBS system by adjusting laser energy and lens distance to quantify Ca, Cr, Al, Ba, Cu, Mg, Mn, K, Na, Fe, P, S, Sr, and Zn concentrations in *Piper betel* (black pepper) leaves. Finally, Jull et al. [181] used LIBS to quantitatively analyze nutrients in fresh and dried pelletized leaves from mixed ryegrass and clover pastures.

4.3. LIBS in Medical Plant Analysis

The World Health Organization predicts that approximately 80% of the global population are related to herbal medicines for primary healthcare [47,129]. Historically, knowledge about herbal remedies was passed down orally through generations by trial and error [60,182]. In the last fifty years, ethnobotanical studies have presented new therapeutic plants that were previously unknown to the scientific community [183–187]. The development of sophisticated analytical methods and techniques for isolating plant phytoconstituents has allowed this research to occur.

LIBS has been utilized successfully in the study of various medicinal plant samples, and to evaluate the elemental content found therein. For example, Sharma et al. [188] discovered numerous medicinal plants' elemental compositions, including carbon, iron, magnesium, silicon, calcium, oxygen, hydrogen, nitrogen, and sodium in various medicinal plants. They reported the concentrations of five medicinal plant samples: *Phyllanthus niruri*, *Barringtonia racemosa*, *Tinospora cordifolia*, *Hygrophila angustifolia*, and the flowers of *Hygrophila angustifolia*. These plant samples, in the form of roots, leaves, and whole plant bodies, were analyzed in powdered form. The study suggested that this analytical method could also be applied to investigate other unknown plant species.

In another study, Andrade et al. [123] analyzed 18 samples of medicinal plants from Poland, Lithuania, and Serbia using LIBS. The elemental concentrations of Ca, K, Mn, and various metals (Na, Co, Cu, Fe, Ni, Zn, Mg, Cd, Cr, and Pb) were determined. These samples represented five species: *Sambucus nigra* L., *Hypericum perforatum* L., *Crataegus oxyacantha auct.* L., *Rubus idaeus* L., and *Betula* species L. Plant parts such as flowers, leaves with flowers, fruits, and whole plants were studied. Variations among herbal teas were noted, with leaves showing higher concentrations of copper and nickel, while flowers and leaves exhibited elevated levels of cobalt, calcium, and manganese. Flowers were also found to have higher sensitivity to K, Na, Mg, and Fe.

Additionally, medicinal plants such as *Taraxacum officinale*, *Hyoscyamus niger*, *Ajuga bracteosa*, *Elaeagnus angustifolia*, *Camellia sinensis*, and *Berberis lyceum*, commonly

used in traditional medicine, were analyzed for their leaves, roots, seeds, and flowers. As detailed in Ref. [189], LIBS determined both the beneficial nutrients and potential disadvantages of detected elements. The study identified elements such as silicon, aluminum, iron, copper, calcium, magnesium, sodium, potassium, manganese, phosphorus, and vanadium, along with molecular carbon and nitrogen bands. Magnesium, calcium, phosphorus, and silicon were highlighted as the primary elements in these samples, while manganese, iron, vanadium, aluminum, and titanium were identified as key medicinal metals. Trace elements such as strontium, silicon, and aluminum were also detected.

In research by Rai et al. [190], 13 herbal compounds, including plants such as *Bauhinia variegata*, *Cinnamomum zeylanicum*, *Cinnamomum tamala*, *Commiphora mukul*, *Crataeva religiosa*, *Elettaria cardamomum*, *Emblica officinalis*, *Embelia ribes*, *Piper longum*, *Piper nigrum*, *Terminalia bellerica*, and *Ocimum sanctum*, were analyzed using LIBS to develop antidiabetic and polyherbal formulas. The LIBS data confirmed the presence of elements such as Na, K, Mg, Ca, H, O, and N in these compounds.

Rai et al. [32] analyzed a group of Indian medicinal plants using a LIBS setup. One of the plants studied was *Cynodon dactylon* (Family: Poaceae), a common weed with antidiabetic properties. LIBS results indicated that its extracts contained elements such as Mg and C. Additionally, the plant *Emblica officinalis* (Family: Euphorbiaceae) was reported to possess antimicrobial, antioxidant, hepatoprotective, anti-tumor, and lipid-lowering properties. Its aqueous seed extract exhibited antidiabetic and antioxidant activity, with the LIBS spectrum confirming the presence of elements such as Mg, Na, Cl, Ca, H, O, and C.

The LIBS analysis of *Ficus bengalensis* (Family: Moraceae) revealed a higher concentration of Mg and Ca compared to other elements in its aqueous extract. Another plant, *Moringa oleifera* (Family: Moringaceae), was also examined using LIBS.

Shahbaz et al. [191] investigated the chemical composition, antioxidant, antimicrobial, cytotoxic, and antihemolytic activities of five different extracts of *G. hispida* and *H. crispum* (Family: Boraginaceae). The elements Si, Fe, Ba, Mg, Ti, Ca, and Cr were identified using LIBS. Their findings indicated that antibacterial activity decreased in the order of methanol > ethanol > chloroform > ethyl acetate > n-hexane in both species. Among the extracts, the ethanolic extract of *G. hispida* demonstrated the highest cytotoxic potential, while the chloroform extract of *H. crispum* exhibited the strongest antihemolytic activity.

The research conducted by Aldakheel et al. [153], used LIBS as a method for determining the elemental composition to investigate the anticancer and antibacterial properties of leaves. Their study specifically analyzed the leaves of *Tinnevelly Senna*, which had bioactive compounds produced in the leaves composed of sennosides, phenols, and flavonoids, making them valuable for treating various diseases. The traditional Ayurveda medicine system also uses different parts of plants, including roots, seeds, bark, and leaves, as noted in Ref. [40].

One example is the analysis of the *Azadirachta indica* plant using LIBS. The technique confirmed the presence of elements such as Fe, Si, Mg, Ca, Ba, Na, Li, N, K, O, Al, Sr, Ti, C, and H in the leaves and bark of *Azadirachta indica*. Likewise, Liang et al. [192] also used the LIBS approach to study *Salvia miltiorrhiza*, which is a keystone plant species of Chinese traditional medicine, known to have biological properties that include, but are not limited to, lowering blood pressure, improving blood flow, and relieving pain, nourishing the heart, and calming the mind. The elemental composition of *Salvia miltiorrhiza* was also reported in the study, further highlighting its medicinal significance.

Watal et al. [193] investigated glycemic elements in plants with hypoglycemic properties using LIBS. This study focused on medicinal plants belonging to the Indian plant category. LIBS is also effective in detecting lead in medicinal plants. For example, Jiang et al. [118] analyzed the *Rheum officinale* plant to determine lead concentrations.

They recommended the LIBS-LIF method for rapid, sensitive, and quantitative analysis of lead in medicinal plants. Additionally, *Baishao* (*Radix Paeoniae Alba*), a widely used medicinal herb, was analyzed using LIBS to determine its geographical origin [194].

The *Saussurea simpsoniana* plant, an environmentally friendly species rich in nutrients, has been used in traditional medicine to treat bronchitis, rheumatic pain, abdominal, and nervous disorders. In research by Fayyaz et al. [195], LIBS analysis confirmed the presence of elements such as Al, Ba, C, Ca, Fe, H, K, Li, Mg, Na, Si, Sr, and Ti. Similarly, Rhatany roots (RRs) are renowned for their antiviral properties and astringent biochemical compounds, which contribute to their therapeutic and medicinal value. In Ref. [196], Rhatany root samples were analyzed for their elemental composition using LIBS.

Furthermore, Alresawum et al. [197] examined ten traditional Ethiopian medicinal plants using LIBS, identifying essential nutrients such as copper, zinc, carbon, manganese, phosphorus, calcium, magnesium, iron, sodium, and potassium. In another study [198], the leaves of *Calotropis procera*, *Chenopodium ambrosioides*, and *Nerium indicum* were analyzed using LIBS (see Figure 16). Elements identified in all three samples included H, Si, Al, Fe, Cu, Ca, Mg, Na, K, N, O, Sr, and Ba. Molecular bands of carbon and nitrogen were also detected.

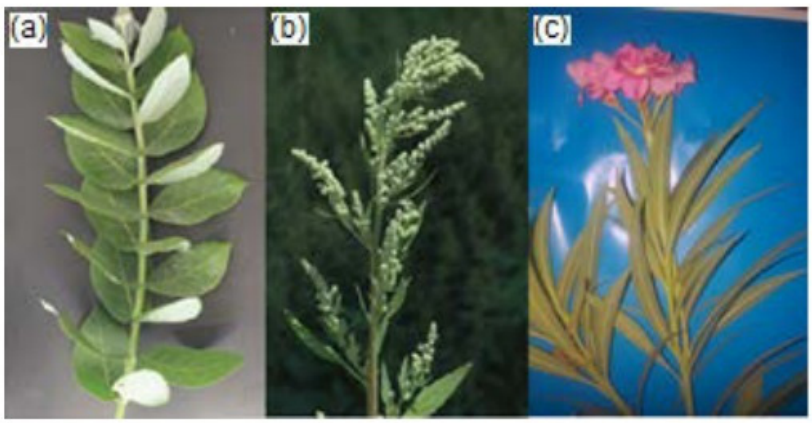

Figure 16. The leaves of different plants: (**a**) *Calotropis procera*, (**b**) *Chenopodium ambrosioides*, and (**c**) *Nerium indicum* utilized in Ref. [198]. Reproduced from Ref. [198] with permission of Gadjah Mada University.

The predominant elements in these plants were nitrogen, hydrogen, and oxygen, while magnesium, iron, potassium, copper, and calcium were identified as significant medicinal metals. Trace elements such as Sr, Si, Ba, and Al were also detected in the leaves of all three plants, highlighting their comprehensive elemental profiles.

Shukla et al. [199] analyzed the aqueous extract of *Ficus religiosa* leaves using LIBS to determine their elemental composition. This analysis proved beneficial in streptozotocin-induced diabetes models. LIBS revealed that this medicinal plant could significantly lower blood glucose levels and increase glucose tolerance tests in diabetic models. Magnesium and calcium were highlighted as key elements contributing to these effects.

Additionally, *Moringa oleifera* was analyzed for its elemental composition and biological effects using LIBS, as discussed in Ref. [200]. The analysis identified essential elements such as Na, Ca, Se, K, Mg, Zn, P, S, Fe, and Mn. Notably, the plant exhibited anticancer properties, as its seed extracts (MOS) inhibited the growth of colon cancer cells (HCT-116) without affecting non-cancerous cells (HEK-293), suggesting its potential non-carcinogenic features.

In Ref. [201], the aqueous extract of *Trichosanthes dioica* fruit, a known herbal antidiabetic medicine, was studied for its elemental composition using LIBS. The analysis detected magnesium, iron, sodium, potassium, zinc, calcium, hydrogen, oxygen, and carbon. High concentrations of Ca^{2+}, Mg^{2+}, and Fe^{2+} ions were found to contribute to the antioxidant potential of *T. dioica*.

The medicinal plant *Panax notoginseng* (*P. notoginseng*), commonly used as a dietary supplement, is known for its properties in reducing blood stasis, alleviating swelling, and pain relief. Chen et al. [202] employed LIBS to detect cadmium (*Cd*), demonstrating this plant's ability to absorb the element from its environment.

Three Chinese medicinal plants—Chuan-Mutong (*Clematidis armandii Caulis*), Mutong (*Aristolochiae manshuriensis Caulis*), and Utong (*Akebiae Caulis*)—were analyzed using LIBS for their elemental composition. Aldakheel et al. [114] also used LIBS to investigate these plants' leaves, identifying elements like magnesium, calcium, copper, manganese, sulfur, phosphorus, and zinc. Additionally, *Moringa oleifera* leaves were noted for their high antioxidant and nutrient content, contributing to benefits such as lowering blood sugar, treating heart diseases, and reducing inflammation.

Chinese medicinal plants, including Lily and Marigold, were analyzed for elemental composition using LIBS by Wang et al. [203]. Their study found potassium, calcium, magnesium, and iron in various plant parts, including the root, stem, and leaf of chrysanthemum; the roots and leaves of *Iris lactea*; and *Salvia miltiorrhiza*, along with its planting soil. Lily showed a significant enrichment of potassium, with the sequence flower > leaf > stem > root. The roots and leaves of Lily were rich in calcium and magnesium, with enrichment patterns for calcium and magnesium being leaf > root. Marigold exhibited a higher enrichment coefficient for calcium and magnesium.

Finally, the elemental composition of the herbal medicinal plant *Gynostemma*, commonly used in traditional Chinese medicine, was studied by Han et al. [204] using LIBS. Elements such as aluminum, calcium, iron, and magnesium were detected in the plant. The study also examined the dissolution of metallic elements in material melting through LIBSology. Copper and cadmium solutions were added to the plant material and analyzed for their elemental composition using the same technique.

In the study by Andrews et al. [205] LIBS was employed to investigate the relationship between silicon concentration, distribution, and phytolith formation in Populus trichocarpa plants. Phytoliths are non-crystalline particles of amorphous silica that form inside plant cells. These structures play a key role in the global carbon cycle because they can sequester organic carbon, which decomposes slowly, contributing to long-term carbon storage. A deeper recognition of the relationship between phytolith formation and silicon levels in plant tissues could allow bioengineered species to optimize carbon sequestration during substrate decomposition.

The study found no correlation between silicon levels in leaves and silicon-expressing genotypes. Instead, silicon concentration was reported to depend heavily on the growth environment, with soil silicon availability being a key factor.

Additionally, LIBS was utilized to evaluate the antidiabetic potential of the aqueous extract of *Trichosanthes dioica* fruits [105]. The plant supported its antidiabetic action with high magnesium, calcium, and iron levels.

4.4. Toxic Elements Evaluation by LIBS

Typically, toxic effects on plants or parts of plants are assessed at the organism, tissue, or cellular level. However, the distribution, bioaccumulation, absorption, and translocation of studied compounds are often evaluated only at the end of exposure. The combined evaluation of these results can provide deeper insights into the effects of certain pollu-

tants. Additionally, information about the spatial distribution of elements can establish a connection between the precise location of an element and its toxic effects.

LIBS has been used to assess the presence and concentration of lead in *Rhododendron* leaves [119]. These leaves are commonly used in medicines for their therapeutic properties, making it essential to monitor lead content for medicinal safety. In Ref. [206], a Russian internal standard technique and standard addition methodology were incorporated into LIBS to track and analyze copper and manganese in *Glycyrrhiza*. This study aimed to identify harmful elements in *Glycyrrhiza*, a traditional Chinese medicine containing active compounds with significant potential in treating COVID-19. Moreover, Wang et al. [207] employed LIBS to analyze dry orange peel and *Ligusticum wallichii* (a medicinal plant) for mercury concentrations. Their results demonstrated the quantitative measurement of copper and lead in *Ligusticum wallichii*. Additionally, this research extended to the analysis of lead and copper in *Coptidis*.

Yang et al. [208] utilized LIBS to detect and investigate heavy metals in mulberry leaves. The results indicated the presence of copper (Cu) and chromium (Cr) in the leaves. Notably, *Morus alba* mulberry leaves from China, as highlighted by Lim and Choi [209], Mahboubi [210], and Wan et al. [211], are rich in nutrients such as mineral elements, proteins, amino acids, fatty acids, and rare bioactive compounds like phenols, alkaloids, flavonoids, and polysaccharides. These properties have made mulberry tea and vegetables highly valued in ancient China. However, mulberry plants are vulnerable to heavy metal contamination through improper irrigation, contaminated soil, and fertilization [211].

LIBS has also been applied to analyze potassium, lead, and manganese concentrations in *Capsicum annuum* L. leaves [60]. Additionally, Krystofova et al. [95] studied the application of LIBS in plant tissues, mapping the spatial distribution of lead and magnesium in sunflower leaves. They achieved high-resolution spatial mapping of these elements on a 4.5 × 2 mm^2 surface area of a sunflower leaf. Figure 17 displays a LIBS spectrum generated using a single laser pulse, where the presence of lead and magnesium is evident within a specific wavelength range. The researchers identified the Mg (I) analytical line at a wavelength of 277.98 nm, as detector saturation prevented the selection of other magnesium emission lines.

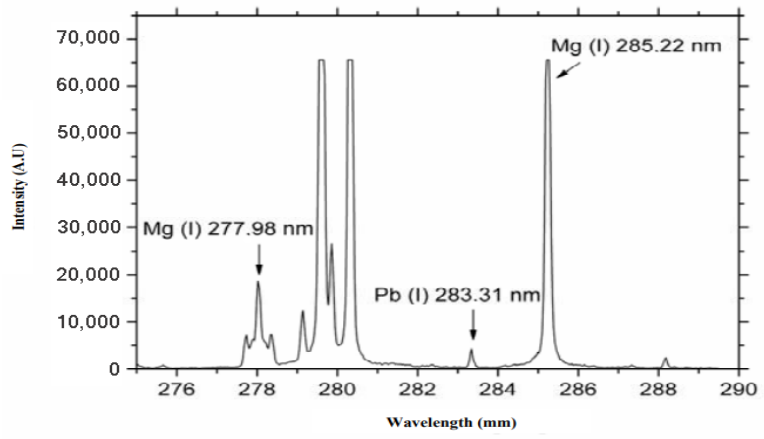

Figure 17. A LIBS spectrum after irradiation of one laser beam to a sample of sunflower leaf subjected to 0.5 mM Pb-EDTA for 3 days. Reproduced from Ref. [95] with permission of Multidisciplinary Digital Publishing Institute.

Singh et al. [133] carried out a speedy and precise analysis of lithium elements and their distribution in leaves of a plant. Their study found that lithium dioxide is released through the veins of *Podocarpus macrophylla* leaves. Their study reported that lithium dioxide was transported through the leaf veins of Podocarpus macrophylla. This also

demonstrated that the xylem carries plant toxins, and that the structural features of the leaf vein were well worth exploring and mapping. The results suggested that plants can effectively manage the flux of lithium into their leaves.

Moreover, Zheng et al. [212], conducted a study using LIBS, and analyzed samples of *Coptidis* (a traditional Chinese medicinal plant) to determine the concentration of heavy metal elements like copper and lead. Since *Coptidis* is commonly affected by heavy metals from irrigation, it is essential to consider possible contamination.

Additionally, Fatima et al. [213] selectively studied ten plant species from the Poaceae family using LIBS. Their findings revealed the presence of essential nutrient elements like K, Mg, Ca, Na, and Fe, alongside toxic elements like Al, Ti, Sr, Ba, Si, Ar, Cs, and Li. The intensity of these elements was particularly higher in species such as *Imperata cylindrica*, *Dichanthium annulatum*, *Sorghum halepense*, *Eleusine indica*, and *Oxalis compressa*.

Martin et al. [75] successfully utilized LIBS to detect carbon in various soil types. They also examined chemical compounds associated with annual growth in tree rings and identified elements in forensic samples. The forensic samples analyzed in their study included two cremated ash samples from a Georgia mortuary. Figure 18 presents the LIBS spectrum for these samples. Figure 18a highlights lead elements, which are more concentrated in one of the samples, Figure 18b displays copper elements, with higher concentrations in one sample, and Figure 18c shows both lead and copper elements, which are more prevalent in a single sample.

The study concluded that LIBS is a valuable technique for detecting various elements, with applications spanning environmental studies, forensic medicine, and beyond.

4.5. Plant Disease Diagnosis

Plant losses caused by different crop diseases from pathogens, including viruses, fungi, and bacteria, continue to be an obstacle in sustainable agriculture, everywhere in the world. Improved diagnostics and control measures for disease are also needed to mitigate damage through the growing season, harvest, and postharvest phases to maximize agricultural yield and sustainability [214]. Plant disease symptoms often appear late in the season than other issues, especially when looking at symptoms after pollination, and may appear in different forms to affect various organs of the plants. Among these, foliar diseases—those that exhibit symptoms on leaves—are distinctive and can often be diagnosed through visual inspection by experienced plant pathologists. Notably, up to 50% of yield losses are attributed to fungal infections [215]. Infectious plant diseases caused by fungi, bacteria, or viruses can range in severity from minor leaf or fruit damage to plant death.

Accurate identification and detection of causative pathogens are essential steps toward managing newly emerging plant diseases. For those with considerable knowledge and expertise in disease diagnosis and plant pathogen isolation, detecting pathogens in symptomatic plants can be a relatively easy. Over the past decade, many types of plant disease, and notably crop diseases affecting specific products such as soybean, citrus, and tobacco, have been detected early using LIBS with great success. LIBS has demonstrated a universal ability to detect a great diversity of microorganisms on surfaces, including molds, bacteria, spores, yeasts, and viruses causing diseases [86,181,214–217]. The application of LIBS-based probes has significantly contributed to the successful detection of microorganisms in agriculture.

In a pioneering study, Pereira et al. [86] employed LIBS in combination with SIMCA to evaluate the organic and inorganic signal profiles of citrus leaves, both healthy and those inoculated with *Candidatus Liberibacter asiaticus* (CLas) bacteria, without prior sample pretreatment. Their findings demonstrated that citrus samples could be classified with 97% accuracy within the first month following inoculation [39]. Similarly, Singh et al. [45]

effectively utilized LIBS to identify intra- and inter-site soil quality differences among various mining sites, exploring its utility in diagnosing microbes responsible for significant agricultural and environmental diseases.

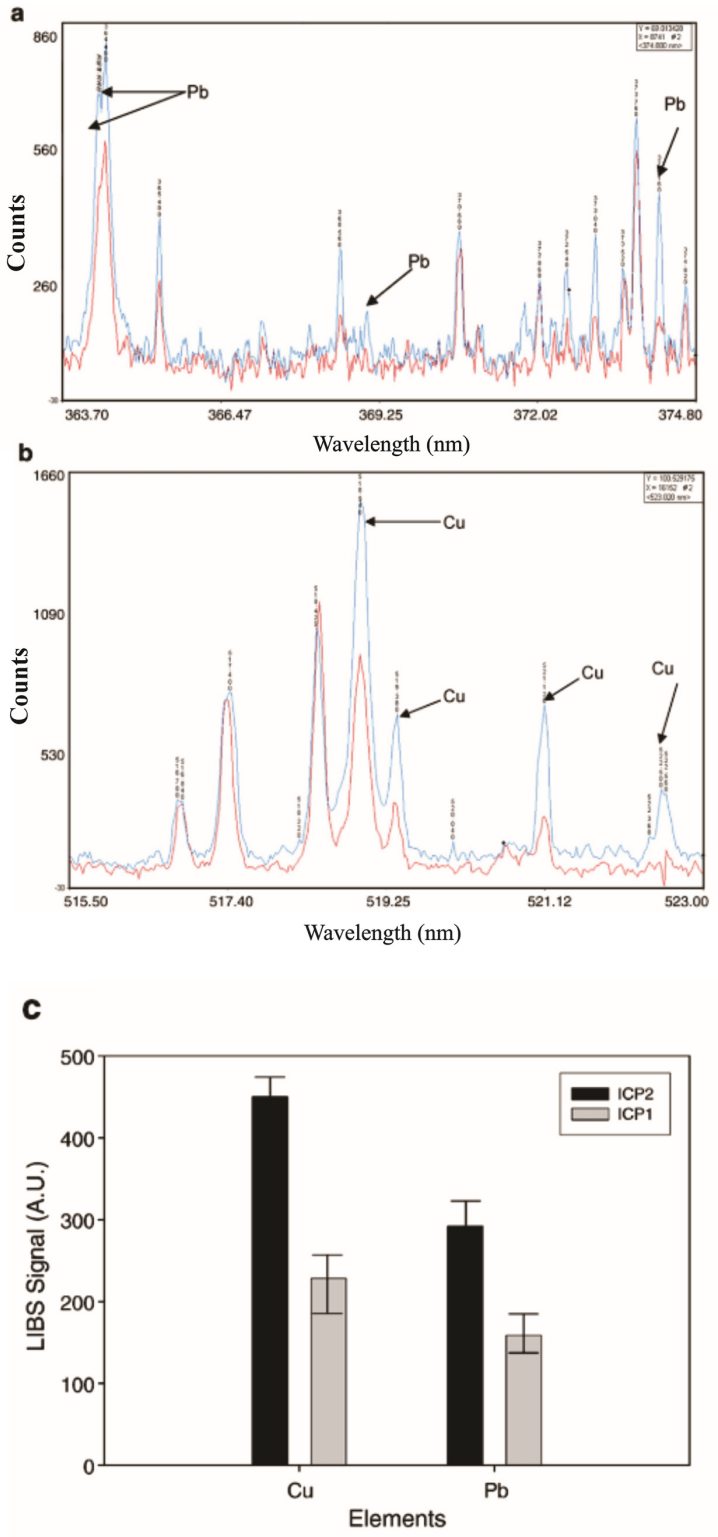

Figure 18. (**a**) LIBS spectral emission for two cremation targets with higher Pb content in one of the samples. (**b**) LIBS spectral emissions for two cremation targets with a more significant amount of Cu in one species. (**c**) LIBS spectral emissions of two cremation species having twice the amount of Pb, and Cu elements. Here, samples are labeled with ICP1, and ICP2. Moreover, #2 refers to sample 2. Reproduced from Ref. [75] with permission of Elsevier.

Sharma et al. [218] successfully combined FTIR, LIBS, and WDXRF spectroscopy to evaluate chemical and elemental changes in papaya plants affected by gall nematodes. They revealed that diseased papaya samples contained higher levels of Mg, Si, Ca, and Al compared to healthy plants, while healthy samples exhibited stronger Na spectral lines and lower nitrogen contents than diseased plants. Such insights into the interactions between mineral nutrients, diseases, and host plants can inform strategies for disease prevention, crop quality enhancement, and yield improvement.

Peng et al. [219] proposed a novel LIBS-based method for distinguishing tobaccos infected with the tobacco mosaic virus (TMV). Spectral analysis was conducted on both fresh leaves and dried leaf pellets. Classification models based on the full spectrum and observed emission lines were developed using partial least-squares discriminant analysis (PLS-DA). In their study, Principal component analysis (PCA) was implemented to visualize symptom distribution, while PLS-DA and support vector machines (SVM) were utilized for quantitative classification. They also studied the effects of moisture content on signal stability, spectral line profiles, and plasma characteristics (temperature and electron density). It was shown that the SVM significantly increased classification results and reduced the impact of moisture content on the classification accuracy and mitigated the effects of moisture content. Finally, Table 7 summarizes various plant diseases and the elements identified, along with the corresponding references.

Table 7. A summary of different diseases identified by LIBS.

Investigated Plant	Diseased Type	Elements Studied	References
Oilseed rape (L.)	Sclerotinia stem rot (SSR)	C, Ca, Na, K	[220]
Tomato	Root Knot Nematode (RKN)	C, Mg	[221]
Tobacco	Cymbidium Ringspot Virus	C, Mg	[221]
Citrus leaves	Huanglongbing, Citrus canker	Fe, Mn, Mg, Zn	[222]
Black tea (*Camellia sinensis*) leaves	-	Fe, Mn, Na, P, Ca, Al, Zn, Cr, Cu, Mn, Ni, Pb	[223]
Citrus	Candidatus Liberibacter asiaticus (CLas) and Citrus tristeza virus (CTV)	C, H, O, Ca, K, N, Cl, Mg, S, Fe, Mn, Ma, Na, Ni, Zn	[86]
Soybean	Green stem and foliar retention (GSFR)	Ca, K, Mg	[223]
Camellia oleifera leaves	Anthracnose	Mn, Ca, Al, Fe	[224]
Citrus leaves	Huanglongbing (HLB)	Ca, Mg, K	[217]
Papaya	Nematode-infested	Mg, Si, Al, Ca, Na, K, N, O, C, Na, Zn, Fe, Ti, Cr, Mn, Cu, Cl	[218]
rice plant	The infection caused by false smut	Ca, Mg, Si, Cu, Fe	[225]
Tobacco leaves	Tobacco mosaic virus (TMV)	C, Mg, Ca, N, H, K, O	[219]
Camellia oleifera industry	Anthracnose of *Camellia oleifera*	Mn, Ca, Ca II, Fe	[224]
Ber fruits	Agrobacterium tumefaciens (*Ziziphus mauritiana*)	Ca, K, Si, Mn, Na, increasing trends of Mg	[226]
Citrus	Huanglongbing (HLB)	Ca, Zn, K	[227]
wheat (*Triticum aestivum*)	fungal infection	Ca, Mg, Si, Fe, Na, K, C, H, O, N	[124]
navel orange	Huanglongbing (HLB)	K, Ca, Mg, Fe, Mn, Cu, P	[228]

Table 7. *Cont.*

Investigated Plant	Diseased Type	Elements Studied	References
Fresh fruit (Citrus)	**Huanglongbing (HLB)**	**Ca, Zn, K**	[229]
Gannan navel oranges	**Huanglongbing (HLB)**	**Ca, Na, Mg, K, C, H, O**	[230]
Mulberry fruit	**thiophanate-methyl**	**Fe, Cs, Th, Sr**	[231]
R. officinale	**toxic metals**	**Ca, K, Mg**	[118]
Citrus	**Huanlongbing (HLB)**	**Ca, Na, N, H, Fe**	[232]

5. New Approaches to LIBS Plant Analysis

5.1. Calibration-Free LIBS

Different methods can be used for the quantitative compositional analysis of plant samples.

The use of data analysis methods such as CF-LIBS has been proposed as a future perspective to improve the accuracy and reliability of LIBS in plant analysis [150,233–236]. CF-LIBS can be performed to quantify elemental concentration in situations where it is challenging to create a calibration dataset. In the CF-LIBS approach a Boltzmann plot is built parameterizing the measured line intensity according to the Boltzmann equation, which is valid in LTE condition as [237,238]:

$$\overline{I_{ij}} = FC^s A_{ij} \frac{g_i e^{-\frac{E_i}{kT}}}{U^s(T)} \quad (1)$$

Here, $\overline{I_{ij}}$ indicates the measured integral line signal (counts), and C_s is the concentration of the radiating species inside the plasma. F is the experimental constant that considers the optical performance of the collecting system, as well as all plasma concentrations and their volume. In Equation (1), the spectroscopic transition parameters A_{ij}, g_i, and E_i are obtained from spectral databases, but F, C_s, and T values must be experimentally evaluated. The partition function of each species $U^s(T)$ is calculated from the specified spectroscopic value when the plasma temperature is known as:

$$U^s(T) = \sum g_k exp\left(\frac{-E_k}{K_B T}\right) \quad (2)$$

By considering the relations [239]

$$y = ln\frac{\overline{I_{ij}}}{g_i A_{ij}} \quad (3)$$

$$x = E_i \quad (4)$$

$$m = -\frac{1}{k_B T} \quad (5)$$

$$q^s = ln\frac{C^s F}{U^s(T)} \quad (6)$$

and taking the logarithms of both sides, Equation (1) can be reformulated in a linear form as [239]:

$$y = mx + q^s \quad (7)$$

A similar relation can be considered for all the species in the plasma: utilizing Equations (3)–(6), the intensity of each experimental LIBS spectral line can be represented as a point in the Boltzmann plot. Therefore, all the points corresponding to spectrum lines

emitted by the same species will be disposed in parallel lines of slope m on the Boltzmann plot, each of them with intercept q_s which depends on the species. The determination of the slope m allows the determination of the plasma electron temperature, since $m = -\frac{1}{k_B T}$; at the same time, the intercept q_s is related to the logarithm of the species concentration multiplied by the experimental factor F, which considers the detection system efficiency.

For calculating the unknown experimental parameter F, according to Equation (6) one can use the determined concentration of an internal standard, if this information is accessible. Otherwise, the normalization relation can be employed as [238]:

$$\sum_e C^s = \frac{1}{F} \sum_s U^s(T) \times exp(q^s) = 100\% \tag{8}$$

because the summation of the relative concentrations of whole elements must be equal to unity.

After that, the number density of each species can be obtained as [238]:

$$C^s = \frac{U^s(T)\ exp(q^s)}{F} \tag{9}$$

where all the factors are measured or calculated.

The number density of one element is the sum of the concentrations of its neutral and single ionized species:

$$C_{el} = C^I + C^{II} \tag{10}$$

In LIBS analysis, higher ionization states can be disregarded because the concentration of twice-ionized species is usually negligible.

When the total number densities of all the elements are obtained, the weight percentage composition is given by the relation [29]:

$$C_{el}(\%) = \frac{\text{Weight composition of one element}}{\text{Net weight composition of all the elements}} \times 100 \tag{11}$$

The relative mass fraction N_a^m of element a can thus be calculated as [235]:

$$N_a^m = \frac{\left(C_a^I + C_a^{II}\right) M_a}{\sum_s C^s M_s} \tag{12}$$

here, M_a is the atomic mass related to the element a, and the sum is done on all of the elements in the plasma.

Aldakheel et al. measured the elemental composition of Senna leaves [155] exploiting the Boltzmann equation [46,131], too.

Muhammad Aslam Khoso et al. [240] used LIBS to perform elemental and comparative analyses of soils from wheat, corn, rice, and okra fields. They collected soil samples from agricultural fields in the southern Sindh province of Pakistan. The emitted spectrum of the corn sample, shown in Figure 19, was obtained within the wavelength range of 200 to 720 nm at two depths: three inches and six inches. Their analysis revealed that elements such as Fe, Si, Mg, Ca, Al, Ba, Hg, Cr, Ni, Mn, H, Cu, Li, Sr, K, Ti, Na, Pb, V, and C were present in all the soil samples. Using a CF-LIBS method, they determined the elemental compositions of various samples.

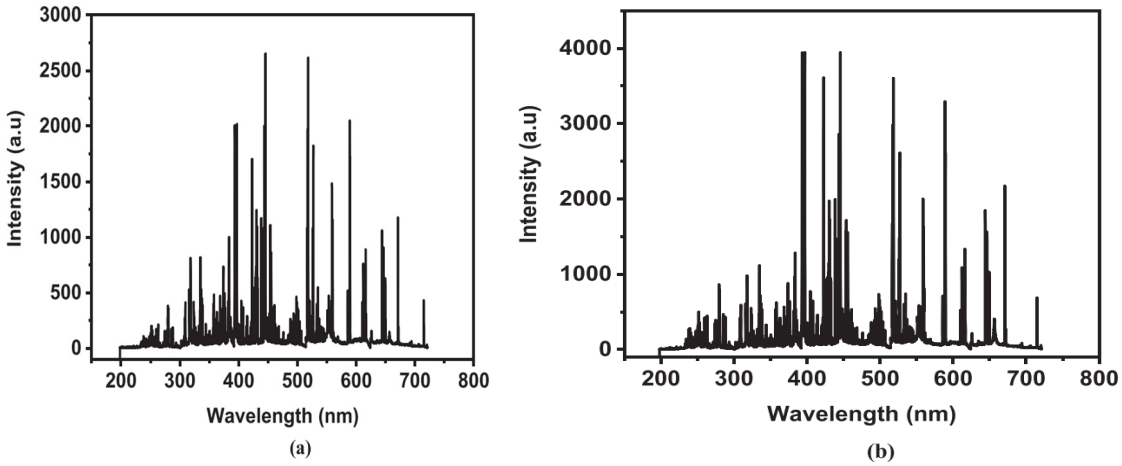

Figure 19. The LIBS spectral emissions of the soil of a corn field in the 200–720 nm wavelength range, at a depth of 3 inches (**a**) and a depth of 6 inches (**b**). Reproduced from Ref. [240] with permission of Elsevier.

Figure 20 compares the weight percentages of elements in soils from cultivated fields (wheat, corn, rice, and okra) at two depths, 3 inches and 6 inches. The detected elements varied with soil depth and were associated with different crops, providing valuable insights into the elemental composition of the samples. Their results at different depths are summarized in Table 8.

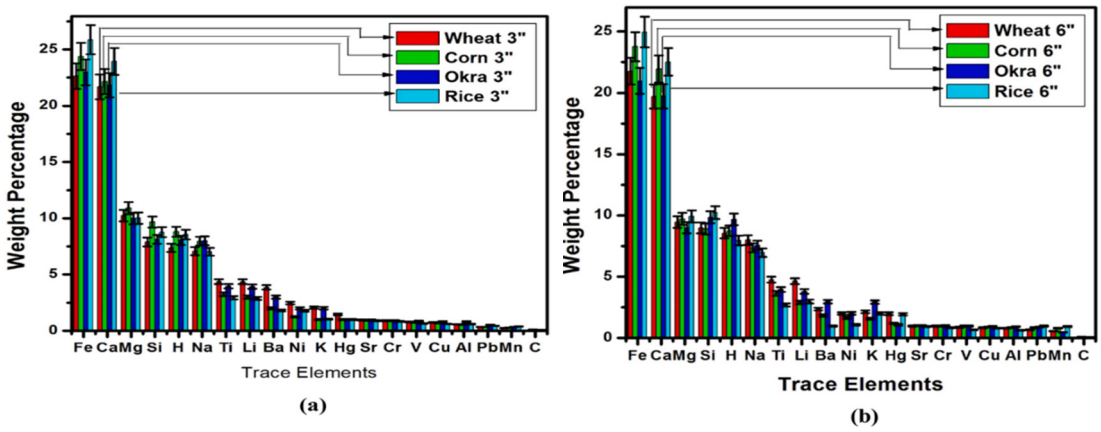

Figure 20. The weight percentage of main elements in the soil at a depth of 3 inches (**a**) and 6 inches (**b**). Reproduced from Ref. [240] with permission of Elsevier.

Table 8. The weight percentage of main elements in rice, okra, wheat, and corn at three and six inches [240].

Nutrient	Fe		K		Cr		Mg	
	3 in.	6 in.	3 in.	6 in.	3 in.	6 in.	3 in.	6 in.
Wheat (%)	22.63	21.77	2.05	2.14	0.90	0.98	10.24	9.45
Corn (%)	24.38	23.77	1.01	1.56	0.89	0.98	10.90	9.72
Okra (%)	22.97	20.98	2.01	2.93	0.89	0.99	9.98	8.99
Rice (%)	25.87	24.96	1.02	1.99	0.83	0.84	10.01	9.92

In the study conducted by Borduchi et al. [151], LIBS was used for comparative elemental analysis of soil samples from wheat, rice, corn, and okra fields. The Boltzmann plot method was employed to measure the electron temperature (T_e), while the Stark broadening profile method was used to determine the electron number density (N_e). Additionally,

the calibration-free method was utilized to realize the weight percentage of each element in the corresponding soil samples.

Furthermore, Borduchi et al. [151,241] proposed combining CF-LIBS with OPC to identify nutrients in five different sets of soybean leaf samples, aiming to reduce matrix effects.

The plasma temperature can be determined using the Boltzmann plot method based on the relative intensities of spectral lines, provided the transition probabilities (A_{ki}) of specific excited states are available [159,240–242]. To enhance the accuracy of temperature measurements, multiple spectral lines must be considered simultaneously in the Boltzmann plot [63].

Trevizan et al. [63] measured the macronutrients P, K, Ca, and Mg in pellets made from plant reference materials. Their study showed that most of the results obtained from LIBS analysis of plant samples were in good agreement with those measured by ICP-OES following wet acid decomposition.

The relative intensity of the spectral lines of specified excited states represents the relative population of the upper energy levels and can be used to evaluate the excitation temperature. Jabbar et al. [149] applied the Boltzmann equation to determine the excitation temperature of plasma generated on the surfaces of root, soil, and shoot samples within the presence of an external electric field.

Figure 21 represents the Boltzmann plots of the root sample with and without electric field irradiation. The temperatures for the soil, root, and shoot samples in condition of without the external electric field were calculated to be 7500 K, 10,000 K, and 8000 K, respectively. These values increased to 8300 K, 12,000 K, and 10,000 K under electric field-assisted LIBS.

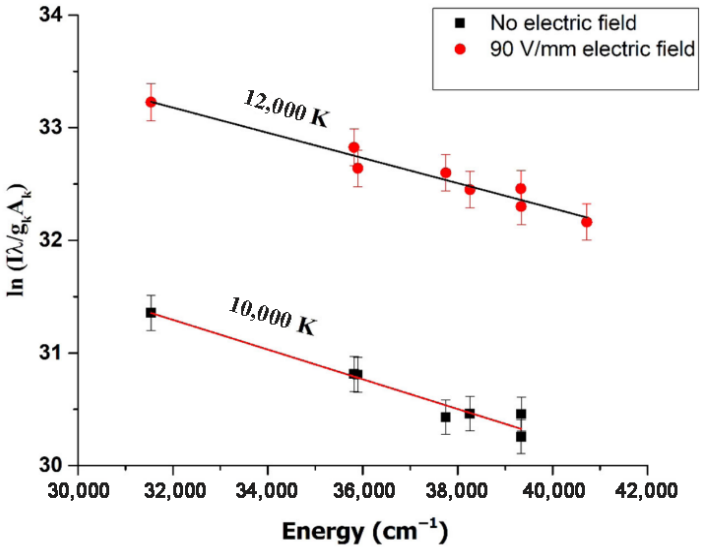

Figure 21. Electron temperature estimation by Boltzmann plot of the Ca I spectral lines obtained in ambient air utilizing a laser beam of 532 nm wavelength, at a 2 μs delay time, with and without a 90 V/mm electric field. Reproduced from Ref. [149] with permission of Taylor & Francis.

Moreover, the ionized species' concentration was calculated using the Saha–Boltzmann equation [34,46]:

$$n_e \frac{C_s^{II}}{C_s^{I}} = 6.04 \times 10^{21} T^{3/2} \frac{U^{II}(T)}{U^{I}(T)} \exp\left(\frac{-E_{\text{ion}}}{kT}\right) \quad (13)$$

The above equation links the concentration ratio of the neutral and singly ionized species of an element. Moreover, Khoso et al. [243] investigated the application of LIBS for rapid and precise elemental analysis of soil samples. By employing a Q-switched Nd:YAG

laser at 1064 nm, their study identified elements such as Fe, Ca, Ti, Si, Al, Mg, and Pb through their distinct spectroscopic fingerprints. The research also examined plasma dynamics, determining electron temperature (14,611 K) and electron number density (4.1×10^{16} cm^{-3}) using Boltzmann's plot and Stark broadening methods, respectively. Their work proposed LIBS as a capable analysis tool for soil composition, offering a valuable framework for surveillance in the environment and agriculture. Additionally, Díaz Pace et al. [29], employed for the first time LIBS to study the extractability of macronutrients, i.e., Mg, Ca, Na, and K, in industrial yerba mate plants. The infusion process was simulated in the lab using powdered leaf material samples. The authors considered the relative percentage reached into water in the infusion as the extractability E_α (%) of element α [29]:

$$E_\alpha = \left(1 - \frac{I^z_{\alpha,f}}{I^z_{\alpha,i}}\right) \times 100 \tag{14}$$

where $I^z_{\alpha,i}$ and $I^z_{\alpha,f}$ are the related integral spectral intensities. The background-subtracted intensities are related to the element's concentration using the Boltzmann equation [29].

A. Alrebdi et al. [141] also studied the composition of Peganum harmala seed samples using the CF-LIBS approach. The excitation temperature was calculated from the Saha-Boltzmann-plot method, which considers numerous spectral emission lines of both ionic and atomic lines according to the relation [63]:

$$\ln\left(\frac{I_1}{g_1}\frac{\lambda_1}{A_1}\right)^* = \ln\left(\frac{I_1}{g_1}\frac{\lambda_1}{A_1}\right) - \ln\left(6.04 \times 10^{21} \times \frac{T^{\frac{3}{2}}}{n_e}\right) \tag{15}$$

The authors employed the relation between Stark width and plasma electron number density for the calculation of n_e as follows [244]:

$$n_e\left(\mathrm{cm}^{-3}\right) = \frac{\Delta\lambda_{\frac{1}{2}}(FWHM)}{2\omega_s(\lambda, T)} \times 10^{16} \tag{16}$$

where ω_s indicates the Stark broadening coefficient, n_e represents the plasma electron number density, and T denotes the electron temperature. Figure 22 illustrates the Saha-Boltzmann plot gained from the Ca (I) and Ca (II) emission lines.

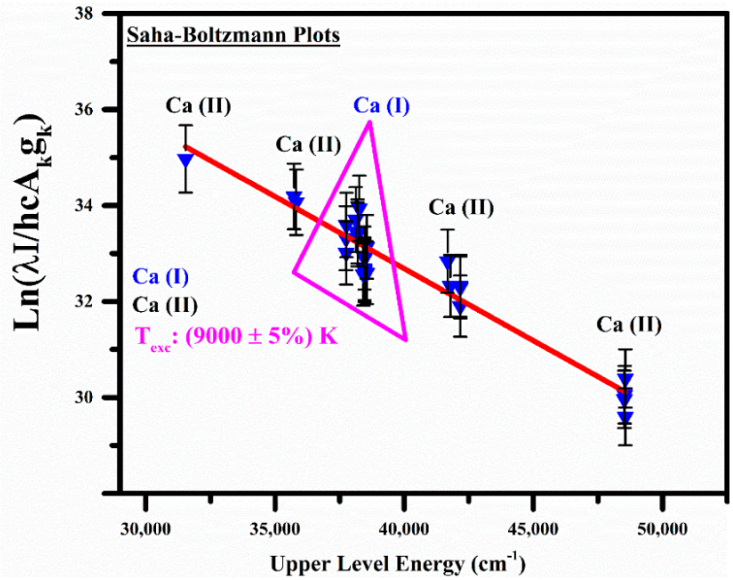

Figure 22. Saha-Boltzmann plots with Ca (I) and Ca (II) emission lines. Reproduced from Ref. [141] with permission of Multidisciplinary Digital Publishing Institute.

Qasim et al. [245] utilized CF-LIBS to analyze the plant's composition using self-absorption corrected line intensities. The comparison of the results with the data extracted by applying ICP-MS analysis indicated that the theoretical model's results at lower pressures were in good agreement. Generally, self-absorption might cause errors in quantitative analysis due to the decrease in line intensity or even the appearance of a dip at the emission peak (self-reversal). A self-absorption (SA) parameter can be defined as:

$$\mathrm{SA_{int}} = \frac{I^{ji}}{\widehat{I}_{ji}} \tag{17}$$

where I^{ji} is the measured integral intensity and $\widehat{I}_{ji}$ is the line intensity that would have been measured if self-absorption effects had been negligible [245].

The SA parameter may vary from 0 to 1, where a smaller SA value corresponds to stronger self-absorption [246].

The self-absorption parameter can be experimentally evaluated as follows:

$$\mathrm{SA_{int}} = \frac{I^{ji} A_{mn} g_m}{I_R^{mn} A_{ji} g_j} exp\left(\frac{E_j - E_m}{k_B T}\right) \tag{18}$$

where A_{ji}, E_j, and g_j are the transition probability, energy, and statistical weight of the emission line, respectively, while k_B is the Boltzmann constant and T is the plasma electron temperature. I_R^{mn}, A_{mn}, and g_m are the measured spectral emission integral intensity, transition probability, and statistical weight of a non-self-absorbed spectral line emitted by an internal reference element with upper level energy E_m.

The self-absorption corrected intensity $\widehat{I}_{ji}$ can be calculated from the SA parameter without the knowledge of the line intensity I^{ji} from Equation (17) [247–250]:

$$\widehat{I}_{ji} = \frac{I^{ji}}{\mathrm{SA_{int}}} \tag{19}$$

5.2. Chemometrics

Nowadays, LIBS combined with chemometric methods is widely used in many applications, although multivariate analysis often requires substantial computational effort and prior chemometric knowledge [125]. Even though LIBS is still constrained by its direct spatial determination, sensitivity, and spatially resolved measurement, advances have been made to overcome these challenges.

Chemometrics integrated with LIBS has a very significant role in plant analysis as it provides deep insights and better interpretation of the experimental results [33]. Moreover, by combining LIBS with multivariate regression models, researchers accurately detected pesticide residues [129]. The resulting 3D LIBS maps showed a clear trend of decreasing pesticide residues with leaf depth. This marked the first instance of in situ and in vivo elemental imaging of plants using LIBS. The reported spatial resolution was 200 µm, which is lower than the resolution achievable with conventional techniques like synchrotron radiation XRF (SRXRF) and secondary ion mass spectrometry.

In 2018, Ponce et al. [232] employed LIBS with principal component analysis (PCA) to classify six *Citrus* varieties, including Macrophylla, Valencia orange, Sugar Belle, Ray Ruby grapefruit, Meyer lemon, and Murcott honey. PCA of the LIBS data achieved high accuracy (~90%) in distinguishing healthy samples from those infected with HLB (Huanglongbing). This study demonstrated that LIBS combined with chemometric methods is a rapid, economical, and effective tool for identifying HLB-infected *Citrus* plants.

Multivariate analysis provides more comprehensive signal information than univariate analysis, making it effective in resolving matrix effects and mitigating shot-to-shot

fluctuation issues. It is also seen to give a quantitative analysis despite overlapping spectral lines [30].

Standard multivariate techniques used in LIBS include partial least squares regression (PLSR) [251,252], multivariate linear regression (MLR), support vector machines (SVM) [40], artificial neural networks (ANN) [253], and principal component regression (PCR) [254,255], among others [255–259]. For a more detailed exploration of multivariate analysis in LIBS, readers are encouraged to consult the recent book "Chemometrics and Numerical Methods in LIBS" [260].

In practical terms, chemometrics is predominantly employed for calibration and classification. Moreover, "fingerprint" characteristics of LIBS and the analytical abilities of chemometrics make the combination of chemometric methods and LIBS a unique approach to discrimination [257]. Typical applications in agriculture include detecting polluted food [91,261,262], classifying soil types [167], conditions under which plants grow [65], and detecting food contamination [109].

As another example, multivariate methods have been used as calibration methods to estimate element concentrations. Some examples of these applications include assessing toxic metals in soils, plants, and food products.

While the benefits of chemometric methods have been proven, some issues remain unresolved. To develop a robust model, it is preferable to use extensive and diversified training samples or incorporate random effects [263]. This approach can significantly improve practical applications and facilitate the development of commercial LIBS systems for agriculture. A deep understanding of chemometrics' capabilities, limitations, and its relationship to the interaction between plasma and samples is also essential. Special attention should be given to addressing overfitting. Due to the large number of wavelengths in LIBS spectra, overfitting can become a significant issue when working with a limited number of samples (tens or hundreds). Therefore, it is recommended to use an appropriate chemometric method that eliminates redundant information (such as noise and irrelevant signals) while retaining the most valuable variables.

For instance, Zhu et al. [264] explored the calorific value and CO_2 emissions of coal at different coalification levels to improve efficiency and decrease emissions in coal-fired power plants. They boosted partial least squares regression (PLSR) by integrating a dual-cycle variable selection mechanism with competitive adaptive reweighted sampling to improve the accuracy of LIBS.

Their methods turned out very useful for estimating elemental and fixed carbon, almost improved the coefficients of determination (R^2) and errors. Their work showed the promise of using LIBS as a real-time measurement tool for coal-fired power plants and for producing cleaner and more efficient energy. In addition, Cai et al. applied a novel technique involving laser induced breakdown spectroscopy and machine learning methods for precise soil contamination detection, while measuring its contribution to the contamination of the crops. Their methods turned out to be very useful for estimating elemental and fixed carbon and improved the coefficients of determination (R^2) and errors. Their work showed the promise of using LIBS as a real-time measurement tool for coal-fired power plants and for producing cleaner and more sustainable energy. Additionally, Cai et al. [265] introduced a new technique using LIBS and machine learning models to detect soil contamination accurately, including calculating its contribution to the contamination of the crops. The study analyzed the uptake of heavy metals in the garlic crops grown in contaminated soil. They found that metals had different distributions in different parts of the plant. Soil classification using LIBS improved the trace-back of contaminated garlic to the soil sampling point. This method has been brought to the forefront as LIBS is an effective tool to monitor agricultural pollution and provide food safety.

In addition, Babos et al. [170] examined the application of LIBS in precision agriculture to rapidly evaluate soil fertility. Multivariate calibration models were developed to predict essential soil properties, exhibiting robust performance across various agricultural conditions. They indicated that Principal Component Analysis (PCA) enabled soil classification by differentiating between fertile and less fertile soils. Furthermore, their study brought to light LIBS as a quick and precise method for quantifying soil heterogeneity without employing complicated extraction methodologies.

5.3. Nanoparticle Enhanced LIBS

In 2013, a new method to increase signal intensity was first introduced, called nanoparticle-enhanced LIBS (NELIBS), by De Giacomo et al. [146]. This method demonstrated signal enhancement of 1–2 orders of magnitude. The fundamental principle of NELIBS [266] lies in improving ablation efficiency by lowering the material's ablation threshold. This is attained by using multiple ignition points and instantly releasing electrons. The signal can increase significantly by dropping a colloidal solution; however, the increase is relative to the type of substrate. For instance, signal intensity improvements of 1–2 orders of magnitude have been observed for metals, while no significant enhancement was recorded for insulators, such as basalt minerals, soil samples, and Teflon pellets [146]. This lack of enhancement for insulators is attributed to their high ablation thresholds. Further research is necessary to understand the effects of NELIBS on various sample types fully and to elucidate the laser-nanoparticle interaction process [30].

Nanoparticles are widely applied across numerous fields. However, their potentially harmful effects on organisms across all trophic levels of the environment must be estimated precisely. Several limited, detailed descriptions of the routine of nanoparticle spread in plants are available; this suggests the application of new analytical techniques to determine their precise spatial distribution. The requirement for large-scale imaging of entire model organisms further compounds this need. To the best of the authors' knowledge, LIBS has rarely been employed to detect nanoparticles in biological matrices, particularly in plants [267].

In recent years, LIBS has been used to investigate the distribution of nanoparticles such as Ag nanoparticles [131], CdTe nanoparticles [132], and photon-upconversion nanoparticles [125] in terrestrial plants (*Vicia faba*, *Raphanus sativus*) and aquatic plants (*Lemna minor*) [33]. The first visualization of nanoparticles in plant tissues using LIBS was published in 2017 by Krajcarová et al. [131]. Their study focused on the roots of *Vicia faba* (commonly known as broad bean) and monitored the distribution and mapping of copper, silver ions, and Ag nanoparticles at specific concentrations. Their findings revealed that Ag nanoparticles could not penetrate the inner root tissues and remained confined to the outermost layer. Furthermore, they also pointed out that concentrations of Ag nanoparticles were an order of magnitude less in the roots of plants cultured in Ag nanoparticle solutions compared to roots on culture on metal ion solutions (Figure 23). They also noted a low uptake rate for Ag nanoparticles, in agreement with previous studies [131,267].

Ohta et al. [268] studied localized surface plasmons (LSPs) and their effect on LIBS, particularly focusing on the emission enhancement effect of metallic particles attributed to localized surface plasmon resonance during the analysis of plant nutrients. Generally, there are two types of plasmonic excitations: surface plasmons (SPs) and localized surface plasmons (LSPs) [269].

In their experiments, they used a Q-switched Nd:YAG laser with an energy output of 0.3 mJ to monitor plant nutrients in *Citrus unshiu* and *Rhododendron obtusum*. For example, Figure 24 illustrates the distribution of *Citrus unshiu* after drying with a heater, while Figure 25 shows the emission spectrum of *Rhododendron obtusum* after applying silver

colloidal particles to its leaf surface. Gold and Ag nanoparticles were utilized in the leaves to increase plasma radiation. This approach assisted the detection and monitoring of plant nutrients using low-energy LIBS without draining the leaves before laser irradiation.

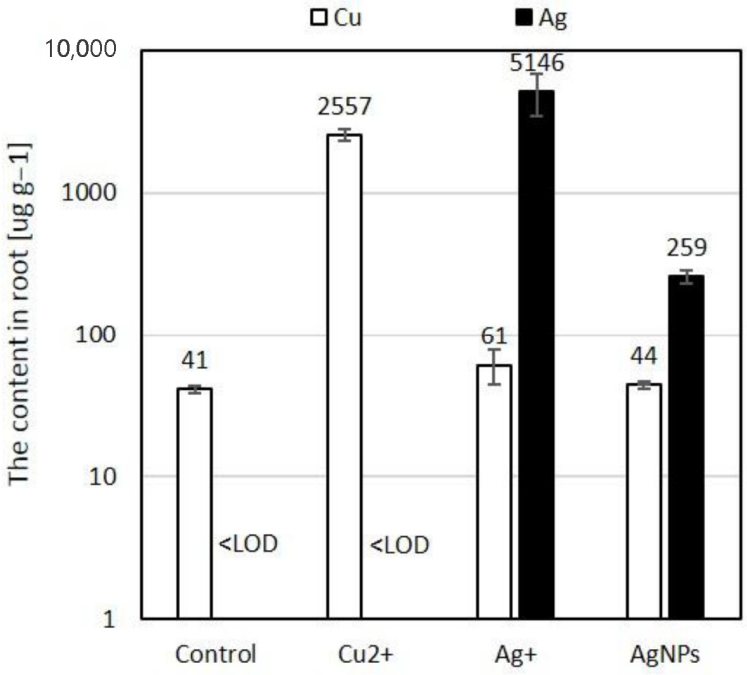

Figure 23. The amount of Ag, and Cu in *Vicia faba* root (dry weight), after passing seven days of cultivation in distilled water (control group), 10 µmol L^{-1} Cu^{2+}, Ag^{+}, and Ag nanoparticle solutions. Reproduced from Ref. [131] with permission of Elsevier.

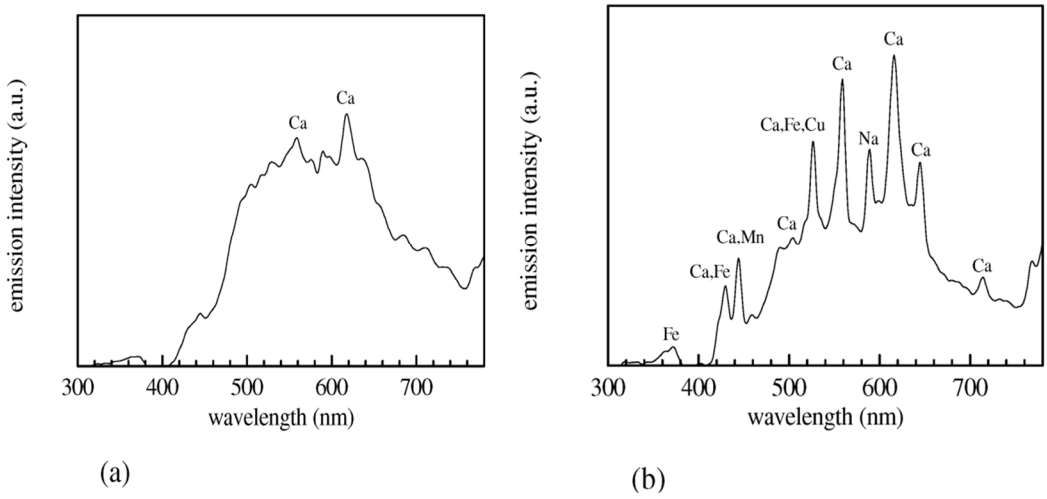

Figure 24. Spectral emission of *Citrus unshiu* post desiccation with a heater (**a**) 3 min, and (**b**) 5 min. Reproduced from Ref. [268] with permission of Optica publishing group.

Additionally, they investigated the influence of metallic particle size and material composition on LSP effects. Their results showed a major improvement in terms of plasma emission when silver particles were used. They also found that the distribution, size and material of the metallic particles had a significant impact on the enhancement factor.

In the study performed by Singh [33], the significant role of medicinal plants and the analysis of their elements in the future potential of LIBS in the fields of medicine and food were discussed. A comprehensive review of recent developments in this area, including

technical progress and recent works related to the identification of nanoparticles in plant samples, was also presented.

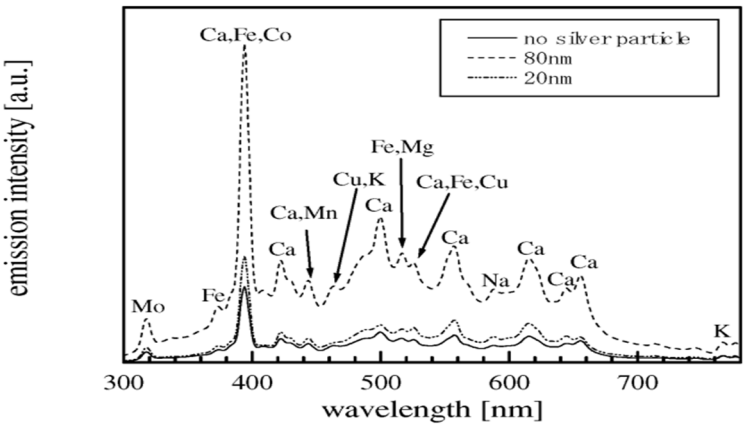

Figure 25. Spectral emission of *Rhododendron obtusum* using silver colloidal nanoparticles injected into the leaf. Reproduced from Ref. [268] with permission of Optica publishing group.

Modlitbová et al. [132] studied the toxicity assessment of two distinct forms of cadmium, namely $CdCl_2$ and Cd-based quantum dots (QDs), on the freshwater model plant *Lemna minor* L. They investigated cadmium telluride QDs capped with two coating ligands: glutathione (GSH) and 3-mercaptopropionic acid (MPA). Their results indicated that GSH- and MPA-capped Cd-based QDs exhibited comparable toxicity towards *Lemna minor* L., although they were considerably less toxic than $CdCl_2$. Nevertheless, in *L. minor* fronds, both Cd sources led to similar trends in Cd distribution and bioaccumulation.

Navarro et al. [270] investigated the uptake of water-dispersible CdSe/ZnS quantum dots (QDs) in the plant *Arabidopsis thaliana*. Their results demonstrated that *Arabidopsis* plants exposed to QDs dispersed in Hoagland's solution for 1–7 days did not internalize intact QDs. Inductively coupled plasma mass spectrometry analysis of Cd and Se concentrations in roots and leaves revealed that Cd and Se from QD-treated plants remained in the *Arabidopsis* root system and were not translocated to the leaves. Furthermore, fluorescence microscopy provided evidence that the QDs were primarily located on the exterior surfaces of the roots; the authors also observed that the QDs absorption depended on their stability in suspension.

Despite its potential, LIBS has been employed by only a small number of studies to image chemical elements in biotic tissues [270,271]. For instance, one study utilized the LipsImag device to analyze the in situ distribution of the pesticide chlorpyrifos using P and Cl imaging in *Zea mays* leaf samples [129]. Additionally, the study applied NELIBS to investigate *Allium schoenoprasum* plant samples in the laboratory [136].

6. Discussion

6.1. Comparison of LIBS with Other Techniques

The accuracy of LIBS in the quantitative and qualitative analysis of agricultural products can be assessed by comparing it with other methods [272]. For example, M. de Oliveira et al. [273] evaluated LIBS in parallel with near-infrared spectroscopy (NIRS) and considered employing them together for simultaneous multi-elemental identification levels of micro- and macronutrients from vegetable samples, specifically *Brachiaria* forages. The authors note that LIBS frequently produced results that were inadequate due to the complexity of the sample matrix; further, NIRS, while sensitive, did not have an adequate indirect correlation to inorganic elemental content. Nevertheless,

combining LIBS with NIRS markedly improved the detection of inorganic nutrients levels in the *Brachiaria* matrix.

Another study demonstrating the utility and advantages of LIBS was conducted by Kaiser et al. [67]. They analyzed the concentrations of magnesium and lead in lettuce samples using both LIBS and LA-ICP-MS techniques. As shown in Figure 26, the study also compared the two laser-based detection methods and monitored the distribution of lead and magnesium in the tested lettuce samples. The results revealed that the controlled samples exhibited the highest magnesium concentrations in the vein structures, while the samples treated with 0.5 mM Pb-EDTA contained the highest concentrations of lead. Furthermore, in the samples treated with 1 mM Pb-EDTA, lead was distributed more homogeneously throughout the tissue, as confirmed by both LIBS and ICP-MS analyses.

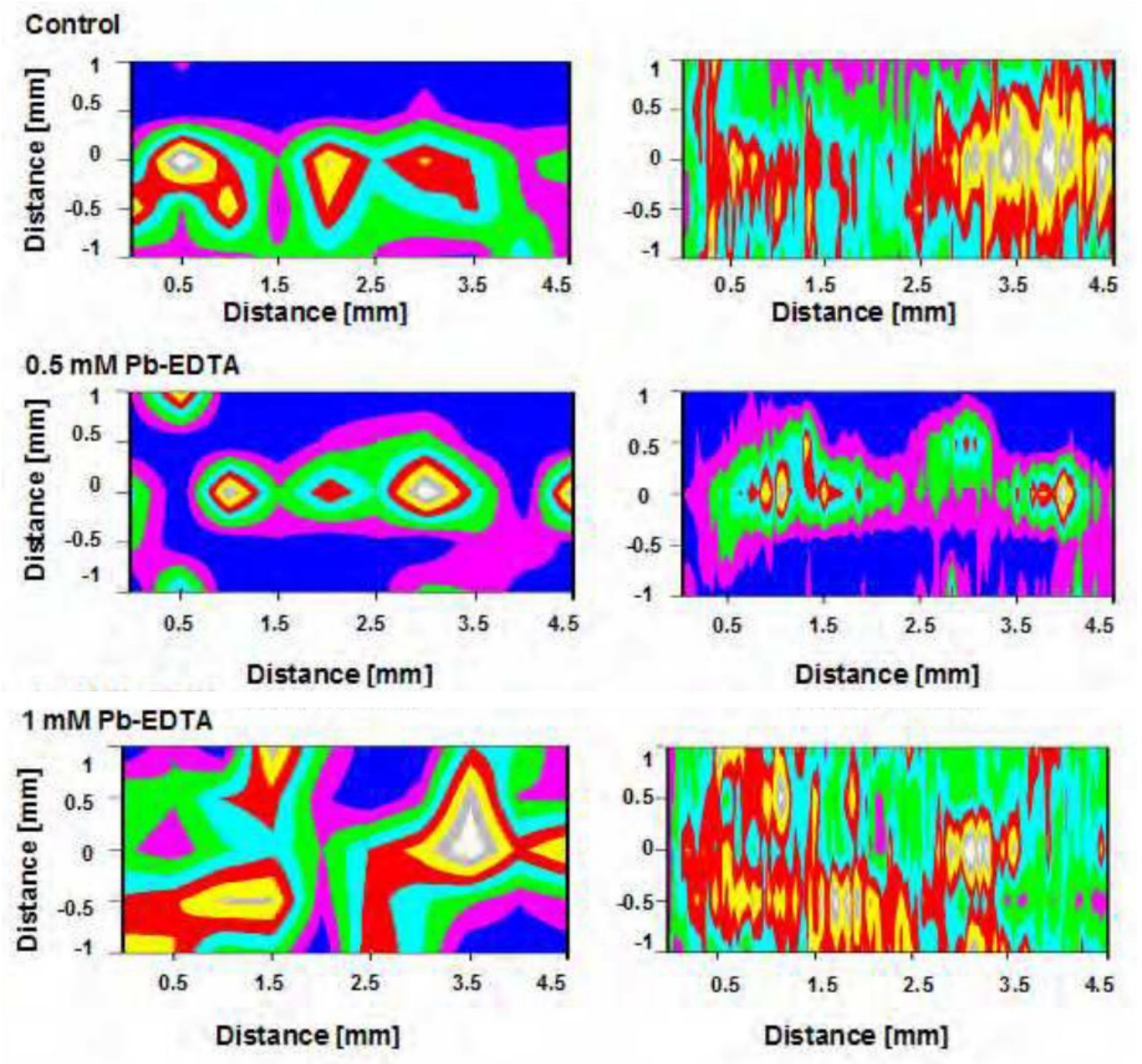

Figure 26. The map showing the diffusion of Mg in the control leaves and Pb in the treated leaf points, attained through LIBS (**left** column) and the LA-ICP-MS method (**right** column). Reproduced from Ref. [67] with permission of Formatex.

In conclusion, the study found that both techniques could assess plant tissue. However, the simplicity of LIBS provided a significant benefit, which could make it very useful for various key in situ applications such as environmental monitoring and remediation. This simplicity, combined with its versatility, highlights LIBS as a promising tool for future agricultural and environmental research advancements.

Monitoring and characterizing macro- and micronutrients in sugarcane leaf samples were carried out by Nunes et al. [82]. In addition to seeking improvements and advancements in the operational conditions of LIBS, the researchers compared the results obtained from LIBS with those from microwave-assisted digestion and ICP-OES analysis [274].

In this study, the authors used a neuro-genetic approach to optimize the operational parameters of LIBS analysis. Neuro-genetic approaches consist of two parts, neural networks and genetic algorithms, which allow us to assess the different operational parameters and optimize LIBS settings. Using these techniques led to the identification of optimal conditions that improved the accuracy of the analysis.

Figure 26 compares the results from the LIBS analysis to the ICP-OES results, in which the ICP-OES results served as reference values. In the case of the LIBS analysis, only the results from PLSR are illustrated. PLSR is a predictive regression method that relies on estimated latent variables and is commonly used to analyze two datasets simultaneously.

The comparison presented in Figure 27 indicates that the results of LIBS analysis are consistent with the reference ICP-OES method. This consistency demonstrates the reliability and accuracy of LIBS when applied as optimized, confirming its potential for high-resolution nutrient analysis in plant tissue.

One of the significant concerns in Brazil regarding soybean cultivation is the plant's susceptibility to green stem and foliar retention (GSFR). A LIBS-based analysis addressing this issue was conducted by Ranulfi et al. [223]. For their experiments, 35 healthy soybean plants and 35 GSFR-affected plants were collected from two farms located 180 km apart in Maranhão, Brazil. Healthy samples were sourced from Xingu (Riachão City), while GSFR-affected samples were collected from Parnaíba City (Balsas City).

In addition to LIBS, Atomic Absorption Spectrometry (AAS) was employed as a reference method. Figure 28 presents the typical averaged broadband LIBS spectra for both sample groups: healthy and GSFR-affected soybean plants. Furthermore, Figure 29 illustrates the correlation between the elemental concentrations measured by the AAS method and the peaks in the LIBS spectrum for three elements—calcium, potassium, and magnesium—occurring at wavelengths of 422.67 nm, 766.49 nm, and 518.36 nm, respectively.

The results of their experiments demonstrated that, in the initial phase, LIBS effectively differentiated between healthy soybean plants and those influenced by GSFR. The study used components of magnesium, potassium, and calcium. The analysis also indicated a Pearson correlation coefficient of 0.8 between LIBS and AAS, indicating a strong agreement and correlation between the two techniques due to the coefficient's proximity to 1.

A. Alrebdi et al. [141] investigated various *Peganum harmala* seed samples using the calibration-free LIBS (CF-LIBS) method. They applied principal component analysis (PCA) to the LIBS data to classify the seed samples into four categories: α, β, γ, and Δ. Additionally, the results obtained through CF-LIBS were compared and integrated with those from XRF and scanning electron microscopy with energy-dispersive X-ray spectroscopy (SEM-EDX).

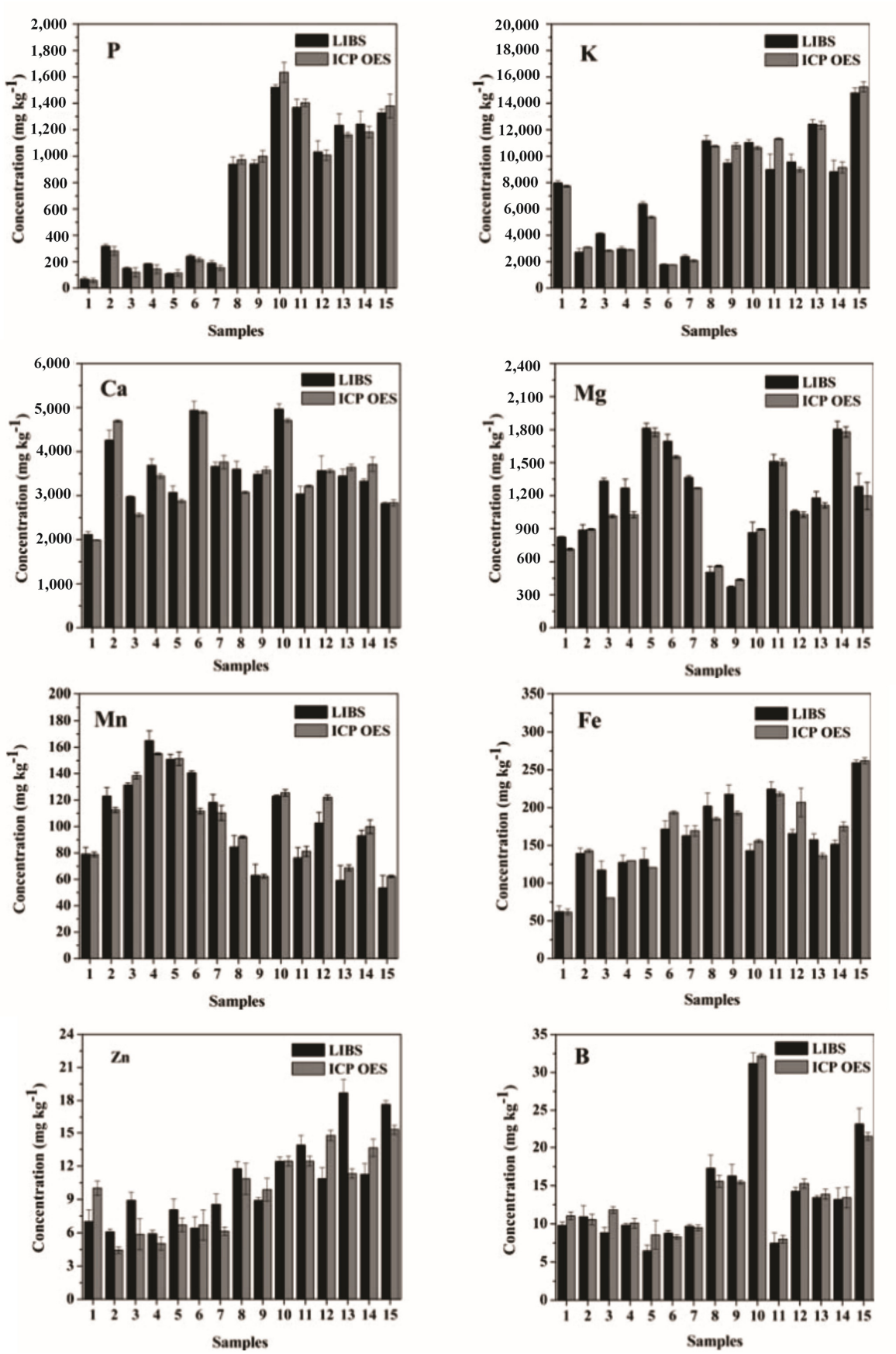

Figure 27. Detection of P, K, Ca, Mg, Mn, Fe, Zn, and B in sugar cane leaf pellets following acid digestion, using ICP-OES and LIBS multivariate PLSR. Error bars represent an estimated standard deviation of 1 (n = 3). Reproduced from Ref. [82] with permission of the Royal Society of Chemistry.

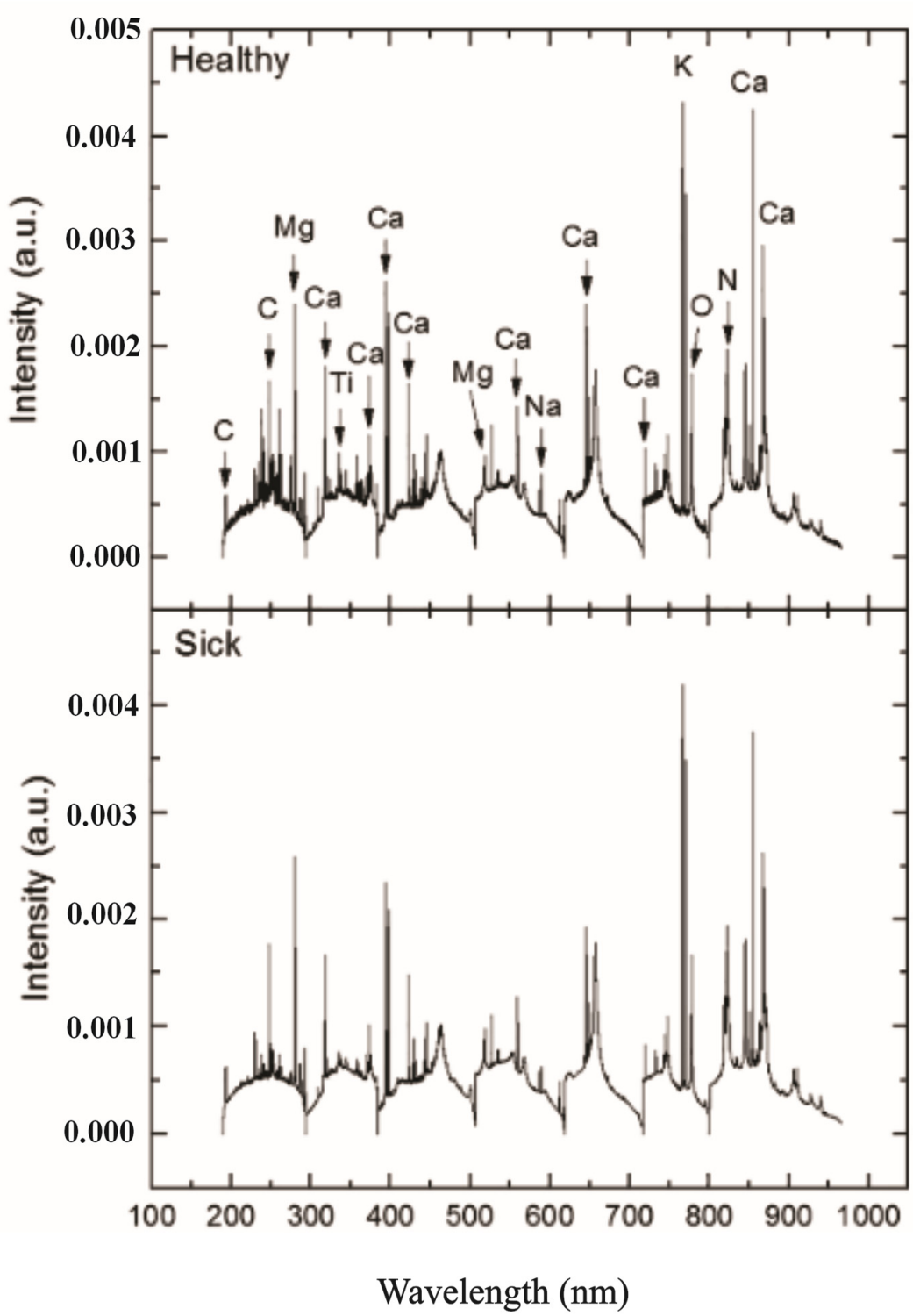

Figure 28. Regular broadband LIBS radiation of healthy and diseased soybean leaves. Reproduced from Ref. [223] with permission of Elsevier.

Figure 30 displays the elemental composition (μg/g) of the *P. harmala* seed sample classified as α, as analyzed using the CF-LIBS, XRF, and EDX methods. The figure clearly shows that XRF detected elements such as Zr, Ru, and Mn. Similarly, LIBS identified Li and C, while EDX uniquely detected Rb due to differences in detection limits and elemental homogeneity among the techniques.

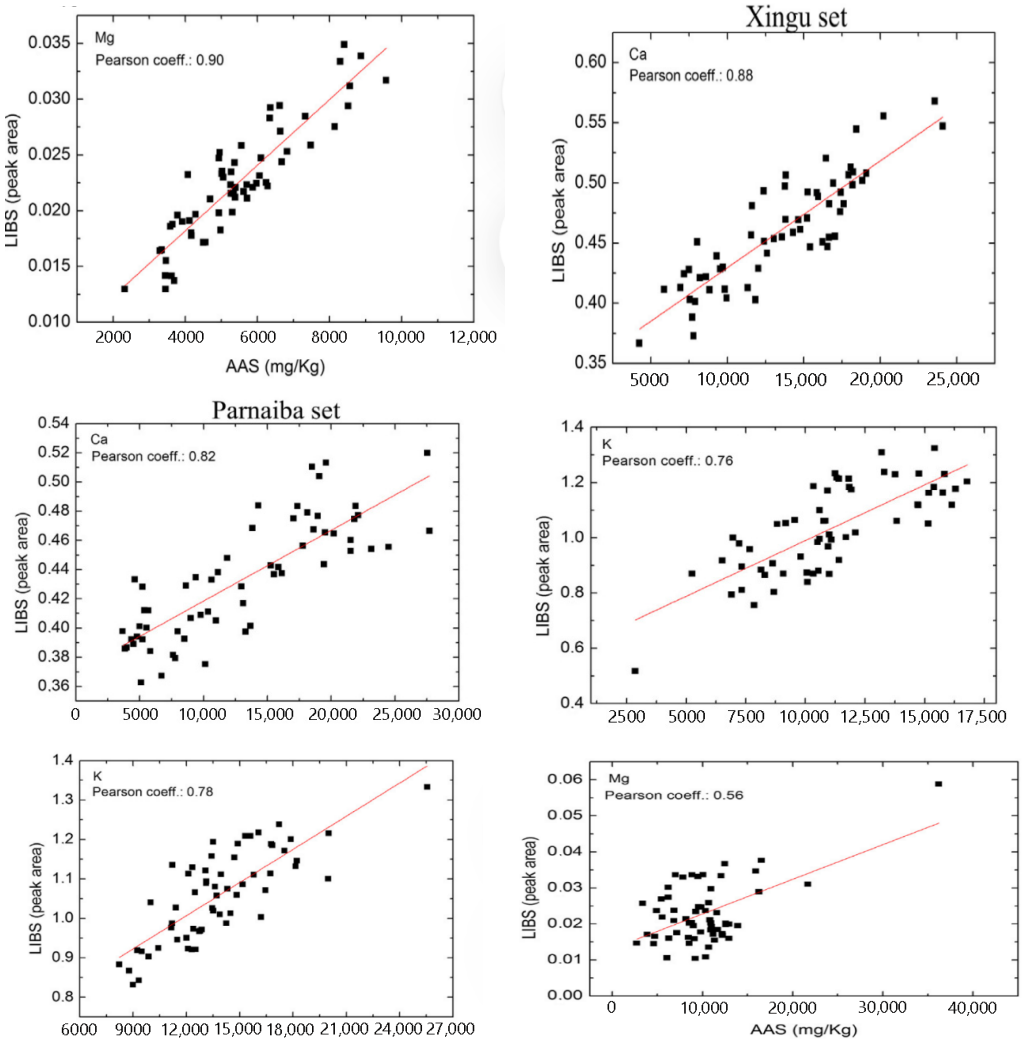

Figure 29. Correlation diagrams showing LIBS emission peak regions for Ca (422.67 nm), K (766.49 nm), and Mg (518.36 nm) alongside the related elemental concentrations estimated through AAS for the Xingu species set (**left**), and the Parnaíba species set (**right**), comprising healthy and damaged leaves. Reproduced from Ref. [223] with permission of Elsevier.

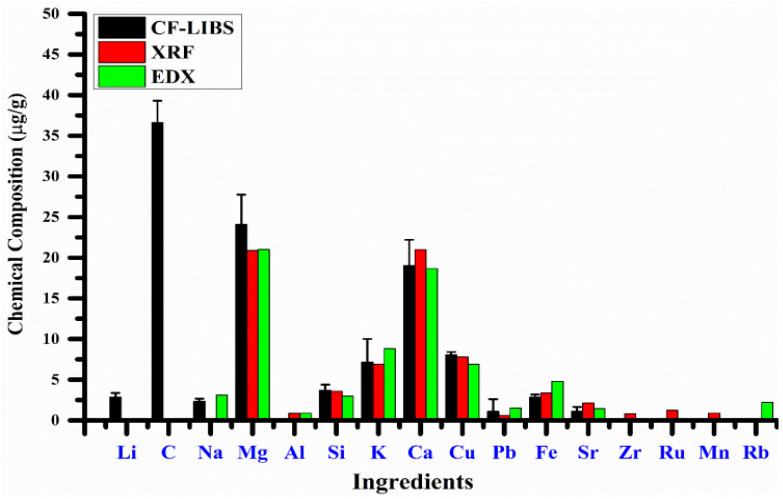

Figure 30. Elemental content (μg/g) of the *P. harmala* seed target-(α) by different CF-LIBS, EDX, and XRF techniques. Reproduced from Ref. [141] with permission of Multidisciplinary Digital Publishing Institute.

Table 9 contains a complete view comparing LIBS with other analytical methods for plant material analysis and describing the positive attributes of LIBS.

Table 9. Comparison of the LIBS methodology with other analytical techniques for plant material analysis, emphasizing LIBS's advantages over traditional methods.

Plant Name	Plant Part	Detected Elements	Method for Comparison with LIBS	Reasons for LIBS Superiority	References
Phylanthus niruri	Roots and leaves	Na, Ni, Al, Mg, Fe, Si, Mn, Ca, Zr, Cr, K, Ba, P, Cu, Ti, Zn, C, H, N, O, Li	ICP-OES	Rapid analysis, multi-elemental detection, high spatial resolution, minimal or no sample preparation, non-destructive technique, all-phase (solid, liquid, and gases) detection	[188]
Barringtonia racemosa	Roots and leaves				
Tinospora cordifolia	Roots and leaves				
Hygrophila angustifolia	Roots and leaves				
Flower sample of *Hygrophila angustifolia*	Flower part				
Apple	leaves	Zn, Mn, P, Al, Ca, Cu, Mg, Fe	AAS	Multi-elemental analysis, minimal sample preparation	[83]
Peach	leaves				
Spinach	leaves				
Tomato	leaves				
Sunflower	leaves	Pb, Cu, Mg	LA-ICP-MS	Instantaneous emission, LA-ICP-MS does not directly offer information related to a particular location within the sample	[97]
Sugar cane	dried leaves,	Cu, Mn, P, K, Ca, Mg, Fe, Zn, B, Si	EDXRF	Multi-element analysis, both macro- and micronutrient detection, real-time measurement, fresh samples analysis	[55]
Soil	collected around the Sultan Iskandar power station	Fe, Ni, Pb, Cu	FAAS	Rapid analysis, real-time analysis, multi-elemental analysis	[113]
Miracle Moringa	leaves	Ca, Na, K, Fe, Mg, Mn, Cu, P, S, Zn	ICP-OES	Minimal sample preparation, rapid analysis, portable and field-deployable	[114]
Black tea	leaves	Fe, Mg, Na, P, Ca, Al, Zn	ICP/AES	Minimal sample preparation, field analysis, high-throughput screening, analyzing delicate samples, portability	[222]
Tinnevelly senna	leaves	Na, Sr, Al, Ba, Ca, Cu, Fe, Mg, Mn, Zn, As, V	ICP-OES	Rapid, eco-friendly, multi-elemental analysis	[153]
Festuca arundinacea	leaves	Ca, Mg, Fe, Mn, Cu, Ni, Zn	ICP-MS	Minimal sample preparation, portability, multi-element analysis	[81]
Sugar cane	leaves	P, K, Fe, Mn, Ca, S, Si	EDXRF	Fast, in situ analysis with minimal sample preparation	[55]
Papaya	Root	N, O, C, Na, Zn, Mg, Si, Al, Ca, Na, K, Ti, Fe, Cr, Mn, Cu, Cl	WDXRF	Minimal sample preparation, portability, depth profiling	[218]

6.2. Advantages and Disadvantages of LIBS for Plant Analysis

As mentioned earlier in this research, LIBS has been proposed for various applications and has some major advantages over more traditional spectrochemical measurements. Some of these advantages include minimal or no sample preparation, rapid and repeatable elemental measurements, and high spatial resolution on the target surface, which offers insight into how elements are spatially distributed in the samples under analysis. LIBS analysis can be performed in either contact or stand-off mode, enabling detailed profiling of layered structures and direct analysis of in situ samples [139].

Qualitative LIBS measurements can identify samples using unique spectral signatures based on their elemental composition. A single laser shot is often sufficient to determine

the composition of a sample. Additionally, LIBS provides spatially resolved information about element distribution, which is unattainable with other traditional methods without extensive sample preparation, such as ashing or acid dilution [153].

Among laser ablation-based techniques, LIBS is unique in enabling quantitative in situ analysis with satisfactory sensitivity and a wide lateral resolution range. Many of the requirements for modern analytical methods, such as minimal sample preparation and real-time analysis, are fulfilled solely by LIBS [46]. The technique is conceptually and experimentally simple and offers excellent potential for microanalysis when integrated with a microscope. LIBS can analyze samples in various states, including solids, liquids, and gases. Furthermore, it is effective in plant analysis to quickly detect and map heavy minerals and nutrients in plant samples, agricultural products, foods, and soils. LIBS is also utilized to identify essential minerals and toxic heavy metals in plants intended for medicinal or dietary purposes [7].

In agricultural science, key challenges such as nutrient management, heavy and toxic metal contamination, and optimal crop productivity significantly impact global agricultural output. Plants, which can grow for decades, incorporate elements in varying proportions. The elements consist of (i) macronutrients such as Ca, K, Mg, N, P, and S and (ii) micronutrients including Fe, Mn, B, Cu, Cl, Mo, Na, and Zn [275]. These elements are necessary for development and growth, and adequate intake is generally associated with a lower risk of several diseases. Therefore, quantifying elements in plant parts is important for understanding their nutritional content, especially in foods such as grains, vegetables, and fruits.

Conversely, heavy and toxic metal elements such as As, Cr, Cd, Li, Pb, and Hg can be harmful even in trace amounts. These metals enter plants through external sources like pesticides, industrial waste, fertilizers, contaminated soil, and water. Once inside plants, these metals bind to sulfur, nitrogen, and oxygen-containing biological molecules like enzymes, nucleic acids, proteins, and carbohydrates, interfering with their normal functions [275].

Trace and metallic elements are essential to the metabolism and functioning of plants. Understanding the movement and distribution of these elements within plants is key to understanding the metabolic pathways. Knowledge about the spatial distribution of minerals is essential for plant science, agriculture, and food technology. In this context, LIBS shows great promise for detecting and mapping trace elements in plant matrices [33].

Mineral analysis during plant growth is a primary application of LIBS in plant science. Micronutrients in plants often occur at trace levels, requiring robust methods for accurate detection. Plants take in minerals from the available soil organic matter or from inorganic fertilizers [276]. Each plant type has specific nutrient needs, and an incorrect combination of nutrients may result in reduced or inhibited growth, disease, or plant death. For understanding how minerals are moved in plants, these functions and pathways for increased crop yield and health can be optimized [34].

Causes of plant diseases from fungi, bacteria, nematodes, environmental stress, and deficiencies from fertilizers are created by urbanization and industrialization [33]. Elemental imaging of plant tissues plays a critical role in diagnosing and addressing these issues because it can expose variation in the distribution of elements, which is necessary for the proper distribution of nutrients and the identification of toxic elements to limit their detrimental effects. Methodologies including SEM-EDS, LIBS, and XRF are commonly employed for elemental imaging and analysis [277].

A variety of methods can directly generate images of elemental distributions within plant tissues, including LIBS, scanning electron microscopy with energy-dispersive X-ray spectroscopy (SEM-EDS), and X-ray fluorescence (XRF) [33]. Additionally, more

advanced techniques are widely regarded as "standard" in elemental imaging, such as laser ablation inductively coupled plasma mass spectrometry (LA-ICP-MS) [99], secondary ion mass spectrometry (SIMS) [278], and particle-induced X-ray emission (PIXE) [279]. Synchrotron methods, including short-range X-ray absorption spectroscopy (XANES), micro-XRF, and extended X-ray absorption fine structure (EXAFS) complement imaging capabilities [142,280]. These spectroscopic methods provide powerful methods with adequate spatial resolution to simultaneously observe and map the mineral elements in plant tissues.

LIBS, in particular, yields key spatial and lateral distribution and is therefore a technique for investigating ion storage and transport across plant compartments. Progress in LIBS methods, such as double-pulse LIBS (DP-LIBS), fs-LIBS, and 3D elemental imaging, have greatly expanded the use of LIBS to plant science. For example, Guerra et al. [55] mapped elements (e.g., P, Ca, Mg, Fe, Mn) in dried leaves of sugarcane (*Saccharum spontaneum* L.), suggesting that this method provides spatial (and lateral distribution) elemental profiles.

Obtaining comprehensive data on the potential impact of various components, compounds, and nanoscale materials on the development and progression of plant tissue is critical. This knowledge is critical for sustainable agricultural production, in determining the nutritional quality and safety of products, and in considering potential negative consequences for plant tissues and cellular structures. Research in plant nutrition and toxicology are focused on examining processes occurring in plant tissues from various levels of essential and non-essential chemical compounds. This includes investigating how these compounds are absorbed, transported, distributed, stored, and utilized within plant tissues [46].

Traditional analytical methods such as atomic absorption/emission spectroscopy (AAS/OES) and mass spectrometry (MS) are widely used to evaluate the chemical composition of bulk plant materials following acid digestion. These methods provide accurate and sensitive measurements of chemical composition and bioaccumulation of compounds. However, they often lack detailed spatial distribution information, which is either lost or limited to specific plant parts (e.g., root, stem, leaves). In recent years, numerous studies [248] have explored the use of LIBS to map elements, materials, and compounds across various plant species (both terrestrial and aquatic) and their different parts (e.g., shoots, leaves, and roots).

Advanced LIBS techniques, including dual-pulse (DP)-LIBS, fs-LIBS, micro-LIBS, NELIBS, and 3D elemental imaging, have been applied to plant studies. For example, DP-LIBS has been highlighted as a signal amplification method in plant science applications [33,275]. Additionally, recent reviews [33,39] have discussed the use of CF-LIBS and univariate and multivariate analysis to minimize matrix effects in plant and soil samples. Given the complexity and variability of plant matrices between species, CF-LIBS is particularly advantageous for quantifying elements in plant samples, even when matrix-matched standards are unavailable.

Since the advent of plant-based diets, considerable effort has gone into developing methods to diagnose nutrient deficiencies and disorders by measuring total nutrient concentrations in plants or their parts. While early methods relied on time-consuming colorimetric or gravimetric techniques, modern approaches employ more precise and rapid methods, such as AAS, ICP-OES, and ICP-MS. LIBS, in particular, has proven valuable for early detection of plant diseases and nutrient deficiencies, especially in crops like Citrus [214,224–226], soybeans [22,89,276–278] and tobacco [218,232,280–282]. For instance, Sankaran et al. [216] used LIBS in 2015 to analyze Citrus leaves for abnormalities, including bacterial Huanglongbing disease (HLB), Citrus canker, and deficiencies in Mn, Zn, Fe, and Mg.

Nutrient deficiencies generally appear visually as symptoms on the leaves, making them easy to diagnose. Some deficiencies, called "hidden errors" may only show up using state-of-the-art analytical techniques. Yield loss can occur due to toxicities caused by excessive nutrient applications as well. Examples include Blossom End Rot in tomatoes and peppers or End Rot in Chinese cabbage, often associated with calcium deficiency [174]. Analyzing nutrient concentrations in specific plant parts can help prevent these problems. However, in some cases, plants may not exhibit visible symptoms despite nutrient shortages, necessitating advanced spectroanalytical techniques like XRF, LIBS, near-infrared spectroscopy (NIR), and chlorophyll fluorescence (Chl) for in situ diagnosis of plant nutrition.

Recently, Ranulfi et al. [217] utilized LIBS to investigate factors underlying Green Stem and Leaf Retention Syndrome (GSFR), or "crazy soybean II," caused by the nematode *Aphelenchoides besseyi* in soybean plants. These studies reaffirm the suitability of LIBS as a non-destructive, environmentally friendly approach for plant analysis.

Recent years have seen rapid progression in the field of LIBS instrumentation and data analysis. In its current state, LIBS does offer many advantages.

Further advances in LIBS data analysis and instrumentation continue to increase the usefulness of this analytical method. For example, the use of CF-LIBS with multivariate analysis is a promising approach for overcoming matrix effects, particularly for complex plant and soil matrices. This approach is especially beneficial for quantifying elements in materials of unknown composition without requiring standard reference materials.

LIBS also plays a significant role in plant-based diet research by diagnosing nutritional disorders through total nutrient concentration analysis. It is also more useful for early detection of plant disease, with Huanglongbing in citrus fruits, nutrient deficiency in crops such as soybeans and tobacco as examples. These are just some examples that illustrate that LIBS could be a green and versatile analytical tool for plant science research.

However, there are still areas of research that are problematic, including those involving lower spatial resolution than that of techniques such as SEM-EDS [144] and poorer precision and reproducibility than that of ICP-MS [282].

Despite the advantages of LIBS, there remain some challenges relating to sample preparation, matrix effects, spectral preprocessing, model calibration, and instrumental development. One major challenge is the sensitivity of LIBS to material heterogeneity, which can significantly affect results. Changes in the chemical or physical features of the sample (matrix effects) can affect the signal intensity of the emission lines. The careful preparation and presentation of the sample and the optimal measurement parameters are essential for yielding reproducible data.

Further advancements are needed in system stability, mitigation of self-absorption effects [283,284], reduction in line broadening, minimization of the high-intensity background continuum, and addressing strong matrix effects. Additionally, the complexity and volume of LIBS data have traditionally led to extended processing and interpretation times, sometimes stretching over weeks or months.

6.3. Future Prospective

Recent developments of LIBS within the area of processed agricultural products such as flour, coffee, wine and others have shown considerable promise and potential; however, advancements in the technique for these analyses have been limited to date. Future studies can focus on investigating the potential for applications of 3D elemental imaging, NELIBS, and novel micro-LIBS methods. Recent feasibility studies demonstrated the analytical potential of these approaches. Wang et al. achieved a tenfold decrease in the detection limits for Hg concentration in tangerine peels by using gold nanoparticles in a NELIBS approach [207]. Similarly, 2D LIBS elemental imaging of plants at the micrometer scale has

already been demonstrated using commercial instrumentation [285], opening the way for the possibility of obtaining 3D high-resolution images with the same equipment.

Additionally, efforts should aim to expand the range of plant species, products, cultivars, and derivatives analyzed with LIBS, many of which remain unexplored [39].

The integration of machine learning methodologies, nanotechnology, and LIBS has the potential to develop innovative diagnostic tools with precise applications in agriculture. This area holds promise for future research, expanding the application of LIBS technology in a broader agricultural context.

To advance LIBS to a new stage of development, particularly for biomedical applications, and to foster collaboration between the spectroscopic and plant science communities, increased efforts are essential. Addressing this gap will support the evolution of LIBS as a robust tool across interdisciplinary domains.

Sensitivity in LIBS can be enhanced by improving the experimental setup (e.g., incorporating a second laser) or modifying the plant sample (e.g., signal amplification using nanoparticles). It is anticipated that ongoing advancements will address current limitations, further enhancing LIBS's advantages, such as its low cost, simple instrumentation, rapid multi-element screening of large sample sets, acceptable limits of detection (LODs) for many experiments, and detection of nearly all elements, including light elements.

While LIBS has plenty of room for improvement and therefore some potential growth, it is very versatile and adaptable, making its future bright. Prospective technological developments may yield portable instruments, better remote analysis, and the integration of advanced chemometric tools for data analysis.

Future research could focus on enhancing signal and reliability, developing new techniques for data processing and signal amplification to improve the LIBS signal, and the precision, reliability, and repeatability of analysis results.

The use of LIBS in combination with other techniques could also be a winning technique. Combining LIBS technology with complementary analytical methods, including Raman spectroscopy or fluorescence, could help make laser spectrometers even more powerful while expanding their use for chemical analysis. Developing portable and specialized tools will also be important, creating portable and customized LIBS instruments for in situ and real-time detection needs in areas such as emergency management, environmental monitoring, and cultural heritage preservation.

Finally, it will be essential to advance in LIBS fundamental research, develop the basic components of LIBS technology, foster inventions, and accelerate the development plan of its entire application in different domains.

Author Contributions: Writing review and editing, F.R., A.E., M.Z., S.B.,V.P.; supervision, F.R. All authors have read and agreed to the published version of the manuscript.

Funding: This research received no external funding.

Acknowledgments: Fatemeh Rezaei dedicates this paper to her mother, who passed away three months ago. Thanks for all of her kindness, support, and good memories.

Conflicts of Interest: The authors declare no conflict of interest.

Abbreviations

LIBS	Laser-induced breakdown spectroscopy
ns-LIBS	Nanosecond laser-induced breakdown spectroscopy
fs-LIBS	Femtosecond laser-induced breakdown spectroscopy
CF-LIBS	Calibration-free laser-induced breakdown spectroscopy
NELIBS	Nanoparticle-enhanced laser-induced breakdown spectroscopy

SAIS-LIBS	Standard addition method and internal standard method into LIBS
LIBS-LIF	Laser-induced breakdown spectroscopy–laser-induced fluorescence
DP-LIBS	Double-pulse LIBS
SP-LIBS	Single-pulse LIBS
Nd:YAG	Neodymium-doped yttrium aluminum garnet
ArF	Argon fluoride
CO_2	Carbon dioxide
Ti-sapphire	Titanium-sapphire
ChemCam	Chemistry and camera
NIST	National institute of standards and technology
NIR	Near-infrared
NIRS	Near-infrared spectroscopy
ICP-OES	Inductively coupled plasma optical emission spectrometry
ICP-MS	Inductively coupled plasma mass spectrometry
PLSR	Predictive regression method
DP	Dual pulse
LOD	Limit of detection
NPs	Nanoparticles
QDs	Quantum Dots
ns	Nanosecond
fs	Femtosecond
UV	Ultraviolet
IR	Infrared
MIR	Mid-infrared
SRXRF	Synchrotron radiation XRF
ANN	Artificial neural network
PCA	Principal component analysis
PLS	Partial least squares
PLSR	Partial least-squares regression
PLS-DA	Partial least squares discriminant analysis
SVM	Support vector machine
PSO-KELM	Particle swarm optimization-kernel extreme learning machine
GA	Genetic algorithm
SIMCA	Soft independent modeling of class analogy
Chl	Chlorophyll
CRM	Certified reference material
AAS	Atomic absorption spectrometry
OES	Optical emission spectrometry
XAS	X-ray absorption spectroscopy
XRF	X-ray fluorescence spectrometry
μXRF	Micro-X-ray fluorescence
LIF	Laser-induced fluorescence
LIP	Laser-induced plasma
AAS/OES	Atomic absorption spectroscopy/optical emission spectroscopy
MS	Mass spectrometry
SIMS	Secondary ion mass spectrometry
GSFR	Green stem and foliar retention
CCD	Charge-coupled device
ICCD	Intensified charge-coupled device
t_d	Time delay
t_{delay}	Delay time
t_{int}	Integration time gate
LA-ICP-MS	Laser ablation inductively coupled plasma mass spectrometry
ns-LAICP-MS	Nanosecond-laser ablation inductively coupled plasma mass spectrometry

fs-LA-ICP-MS	Femtosecond-laser ablation inductively coupled plasma mass spectrometry
SPs	Surface plasmons
LSPs	Localized surface plasmons
SR	Sufficiency ranges
CTC	Critical threshold concentrations
TMV	Tobacco mosaic virus
LTE	Local thermal equilibrium
PI	Propidium iodide
RWMRI	Relaxation Weighted Magnetic Resonance Imaging
S. aureus	*Staphylococcus aureus*
P. guajava	*Psidium guajava*
OPC	One-point calibration
MOS	*Moringa oleifera* seed
RRs	Rhatany roots
P. notoginseng	*Panax notoginseng*
CLas	*Candidatus Liberibacter asiaticus*
CTV	*Citrus tristeza* virus
WDXRF	Wavelength dispersive X-ray fluorescence
Pb-EDTA	Pb-ethylenediaminetetraacetate sodium salt
EDX	Energy-dispersive X-ray spectroscopy
SEM-EDX	Scanning electron microscopy-energy dispersive X-ray spectroscopy
EDXRF	Energy-dispersive X-ray fluorescence spectrometry
TEM	Transmission electron microscopy
GSH	Glutathione
MPA	3-mercaptopropionic acid
ppm	Parts per million
PIXE	Particle-induced X-ray emission
XANES	X-ray absorption spectroscopy near edge structure
EXAFS	Extended X-ray absorption fine structure
HLB	Huanglongbing disease
SSR	Sclerotinia stem rot
RKN	Root Knot Nematode
FAW	First Automobile Works

References

1. Kumar, R.; Alamelu, D.; Acharya, R.; Rai, A.K. Determination of Concentrations of Chromium and Other Elements in Soil and Plant Samples from Leather Tanning Area by Instrumental Neutron Activation Analysis. *J. Radioanal. Nucl. Chem.* **2014**, *300*, 213–218. [CrossRef]
2. Busser, B.; Moncayo, S.; Coll, J.L.; Sancey, L.; Motto-Ros, V. Elemental Imaging Using Laser-Induced Breakdown Spectroscopy: A New and Promising Approach for Biological and Medical Applications. *Coord. Chem. Rev.* **2018**, *358*, 70–79. [CrossRef]
3. DeLucia, F.C.; Samuels, A.C.; Harmon, R.S.; Walters, R.A.; McNesby, K.L.; LaPointe, A.; Winkel, R.J.; Miziolek, A.W. Laser-Induced Breakdown Spectroscopy (LIBS): A Promising Versatile Chemical Sensor Technology for Hazardous Material Detection. *IEEE Sens. J.* **2005**, *5*, 681–689. [CrossRef]
4. Noll, R.; Sturm, V.; Aydin, Ü.; Eilers, D.; Gehlen, C.; Höhne, M.; Lamott, A.; Makowe, J.; Vrenegor, J. Laser-Induced Breakdown Spectroscopy—From Research to Industry, New Frontiers for Process Control. *Spectrochim. Acta Part B At. Spectrosc.* **2008**, *63*, 1159–1166. [CrossRef]
5. Noll, R.; Cord Fricke-Begemann, A.; Connemann, S.; Meinhardt, C.; Sturm, V. LIBS Analyses for Industrial Applications–an Overview of Developments from 2014 to 2018. *J. Anal. At. Spectrom.* **2018**, *33*, 945–956. [CrossRef]
6. Pedarnig, J.D.; Pedarnig, S.; Trautner, S.; Grünberger, N.; Giannakaris, S.; Eschlböck-Fuchs, J.H. Review of Element Analysis of Industrial Materials by In-Line Laser—Induced Breakdown Spectroscopy (LIBS). *Appl. Sci.* **2021**, *11*, 9274. [CrossRef]
7. Markiewicz-Keszycka, M.; Cama-Moncunill, X.; Casado-Gavalda, M.P.; Dixit, Y.; Cama-Moncunill, R.; Cullen, P.J.; Sullivan, C. Laser-Induced Breakdown Spectroscopy (LIBS) for Food Analysis: A Review. *Trends Food Sci. Technol.* **2017**, *65*, 80–93. [CrossRef]
8. Rezaei, F.; Tavassoli, S.H. Numerical and Experimental Investigation of Laser Induced Plasma Spectrum of Aluminum in the Presence of a Noble Gas. *Spectrochim. Acta Part B At. Spectrosc.* **2012**, *78*, 29–36. [CrossRef]

9. D'Angelo, C.A.; Díaz Pace, D.M.; Bertuccelli, G. Semiempirical Model for Analysis of Inhomogeneous Optically Thick Laser-Induced Plasmas. *Spectrochim. Acta Part B At. Spectrosc.* **2009**, *64*, 999–1008. [CrossRef]
10. Bohling, C.; Hohmann, K.; Scheel, D.; Bauer, C.; Schippers, W.; Burgmeier, J.; Willer, U.; Holl, G.; Schade, W. All-Fiber-Coupled Laser-Induced Breakdown Spectroscopy Sensor for Hazardous Materials Analysis. *Spectrochim. Acta Part B At. Spectrosc.* **2007**, *62*, 1519–1527. [CrossRef]
11. Ralchenko, Y. NIST Atomic Spectra Database. *Mem. Della Soc. Astron. Ital. Suppl.* **2005**, *8*, 96.
12. Guezenoc, J.; Gallet-Budynek, A.; Bousquet, B. Critical Review and Advices on Spectral-Based Normalization Methods for LIBS Quantitative Analysis. *Spectrochim. Acta Part B At. Spectrosc.* **2019**, *160*, 105688. [CrossRef]
13. Hai, B.; Zhu, X.L.; Hu, Z.Q.; Ma, X.; Zhu, J.F.; Su, Y.B.; Zhang, D.C. Simple Method for Liquid Analysis by Laser-Induced Breakdown Spectroscopy (LIBS). *Opt. Express* **2018**, *26*, 18794–18802. [CrossRef]
14. Lei, W.; Motto-Ros, V.; Boueri, M.; Ma, Q.; Zhang, D.; Zheng, L.; Zeng, H.; Yu, J. Time-Resolved Characterization of Laser-Induced Plasma from Fresh Potatoes. *Spectrochim. Acta Part B At. Spectrosc.* **2009**, *64*, 891–898. [CrossRef]
15. Liu, P.; Cuerda-Gil, D.; Shahid, S.; Slotkin, R.K. The Epigenetic Control of the Transposable Element Life Cycle in Plant Genomes and Beyond. *Annu. Rev. Genet.* **2022**, *56*, 63–87. [CrossRef]
16. Soetan, K.O.; Olaiya, C.O.; Oyewole, O.E. The Importance of Mineral Elements for Humans, Domestic Animals and Plants: A Review. *Afr. J. Food Sci.* **2010**, *4*, 200–222.
17. Dalcorso, G.; Manara, A.; Piasentin, S.; Furini, A. Nutrient Metal Elements in Plants. *Metallomics* **2014**, *6*, 1770–1788. [CrossRef]
18. Pilon-Smits, E.A.; Quinn, C.F.; Tapken, W.; Malagoli, M.; Schiavon, M. Physiological Functions of Beneficial Elements. *Curr. Opin. Plant Biol.* **2009**, *12*, 267–274. [CrossRef]
19. 7 Most Abundant Metal Elements in Earth's Crust | Refractory Metals and Alloys. Available online: https://www.refractorymetal.org/7-most-abundant-metal-elements-in-earths-crust/ (accessed on 2 September 2025).
20. Kochian, L.V.; Hoekenga, O.A.; Piñeros, M.A. How Do Crop Plants Tolerate Acid Soils? Mechanisms of Aluminum Tolerance and Phosphorous Efficiency. *Annu. Rev. Plant Biol.* **2004**, *55*, 459–493. [CrossRef] [PubMed]
21. Wei, Y.; Han, R.; Xie, Y.; Jiang, C.; Yu, Y. Recent Advances in Understanding Mechanisms of Plant Tolerance and Response to Aluminum Toxicity. *Sustainability* **2021**, *13*, 1782. [CrossRef]
22. Zheng, S.J. Crop Production on Acidic Soils: Overcoming Aluminium Toxicity and Phosphorus Deficiency. *Ann. Bot.* **2010**, *106*, 183–184. [CrossRef]
23. Khan, F.; Siddique, A.B.; Shabala, S.; Zhou, M.; Zhao, C. Phosphorus Plays Key Roles in Regulating Plants' Physiological Responses to Abiotic Stresses. *Plants* **2023**, *12*, 2861. [CrossRef]
24. Bechtaoui, N.; Rabiu, M.K.; Raklami, A.; Oufdou, K.; Hafidi, M.; Jemo, M. Phosphate-Dependent Regulation of Growth and Stresses Management in Plants. *Front. Plant Sci.* **2021**, *12*, 679916. [CrossRef] [PubMed]
25. Vance, C.P.; Uhde-Stone, C.; Allan, D.L. Phosphorus Acquisition and Use: Critical Adaptations by Plants for Securing a Nonrenewable Resource. *New Phytol.* **2003**, *157*, 423–447. [CrossRef] [PubMed]
26. Niu, Y.F.; Chai, R.S.; Jin, G.L.; Wang, H.; Tang, C.X.; Zhang, Y.S. Responses of Root Architecture Development to Low Phosphorus Availability: A Review. *Ann. Bot.* **2013**, *112*, 391. [CrossRef] [PubMed]
27. Rahman, A.; Lee, S.; Ji, H.C.; Kabir, A.H.; Jones, C.S.; Lee, K. Importance of Mineral Nutrition for Mitigating Aluminum Toxicity in Plants on Acidic Soils: Current Status and Opportunities. *Int. J. Mol. Sci.* **2018**, *19*, 3073. [CrossRef]
28. Santos, D.; Nunes, L.C.; De Carvalho, G.G.A.; Gomes, M.D.S.; De Souza, P.F.; Leme, F.D.O.; Dos Santos, L.G.C.; Krug, F.J. Laser-Induced Breakdown Spectroscopy for Analysis of Plant Materials: A Review. *Spectrochim. Acta Part B At. Spectrosc.* **2012**, *71–72*, 3–13. [CrossRef]
29. Díaz Pace, D.; Molina, J.; Rodríguez, C.I. Rapid Assessment of Extractability of Macronutrients from Yerba Mate (*Illex paraguariensis*) Leaves Based on Laser-Induced Breakdown Spectroscopy. *Chemosensors* **2024**, *12*, 18. [CrossRef]
30. Peng, J.; Liu, F.; Zhou, F.; Song, K.; Zhang, C.; Ye, L.; He, Y. Challenging Applications for Multi-Element Analysis by Laser-Induced Breakdown Spectroscopy in Agriculture: A Review. *TrAC-Trends Anal. Chem.* **2016**, *85*, 260–272. [CrossRef]
31. Kamil, Z.J.; Zoory, M.J.; Mohamad, H.J. LIBS technique for plant mineral ratio analysis and environmental and agricultural importance: A comprehensive review. *Eur. Phys. J. D* **2024**, *78*, 27. [CrossRef]
32. Rai, P.K.; Srivastava, A.K.; Sharma, B.; Dhar, P.; Mishra, A.K.; Watal, G. Use of Laser-Induced Breakdown Spectroscopy for the Detection of Glycemic Elements in Indian Medicinal Plants. *Evid.-Based Complement. Altern. Med.* **2013**, *2013*, 406365. [CrossRef] [PubMed]
33. Singh, V.K.; Sharma, N.; Verma, O.N.; Singh, V.K.; Tripathi, D.K.; Lee, Y.; Kumar, S.; Rai, P.K.; Gondal, M.A. Review: Application of Libs to Elemental Analysis and Mapping of Plant Samples. *At. Spectrosc.* **2021**, *42*, 99–113. [CrossRef]
34. de Carvalho, G.G.A.; Guerra, M.B.B.; Adame, A.; Nomura, C.S.; Oliveira, P.V.; de Carvalho, H.W.P.; Santos, D., Jr.; Nunes, L.C.; Krug, F.J. Recent Advances in LIBS and XRF for the Analysis of Plants. *J. Anal. At. Spectrom.* **2018**, *33*, 919–944. [CrossRef]
35. Yu, K.; Ren, J.; Zhao, Y. Principles, Developments and Applications of Laser-Induced Breakdown Spectroscopy in Agriculture: A Review. *Artif. Intell. Agric.* **2020**, *4*, 127–139. [CrossRef]

36. Yang, P.; Fu, G.; Wang, J.; Luo, Z.; Yao, M. A Tutorial Review on Methods of Agricultural Product Sample Pretreatment and Target Analysis by Laser-Induced Breakdown Spectroscopy. *J. Anal. At. Spectrom.* **2022**, *37*, 1948–1960. [CrossRef]
37. Zhang, Y.; Zhang, T.; Li, H. Application of Laser-Induced Breakdown Spectroscopy (LIBS) in Environmental Monitoring. *Spectrochim. Acta Part B At. Spectrosc.* **2021**, *181*, 106218. [CrossRef]
38. Ren, J.; Zhao, Y.; Yu, K. LIBS in Agriculture: A Review Focusing on Revealing Nutritional and Toxic Elements in Soil, Water, and Crops. *Comput. Electron. Agric.* **2022**, *197*, 106986. [CrossRef]
39. Senesi, G.S.; Cabral, J.; Menegatti, C.R.; Marangoni, B.; Nicolodelli, G. Recent Advances and Future Trends in LIBS Applications to Agricultural Materials and Their Food Derivatives: An Overview of Developments in the Last Decade (2010–2019). Part II. Crop Plants and Their Food Derivatives. *Trends Anal. Chem.* **2019**, *118*, 453–469. [CrossRef]
40. Zaman, M.H.; Rehman, F.; Tahir, M.S.; Faheem, M.; Jamil, Y. A Study on the Effect of Preprocessing and Normalization on Classification of Plant Samples in Machine Learning Assisted Laser-Induced Breakdown Spectroscopy. *Arab. J. Sci. Eng.* **2024**, *49*, 10003–10019. [CrossRef]
41. Tavares, T.R. VNIR, XRF, and LIBS Spectroscopies for Soil Sensing on Precision Agriculture. Ph.D. Thesis, University of São Paulo "Luiz de Queiroz", College of Agriculture VNIR, São Paulo, Brazil, 2021; pp. 1–164.
42. Yang, N. Elemental Analysis of Soils Using Laser-Induced Breakdown Spectroscopy (LIBS). Master's Thesis, University of Tennessee, Knoxville, TN, USA, 2009; pp. 1–61.
43. Barra, I. *Soil Spectroscopy: When Spectroscopy and Machine Learning Combine to Solve Agricultural Soil Diagnostic Problems*; Springer: Cham, Switzerland, 2024; pp. 499–507. [CrossRef]
44. Beć, K.B.; Grabska, J.; Huck, C.W. X-Ray, LIBS, NMR, and MS Applications in Food, Feed, and Agriculture. Portable. In *Spectroscopy and Spectrometry*; John Wiley & Sons, Ltd.: Hoboken, NJ, USA, 2021; pp. 299–323. [CrossRef]
45. Singh, V.K.; Sharma, J.; Pathak, A.K.; Ghany, C.T.; Gondal, M.A. Laser-Induced Breakdown Spectroscopy (LIBS): A Novel Technology for Identifying Microbes Causing Infectious Diseases. *Biophys. Rev.* **2018**, *10*, 1221–1239. [CrossRef]
46. Modlitbová, P.; Pořízka, P.; Kaiser, J. Laser-Induced Breakdown Spectroscopy as a Promising Tool in the Elemental Bioimaging of Plant Tissues. *Trends Anal. Chem.* **2020**, *122*, 115729. [CrossRef]
47. Trevizan, L.C.; Santos, D.; Samad, R.E.; Vieira, N.D.; Nunes, L.C.; Rufini, I.A.; Krug, F.J. Evaluation of Laser Induced Breakdown Spectroscopy for the Determination of Micronutrients in Plant Materials. *Spectrochim. Acta Part B At. Spectrosc.* **2009**, *64*, 369–377. [CrossRef]
48. Martelli, M.R.; Brygo, F.; Sadoudi, A.; Delaporte, P.; Barron, C. Laser-Induced Breakdown Spectroscopy and Chemometrics: A Novel Potential Method to Analyze Wheat Grains. *J. Agric. Food Chem.* **2010**, *58*, 7126–7134. [CrossRef]
49. Bossu, M.; Hao, Z.Q.; Baudelet, M.; Yu, J.; Zhang, Z.; Zhang, J. Femtosecond Laser-Induced Breakdown Spectroscopy for Detection of Trace Elements in Sophora Leaves. *Chin. Phys. Lett.* **2007**, *24*, 3466–3468. [CrossRef]
50. Fortes, F.J.; Moros, J.; Lucena, P.; Cabalín, L.M.; Laserna, J.J. Laser-Induced Breakdown Spectroscopy. *Anal. Chem.* **2013**, *85*, 640–669. [CrossRef]
51. Assion, A.; Wollenhaupt, M.; Haag, L.; Mayorov, F.; Sarpe-Tudoran, C.; Winter, M.; Kutschera, U.; Baumert, T. Femtosecond Laser-Induced-Breakdown Spectrometry for Ca^{2+} Analysis of Biological Samples with High Spatial Resolution. *Appl. Phys. B* **2003**, *77*, 391–397. [CrossRef]
52. Idris, N.; Ramli, M.; Kurihara, K. Detection of Salt in Soil by Employing the Unique Sub-Target Effect in a Pulsed Carbon Dioxide (CO_2) Laser-Induced Breakdown Spectroscopy. In Proceedings of the 2016 International Seminar on Sensors, Instrumentation, Measurement and Metrology (ISSIMM), Malang, Indonesia, 10–11 August 2016. [CrossRef]
53. Khumaeni, A.; Ramli, M.; Deguchi, Y.; Lee, Y.; Idris, N.; Kurniawan, K.H.; Lie, T.J.J.; Kagawa, K. New Technique for the Direct Analysis of Food Powders Confined in a Small Hole Using Transversely Excited Atmospheric CO_2 Laser-Induced Gas Plasma. *Appl. Spectrosc.* **2008**, *62*, 1344–1348. [CrossRef]
54. Tamboli, M.M.; Unnikrishnan, V.K.; Nayak, R.; Devangad, P.; Muhammed Shameem, K.M.; Kartha, V.B.; Santhosh, C. Development of a Stand-off Laser Induced Breakdown Spectroscopy (ST-LIBS) System for the Analysis of Complex Matrices. *J. Instrum.* **2016**, *11*, P08021. [CrossRef]
55. Braga Bueno Guerra, M.; Adame, A.; de Almeida, E.; Gustinelli Arantes de Carvalho, G.; Augusto Stolf Brasil, M.; Santos, D., Jr.; José Krug, F. Direct Analysis of Plant Leaves by EDXRF and LIBS: Microsampling Strategies and Cross-Validation. *J. Anal. At. Spectrom.* **2015**, *7*, 1646–1654. [CrossRef]
56. Harmon, R.S.; De Lucia, F.C.; Miziolek, A.W.; Mcnesby, K.L.; Walters, R.A.; French, P.D. Laser-Induced Breakdown Spectroscopy (LIBS)–an Emerging Field-Portable Sensor Technology for Real-Time, in-Situ Geochemical and Environmental Analysis. *Geochem. Explor. Environ. Anal.* **2005**, *5*, 21–28. [CrossRef]
57. Noharet, B.; Sterner, C.; Irebo, T.; Gurell, J.; Bengtson, A.; Vanik, R.; Karlsson, H.; Illy, E. A Compact LIBS System for Industrial Applications. *Photonic Instrum. Eng. II* **2015**, *9369*, 936904.
58. Whitehouse, A.I. Laser-Induced Breakdown Spectroscopy and Its Applications to the Remote Characterization of Hazardous Materials. *Spectrosc. Eur./World* **2006**, *18*, 14–21. [CrossRef]

59. Gondal, M.; Talanta, T.H. Determination of Poisonous Metals in Wastewater Collected from Paint Manufacturing Plant Using Laser-Induced Breakdown Spectroscopy. *Talanta* **2007**, *71*, 73–80. [CrossRef]
60. Galiová, M.; Kaiser, J.; Novotný, K.; Hartl, M.; Kizek, R.; Babula, P. Utilization of Laser-Assisted Analytical Methods for Monitoring of Lead and Nutrition Elements Distribution in Fresh and Dried *Capsicum annuum* l. Leaves. *Microsc. Res. Tech.* **2011**, *74*, 845–852. [CrossRef]
61. Pořízka, P.; Prochazka, D.; Pilát, Z.; Krajcarová, L.; Kaiser, J.; Malina, R.; Novotný, J.; Zemánek, P.; Ježek, J.; Šerý, M.; et al. Application of Laser-Induced Breakdown Spectroscopy to the Analysis of Algal Biomass for Industrial Biotechnology. *Spectrochim. Acta Part B At. Spectrosc.* **2012**, *74–75*, 169–176. [CrossRef]
62. Kaiser, J.; Novotný, K.; Hrdlička, A.; Malina, R.; Novotný, J.; Prochazka, D.; Petrilak, M.; Krajcarová, L.; Vítková, G.; Kučerová, P. Utilization of Selected Laser-Ablation-Based Diagnostic Methods for Study of Elemental Distribution in Various Solid Samples. In Proceedings of the 17th Slovak-Czech-Polish Optical Conference on Wave and Quantum Aspects of Contemporary Optics, Liptovský Ján, Slovakia, 6–10 September 2010; Volume 7746, p. 774604. [CrossRef]
63. Trevizan, L.C.; Santos, D.; Samad, R.E.; Vieira, N.D.; Nomura, C.S.; Nunes, L.C.; Rufini, I.A.; Krug, F.J. Evaluation of Laser Induced Breakdown Spectroscopy for the Determination of Macronutrients in Plant Materials. *Spectrochim. Acta Part B At. Spectrosc.* **2008**, *63*, 1151–1158. [CrossRef]
64. Sun, D.; Su, M.; Dong, C.; Zhang, D.; Ma, X. A Semi-Quantitative Analysis of Essential Micronutrient in Folium Lycii Using Laser-Induced Breakdown Spectroscopy Technique. *Plasma Sci. Technol.* **2010**, *12*, 478. [CrossRef]
65. El-Deftar, M.M.; Robertson, J.; Foster, S.; Lennard, C. Evaluation of Elemental Profiling Methods, Including Laser-Induced Breakdown Spectroscopy (LIBS), for the Differentiation of Cannabis Plant Material Grown in Different Nutrient Solutions. *Forensic Sci. Int.* **2015**, *251*, 95–106. [CrossRef]
66. Zhang, D.C.; Ma, X.; Wen, W.Q.; Liu, H.P.; Zhang, P.J. Studies of Laser Induced-Breakdown Spectroscopy of Holly Leaves. *J. Phys. Conf. Ser.* **2009**, *185*, 8–11. [CrossRef]
67. Kaiser, J.; Galiová, M.; Novotný, K.; Reale, L.; Stejskal, K.; Samek, O.; Malina, R.; Páleníková, K.; Adam, V.; Kizek, R. Utilization of the Laser Induced Plasma Spectroscopy for monitoring of the metal accumulation in plant tissues with high spatial resolution. *Mod. Res. Educ. Top. Microsc.* **2007**, *1*, 434–441.
68. Chauhan, D.K.; Tripathi, D.K.; Rai, N.K.; Rai, A.K. Detection of Biogenic Silica in Leaf Blade, Leaf Sheath, and Stem of Bermuda Grass (*Cynodon dactylon*) Using LIBS and Phytolith Analysis. *Food Biophys.* **2011**, *6*, 416–423. [CrossRef]
69. Samek, O.; Lambert, J.; Hergenröder, R.; Liška, M.; Kaiser, J.; Novotný, K.; Kukhlevsky, S. Femtosecond Laser Spectrochemical Analysis of Plant Samples. *Laser Phys. Lett.* **2006**, *3*, 21–25. [CrossRef]
70. Khumaeni, A.; Lie, Z.S.; Niki, H.; Kurniawan, K.H.; Tjoeng, E.; Lee, Y.I.; Kurihara, K.; Deguchi, Y.; Kagawa, K. Direct Analysis of Powder Samples Using Transversely Excited Atmospheric CO_2 Laser-Induced Gas Plasma at 1 Atm. *Anal. Bioanal. Chem.* **2011**, *400*, 3279–3287. [CrossRef] [PubMed]
71. Khumaeni, A.; Niki, H.; Fukumoto, K.I.; Deguchi, Y.; Kurihara, K.; Kagawa, K.; Lee, Y.I. A Unique Technique of Laser-Induced Breakdown Spectroscopy Using Transversely Excited Atmospheric CO_2 Laser for the Sensitive Analysis of Powder Samples. *Curr. Appl. Phys.* **2011**, *11*, 423–427. [CrossRef]
72. Soniya, V.P.; Bhindhu, P.S.; Sujaina, M. Laser Induced Breakdown Spectroscopy: A Rapid Analytical Technique for Soil and Plant. *Int. J. Environ. Clim. Change* **2023**, *13*, 1813–1820. [CrossRef]
73. Schenk, E.R.; Almirall, J.R. Elemental Analysis of Cotton by Laser-Induced Breakdown Spectroscopy. *Appl. Opt.* **2010**, *49*, C153–C160. [CrossRef]
74. Braga, J.W.B.; Trevizan, L.C.; Nunes, L.C.; Rufini, I.A.; Santos, D.; Krug, F.J. Comparison of Univariate and Multivariate Calibration for the Determination of Micronutrients in Pellets of Plant Materials by Laser Induced Breakdown Spectrometry. *Spectrochim. Acta Part B At. Spectrosc.* **2010**, *65*, 66–74. [CrossRef]
75. Martin, M.Z.; Labbé, N.; André, N.; Harris, R.; Ebinger, M.; Wullschleger, S.D.; Vass, A.A. High Resolution Applications of Laser-Induced Breakdown Spectroscopy for Environmental and Forensic Applications. *Spectrochim. Acta Part B At. Spectrosc.* **2007**, *62*, 1426–1432. [CrossRef]
76. Gomes, M.D.S.; Santos, D.; Nunes, L.C.; De Carvalho, G.G.A.; De Oliveira Leme, F.; Krug, F.J. Evaluation of Grinding Methods for Pellets Preparation Aiming at the Analysis of Plant Materials by Laser Induced Breakdown Spectrometry. *Talanta* **2011**, *85*, 1744–1750. [CrossRef]
77. De Carvalho, G.G.A.; Santos, D.; Nunes, L.C.; Gomes, M.D.S.; Leme, F.D.O.; Krug, F.J. Effects of Laser Focusing and Fluence on the Analysis of Pellets of Plant Materials by Laser-Induced Breakdown Spectroscopy. *Spectrochim. Acta Part B At. Spectrosc.* **2012**, *74–75*, 162–168. [CrossRef]
78. Jabbar, A.; Akhtar, M.; Mehmmod, S.; Iqbal, M.; Ahmed, R.; Baig, M.A. Quantification of Copper Remediation in the *Allium cepa*, L. Leaves Using Electric Field Assisted Laser Induced Breakdown Spectroscopy. *Spectrochim. Acta Part B At. Spectrosc.* **2019**, *162*, 105719. [CrossRef]

79. Hassan, M.; Sighicelli, M.; Lai, A.; Colao, F.; Ahmed, A.H.H.; Fantoni, R.; Harith, M.A. Studying the Enhanced Phytoremediation of Lead Contaminated Soils via Laser Induced Breakdown Spectroscopy. *Spectrochim. Acta Part B At. Spectrosc.* **2008**, *63*, 1225–1229. [CrossRef]
80. Ma, S.; Gao, X.; Kaimin, G.; Medhanie, K.; JingQuan, L. Analysis of the Element Content in Poplar Tree Leaves by Femtosecond Laser-Induced Breakdown Spectroscopy. *Sci. China Phys. Mech. Astron.* **2011**, *54*, 1953–1957. [CrossRef]
81. Martin, M.Z.; Stewart, A.J.; Gwinn, K.D.; Waller, J.C. Laser-Induced Breakdown Spectroscopy Used to Detect Endophyte-Mediated Accumulation of Metals by Tall Fescue. *Appl. Opt.* **2010**, *49*, C161–C167. [CrossRef]
82. Nunes, L.C.; Batista Braga, J.W.; Trevizan, L.C.; Florêncio De Souza, P.; Arantes De Carvalho, G.G.; Júnior, D.S.; Poppi, R.J.; Krug, F.J. Optimization and Validation of a LIBS Method for the Determination of Macro and Micronutrients in Sugar Cane Leaves. *J. Anal. At. Spectrom.* **2010**, *25*, 1453–1460. [CrossRef]
83. Pouzar, M.; Ernohorský, T.; Průová, M.; Prokopáková, P.; Krejová, A. LIBS Analysis of Crop Plants. *J. Anal. At. Spectrom.* **2009**, *24*, 953–957. [CrossRef]
84. Han, J.; Sun, D.; Su, M.; Peng, L.; Dong, C. Quantitative Analysis of Metallic Elements in Tobacco and Tobacco Ash by Calibration Free Laser-Induced Breakdown Spectroscopy. *Anal. Lett.* **2012**, *45*, 1936–1945. [CrossRef]
85. Zhang, D.C.; Ma, X.W.; Zhu, X.L.; Li, B.; Zu, K.L. Application of Laser-Induced Breakdown Spectroscopy in Analyzing Microelements in Three Kinds of Fruit Samples. *Acta Phys. Sin.* **2008**, *57*, 6348–6353. [CrossRef]
86. Pereira, F.M.V.; Milori, D.M.B.P.; Venâncio, A.L.; Russo, M.D.S.T.; Martins, P.K.; Freitas-Astúa, J. Evaluation of the Effects of Candidatus Liberibacter Asiaticus on Inoculated Citrus Plants Using Laser-Induced Breakdown Spectroscopy (LIBS) and Chemometrics Tools. *Talanta* **2010**, *83*, 351–356. [CrossRef] [PubMed]
87. Beldjilali, S.; Borivent, D.; Mercadier, L.; Mothe, E.; Clair, G.; Hermann, J. Evaluation of Minor Element Concentrations in Potatoes Using Laser-Induced Breakdown Spectroscopy. *Spectrochim. Acta Part B At. Spectrosc.* **2010**, *65*, 727–733. [CrossRef]
88. Uhl, A.; Loebe, K.; Kreuchwig, L. Fast Analysis of Wood Preservers Using Laser Induced Breakdown Spectroscopy. *Spectrochim. Acta Part B At. Spectrosc.* **2001**, *56*, 795–806. [CrossRef]
89. Boyain-Goitia, A.R.; Beddows, D.C.S.; Griffiths, B.C.; Telle, H.H. Single-Pollen Analysis by Laser-Induced Breakdown Spectroscopy and Raman Microscopy. *Appl. Opt.* **2003**, *42*, 6119. [CrossRef]
90. Aragón, C.; Aguilera, J.A. Characterization of Laser Induced Plasmas by Optical Emission Spectroscopy: A Review of Experiments and Methods. *Spectrochim. Acta Part B At. Spectrosc.* **2008**, *63*, 893–916. [CrossRef]
91. Arantes de Carvalho, G.G.; Moros, J.; Santos, D.; Krug, F.J.; Laserna, J.J. Direct Determination of the Nutrient Profile in Plant Materials by Femtosecond Laser-Induced Breakdown Spectroscopy. *Anal. Chim. Acta* **2015**, *876*, 26–38. [CrossRef] [PubMed]
92. Juvé, V.; Portelli, R.; Boueri, M.; Baudelet, M.; Yu, J. Space-Resolved Analysis of Trace Elements in Fresh Vegetables Using Ultraviolet Nanosecond Laser-Induced Breakdown Spectroscopy. *Spectrochim. Acta Part B At. Spectrosc.* **2008**, *63*, 1047–1053. [CrossRef]
93. Kim, G.; Kwak, J.; Choi, J.; Park, K. Detection of Nutrient Elements and Contamination by Pesticides in Spinach and Rice Samples Using Laser-Induced Breakdown Spectroscopy (LIBS). *J. Agric. Food Chem.* **2012**, *60*, 718–724. [CrossRef] [PubMed]
94. Krajcarova, L.; Novotny, K.; Babula, P.; Provaznik, I.; Kucerova, P.; Adam, V.; Martin, M.Z.; Kizek, R.; Kaiser, J. Copper Transport and Accumulation in Spruce Stems (*Picea abies* (L.) Karsten) Revealed by Laser-Induced Breakdown Spectroscopy. *Int. J. Electrochem. Sci.* **2013**, *8*, 4485–4504. [CrossRef]
95. Krystofova, O.; Shestivska, V.; Galiova, M.; Novotny, K.; Kaiser, J.; Zehnalek, J.; Babula, P.; Opatrilova, R.; Adam, V.; Kizek, R. Sunflower Plants as Bioindicators of Environmental Pollution with Lead (II) Ions. *Sensors* **2009**, *9*, 5040–5058. [CrossRef]
96. Diopan, V.; Shestivska, V.; Zitka, O.; Galiova, M.; Adam, V.; Kaiser, J.; Horna, A.; Novotny, K.; Liska, M.; Havel, L.; et al. Determination of Plant Thiols by Liquid Chromatography Coupled with Coulometric and Amperometric Detection in Lettuce Treated by Lead (II) Ions. *Electroanalysis* **2010**, *22*, 1248–1259. [CrossRef]
97. Kaiser, J.; Galiová, M.; Novotný, K.; Červenka, R.; Reale, L.; Novotný, J.; Liška, M.; Samek, O.; Kanický, V.; Hrdlička, A.; et al. Mapping of Lead, Magnesium and Copper Accumulation in Plant Tissues by Laser-Induced Breakdown Spectroscopy and Laser-Ablation Inductively Coupled Plasma Mass Spectrometry. *Spectrochim. Acta Part B At. Spectrosc.* **2009**, *64*, 67–73. [CrossRef]
98. Krizkova, S.; Ryant, P.; Krystofova, O.; Adam, V.; Galiova, M.; Beklova, M.; Babula, P.; Kaiser, J.; Novotny, K.; Novotny, J.; et al. Multi-Instrumental Analysis of Tissues of Sunflower Plants Treated with Silver(I) Ions—Plants as Bioindicators of Environmental Pollution. *Sensors* **2008**, *8*, 445–463. [CrossRef] [PubMed]
99. Galiová, M.; Kaiser, J.; Novotný, K.; Novotný, J.; Vaculovič, T.; Liška, M.; Malina, R.; Stejskal, K.; Adam, V.; Kizek, R. Investigation of Heavy-Metal Accumulation in Selected Plant Samples Using Laser Induced Breakdown Spectroscopy and Laser Ablation Inductively Coupled Plasma Mass Spectrometry. *Appl. Phys. A Mater. Sci. Process* **2008**, *93*, 917–922. [CrossRef]
100. Peng, J.; He, Y.; Ye, L.; Shen, T.; Liu, F.; Kong, W.; Liu, X.; Zhao, Y. Moisture Influence Reducing Method for Heavy Metals Detection in Plant Materials Using Laser-Induced Breakdown Spectroscopy: A Case Study for Chromium Content Detection in Rice Leaves. *Anal. Chem.* **2017**, *89*, 7593–7600. [CrossRef]

101. Rai, D.; Agrawal, R.; Kumar, R.; Rai, A.K.; Rai, G.K. Effect of Processing on Magnesium Content of Green Leafy Vegetables. *J. Appl. Spectrosc.* **2014**, *80*, 878–883. [CrossRef]
102. Dhar, P.; Gembitsky, I.; Rai, P.K.; Rai, N.K.; Rai, A.K.; Watal, G. A Possible Connection Between Antidiabetic & Antilipemic Properties of Psoralea Corylifolia Seeds and the Trace Elements Present: A LIBS Based Study. *Food Biophys.* **2013**, *8*, 95–103. [CrossRef]
103. Tripathi, D.K.; Kumar, R.; Chauhan, D.K.; Rai, A.K.; Bicanic, D. Laser-Induced Breakdown Spectroscopy for the Study of the Pattern of Silicon Deposition in Leaves Of Saccharum Species. *Instrum. Sci. Technol.* **2011**, *39*, 510–521. [CrossRef]
104. Jabbar, A.; Akhtar, M.; Mehmood, S.; Ahmed, N.; Umar, Z.A.; Ahmed, R.; Baig, M.A. On the Detection of Heavy Elements in the: Euphorbia Indica Plant Using Laser-Induced Breakdown Spectroscopy and Laser Ablation Time of Flight Mass Spectrometry. *J. Anal. At. Spectrom.* **2019**, *34*, 954–962. [CrossRef]
105. Rai, P.K.; Chatterji, S.; Rai, N.K.; Rai, A.K.; Bicanic, D.; Watal, G. The Glycemic Elemental Profile of Trichosanthes Dioica: A LIBS-Based Study. *Food Biophys.* **2010**, *5*, 17–23. [CrossRef]
106. Jaiswal, D.; Rai, P.K.; Watal, G. Hypoglycemic and Antidiabetic Effects of Withania Coagulans Fruit Ethanolic Extract in Normal and Streptozotocin-Induced Diabetic Rats. *J. Food Biochem.* **2010**, *34*, 764–778. [CrossRef]
107. Rai, N.K.; Rai, P.K.; Pandhija, S.; Watal, G.; Rai, A.K.; Bicanic, D. Application of LIBS in Detection of Antihyperglycemic Trace Elements in Momordica Charantia. *Food Biophys.* **2009**, *4*, 167–171. [CrossRef]
108. Rai, P.K.; Rai, N.K.; Rai, A.K.; Watal, G. Role of LIBS in Elemental Analysis of Psidium Guajava Responsible for Glycemic Potential. *Instrum. Sci. Technol.* **2007**, *35*, 507–522. [CrossRef]
109. Tiwari, M.; Agrawal, R.; Pathak, A.K.; Rai, A.K.; Rai, G.K. Laser-Induced Breakdown Spectroscopy: An Approach to Detect Adulteration in Turmeric. *Spectrosc. Lett.* **2013**, *46*, 155–159. [CrossRef]
110. Mbesse Kongbonga, Y.G.; Ghalila, H.; Onana, M.B.; Ben Lakhdar, Z. Classification of Vegetable Oils Based on Their Concentration of Saturated Fatty Acids Using Laser Induced Breakdown Spectroscopy (LIBS). *Food Chem.* **2014**, *147*, 327–331. [CrossRef]
111. Nunes, L.C.; da Silva, G.A.; Trevizan, L.C.; Santos Júnior, D.; Poppi, R.J.; Krug, F.J. Simultaneous Optimization by Neuro-Genetic Approach for Analysis of Plant Materials by Laser Induced Breakdown Spectroscopy. *Spectrochim. Acta Part B At. Spectrosc.* **2009**, *64*, 565–572. [CrossRef]
112. Dhanada, V.S.; George, S.D.; Kartha, V.B.; Chidangil, S.; Unnikrishnan, V.K. Hybrid LIBS-Raman-LIF Systems for Multi-Modal Spectroscopic Applications: A Topical Review. *Appl. Spectrosc. Rev.* **2021**, *56*, 463–491. [CrossRef]
113. Badday, M.A.; Bidin, N.; Rizvi, Z.H.; Hosseinian, R. Determination of Environmental Safety Level with Laser-Induced Breakdown Spectroscopy Technique. *Chem. Ecol.* **2015**, *31*, 379–387. [CrossRef]
114. Aldakheel, R.K.; Gondal, M.A.; Nasr, M.M.; Almessiere, M.A.; Idris, N. Spectral Analysis of Miracle Moringa Tree Leaves Using X-Ray Photoelectron, Laser Induced Breakdown and Inductively Coupled Plasma -Optical Emission Spectroscopic Techniques. *Talanta* **2020**, *217*, 121062. [CrossRef] [PubMed]
115. Ercioglu, E.; Velioglu, H.M.; Boyaci, I.H. Chemometric Evaluation of Discrimination of Aromatic Plants by Using NIRS, LIBS. *Food Anal. Methods* **2018**, *11*, 1656–1667. [CrossRef]
116. Zhao, S.; Song, W.; Hou, Z.; Wang, Z. Classification of Ginseng According to Plant Species, Geographical Origin, and Age Using Laser-Induced Breakdown Spectroscopy and Hyperspectral Imaging. *J. Anal. At. Spectrom.* **2021**, *36*, 1704–1711. [CrossRef]
117. Gamela, R.R.; Speranca, M.A.; Andrade, D.F.; Pereira-Filho, E.R. Hyperspectral Images: A Qualitative Approach to Evaluate the Chemical Profile Distribution of Ca, K, Mg, Na and P in Edible Seeds Employing Laser-Induced Breakdown Spectroscopy. *Anal. Methods* **2019**, *11*, 5543–5552. [CrossRef]
118. Jiang, Y.; Kang, J.; Wang, Y.; Chen, Y.; Li, R. Rapid and Sensitive Analysis of Trace Leads in Medicinal Herbs Using Laser-Induced Breakdown Spectroscopy–Laser-Induced Fluorescence (LIBS-LIF). *Appl. Spectrosc.* **2019**, *73*, 1284–1291. [CrossRef] [PubMed]
119. Zhu, C.; Tang, Z.; Li, Q.; Zhou, R.; Lv, J.; Zhang, W.; Zhan, K.; Li, X.; Zeng, X. Lead of Detection in Rhododendron Leaves Using Laser-Induced Breakdown Spectroscopy Assisted by Laser-Induced Fluorescence. *Sci. Total Environ.* **2020**, *738*, 139402. [CrossRef]
120. Whatley, C.R.; Wijewardane, N.K.; Bheemanahalli, R.; Reddy, K.R.; Lu, Y. Effects of Fine Grinding on Mid-Infrared Spectroscopic Analysis of Plant Leaf Nutrient Content. *Sci. Rep.* **2023**, *13*, 6314. [CrossRef]
121. Marie-Christine, M. Comparison of the Performance of Laser-Induced Breakdown Spectroscopy and Color, Visible, Near-Infrared and Mid-Infrared Spectroscopy in the Prediction of Various Soil Properties. Master's Thesis, McGill University, Montreal, QC, Canada, 2020.
122. Singh, J.P.; Thakur, S.N. *Laser-Induced Breakdown Spectroscopy*, 2nd ed.; Elsevier: Amsterdam, The Netherlands, 2020; ISBN 9780128188293.
123. Andrade, D.F.; Pereira-Filho, E.R.; Konieczynski, P. Comparison of ICP OES and LIBS Analysis of Medicinal Herbs Rich in Flavonoids from Eastern Europe. *J. Braz. Chem. Soc.* **2017**, *28*, 838–847. [CrossRef]
124. Tripathi, D.K.; Kumar, R.; Pathak, A.K.; Chauhan, D.K.; Rai, A.K. Laser-Induced Breakdown Spectroscopy and Phytolith Analysis: An Approach to Study the Deposition and Distribution Pattern of Silicon in Different Parts of Wheat (*Triticum aestivum* L.) Plant. *Agric. Res.* **2012**, *1*, 352–361. [CrossRef]

125. Modlitbová, P.; Hlaváček, A.; Švestková, T.; Pořízka, P.; Šimoníková, L.; Novotný, K.; Kaiser, J. The Effects of Photon-Upconversion Nanoparticles on the Growth of Radish and Duckweed: Bioaccumulation, Imaging, and Spectroscopic Studies. *Chemosphere* **2019**, *225*, 723–734. [CrossRef] [PubMed]
126. Kaiser, J.; Samek, O.; Reale, L.; Liška, M.; Malina, R.; Ritucci, A.; Poma, A.; Tucci, A.; Flora, F.; Lai, A.; et al. Monitoring of the Heavy-Metal Hyperaccumulation in Vegetal Tissues by X-Ray Radiography and by Femto-Second Laser Induced Breakdown Spectroscopy. *Microsc. Res. Tech.* **2007**, *70*, 147–153. [CrossRef]
127. Da Silva Gomes, M.; De Carvalho, G.G.A.; Santos, D.; Krug, F.J. A Novel Strategy for Preparing Calibration Standards for the Analysis of Plant Materials by Laser-Induced Breakdown Spectroscopy: A Case Study with Pellets of Sugar Cane Leaves. *Spectrochim. Acta Part B At. Spectrosc.* **2013**, *86*, 137–141. [CrossRef]
128. Zhao, X.; Zhao, C.; Du, X.; Dong, D. Detecting and Mapping Harmful Chemicals in Fruit and Vegetables Using Nanoparticle-Enhanced Laser-Induced Breakdown Spectroscopy. *Sci. Rep.* **2019**, *9*, 906. [CrossRef]
129. Zhao, C.; Dong, D.; Du, X.; Zheng, W. In-Field, In Situ, and In Vivo 3-Dimensional Elemental Mapping for Plant Tissue and Soil Analysis Using Laser-Induced Breakdown Spectroscopy. *Sensors* **2016**, *16*, 1764. [CrossRef]
130. Barbafieri, M.; Pini, R.; Ciucci, A.; Tassi, E. Field Assessment of Pb in Contaminated Soils and in Leaf Mustard (*Brassica juncea*): The LIBS Technique. *Chem. Ecol.* **2011**, *27*, 161–169. [CrossRef]
131. Krajcarová, L.; Novotný, K.; Kummerová, M.; Dubová, J.; Gloser, V.; Kaiser, J. Mapping of the Spatial Distribution of Silver Nanoparticles in Root Tissues of Vicia Faba by Laser-Induced Breakdown Spectroscopy (LIBS). *Talanta* **2017**, *173*, 28–35. [CrossRef]
132. Modlitbová, P.; Novotný, K.; Pořízka, P.; Klus, J.; Lubal, P.; Zlámalová-Gargošová, H.; Kaiser, J. Comparative Investigation of Toxicity and Bioaccumulation of Cd-Based Quantum Dots and Cd Salt in Freshwater Plant *Lemna minor* L. *Ecotoxicol. Environ. Saf.* **2018**, *147*, 334–341. [CrossRef]
133. Singh, V.K.; Tripathi, D.K.; Mao, X.; Russo, R.E.; Zorba, V. Elemental Mapping of Lithium Diffusion in Doped Plant Leaves Using Laser-Induced Breakdown Spectroscopy (LIBS). *Appl. Spectrosc.* **2019**, *73*, 387–394. [CrossRef]
134. Peng, J.; He, Y.; Zhao, Z.; Jiang, J.; Zhou, F.; Liu, F.; Shen, T. Fast Visualization of Distribution of Chromium in Rice Leaves by Re-Heating Dual-Pulse Laser-Induced Breakdown Spectroscopy and Chemometric Methods. *Environ. Pollut.* **2019**, *252*, 1125–1132. [CrossRef]
135. Hahn, D.W.; Omenetto, N. Laser-Induced Breakdown Spectroscopy (LIBS), Part I: Review of Basic Diagnostics and Plasma-Particle Interactions: Still-Challenging Issues within the Analytical Plasma Community. *Appl. Spectrosc.* **2010**, *64*, 335–366. [CrossRef]
136. Tognoni, E.; Cristoforetti, G. Basic Mechanisms of Signal Enhancement in Ns Double-Pulse Laser-Induced Breakdown Spectroscopy in a Gas Environment. *J. Anal. At. Spectrom.* **2014**, *29*, 1318–1338. [CrossRef]
137. Cremers, D.A.; Radziemski, L.J. *Handbook of Laser-Induced Breakdown Spectroscopy*, 2nd ed.; Wiley: Hoboken, NJ, USA, 2013. [CrossRef]
138. Nicolodelli, G.; Senesi, G.S.; Ranulfi, A.C.; Marangoni, B.S.; Watanabe, A.; de Melo Benites, V.; de Oliveira, P.P.A.; Villas-Boas, P.; Milori, D.M.B.P. Double-Pulse Laser Induced Breakdown Spectroscopy in Orthogonal Beam Geometry to Enhance Line Emission Intensity from Agricultural Samples. *Microchem. J.* **2017**, *133*, 272–278. [CrossRef]
139. Rakovský, J.; Čermák, P.; Musset, O.; Veis, P. A Review of the Development of Portable Laser Induced Breakdown Spectroscopy and Its Applications. *Spectrochim. Acta Part B At. Spectrosc.* **2014**, *101*, 269–287. [CrossRef]
140. Peng, J.; He, Y.; Jiang, J.; Zhao, Z.; Zhou, F.; Liu, F. High-Accuracy and Fast Determination of Chromium Content in Rice Leaves Based on Collinear Dual-Pulse Laser-Induced Breakdown Spectroscopy and Chemometric Methods. *Food Chem.* **2019**, *295*, 327–333. [CrossRef]
141. Alrebdi, T.A.; Fayyaz, A.; Asghar, H.; Kamal, A.; Iqbal, J.; Piracha, N.K. Chemometrics and Spectroscopic Analyses of Peganum Harmala Plant's Seeds by Laser-Induced Breakdown Spectroscopy. *Appl. Sci.* **2023**, *13*, 2780. [CrossRef]
142. Jabbar, A.; Akhtar, M.; Ali, A.; Mehmood, S.; Iftikhar, S.; Baig, M.A. Elemental Composition of Rice Using Calibration Free Laser Induced Breakdown Spectroscopy. *Optoelectron. Lett.* **2019**, *15*, 57–63. [CrossRef]
143. Cho, H.H.; Kim, Y.J.; Jo, Y.S.; Kitagawa, K.; Arai, N.; Lee, Y.I. Application of Laser-Induced Breakdown Spectrometry for Direct Determination of Trace Elements in Starch-Based Flours. *J. Anal. At. Spectrom.* **2001**, *16*, 622–627. [CrossRef]
144. De Lucia, F.C., Jr.; Harmon, R.S.; McNesby, K.L.; Winkel, R.J., Jr.; Miziolek, A.W. Laser-Induced Breakdown Spectroscopy Analysis of Energetic Materials. *Appl. Opt.* **2003**, *42*, 6148–6152. [CrossRef]
145. Kunz, J.N.; Voronine, D.V.; Ko, B.A.; Lee, H.W.H.; Rana, A.; Bagavathiannan, M.V.; Sokolov, A.V.; Scully, M.O. Interaction of Femtosecond Laser Pulses with Plants: Towards Distinguishing Weeds and Crops Using Plasma Temperature. *J. Mod. Opt.* **2017**, *64*, 942–947. [CrossRef]
146. De Giacomo, A.; Gaudiuso, R.; Koral, C.; Dell'Aglio, M.; De Pascale, O. Nanoparticle-Enhanced Laser-Induced Breakdown Spectroscopy of Metallic Samples. *Anal. Chem.* **2013**, *85*, 10180–10187. [CrossRef]
147. Kumar, S.; Sharma, N.; Bali, V.; Singh, V.K.; Nam, S.H.; Lee, Y.; Singh, V.K. Classification of Healthy and Nematode-Infested Pea Root Using Laser-Induced Breakdown Spectroscopy and k-Nearest Neighbors Modeling. *Anal. Lett.* **2025**, 1–12. [CrossRef]

148. Andrews, H.B.; Martin, M.Z.; Wymore, A.M.; Kalluri, U.C. Rapid in Situ Nutrient Element Distribution in Plants and Soils Using Laser-Induced Breakdown Spectroscopy (LIBS). *Plant Soil.* **2024**, *495*, 3–12. [CrossRef]
149. Jabbar, A.; Rehman, B.; Iqbal, M.; Ahmed, R.; Mahmood, S.; Baig, M.A. Elemental Analysis of Plants Cultivated in Saline Soil by Laser-Induced Breakdown Spectroscopy (LIBS). *Anal. Lett.* **2021**, *54*, 1351–1365. [CrossRef]
150. Silvestre, D.M.; Barbosa, F.M.; Aguiar, B.T.; Leme, F.O.; Nomura, C.S. Feasibility Study of Calibration Strategy for Direct Quantitative Measurement of K and Mg in Plant Material by Laser-Induced Breakdown Spectrometry. *Anal. Chem. Res.* **2015**, *5*, 28–33. [CrossRef]
151. Borduchi, L.C.L.; Milori, D.M.B.P.; Meyer, M.C.; Villas-Boas, P.R. Reducing Matrix Effects on the Quantification of Ca, Mg, and Fe in Soybean Leaf Samples Using Calibration-Free LIBS and One-Point Calibration. *Spectrochim. Acta Part B At. Spectrosc.* **2022**, *198*, 106561. [CrossRef]
152. Rehan, I.; Rehan, K.; Sultana, S.; Khan, M.Z.; Muhammad, R. LIBS Coupled with ICP/OES for the Spectral Analysis of Betel Leaves. *Appl. Phys. B* **2018**, *124*, 76. [CrossRef]
153. Aldakheel, R.K.; Gondal, M.A.; Almessiere, M.A.; Rehman, S.; Nasr, M.M.; Alsalem, Z.; Khan, F.A. Spectrochemical Analysis Using LIBS and ICP-OES Techniques of Herbal Medicine (*Tinnevelly senna* Leaves) and Its Anti-Cancerous/Antibacterial Applications. *Arab. J. Chem.* **2021**, *14*, 202112. [CrossRef]
154. Umar, Z.A.; Liaqat, U.; Ahmed, R.; Hedwig, R.; Ramli, M.; Marpaung, M.A.; Kurniawan, K.H.; Pardede, M.; Baig, M.A. Determination of Micronutrients and Toxic Elements in *Moringa oleifera* Leaves by Calibration Free Laser-Induced Breakdown Spectroscopy (LIBS). *Anal. Lett.* **2022**, *55*, 755–769. [CrossRef]
155. Martelli, M.R.; Barron, C.; Delaporte, P.; Viennois, G.; Rouau, X.; Sadoudi, A. Pulsed Laser Ablation: A New Approach to Reveal Wheat Outer Layer Properties. *J. Cereal Sci.* **2009**, *49*, 354–362. [CrossRef]
156. Iqbal, J.; Iqbal, J.; Asghar, H.; Asghar, H.; Asghar, H.; Shah, S.K.H.; Naeem, M.; Abbasi, S.A.; Ali, R. Elemental Analysis of Sage (Herb) Using Calibration-Free Laser-Induced Breakdown Spectroscopy. *Appl. Opt.* **2020**, *59*, 4927–4932. [CrossRef]
157. Shukla, P.; Kumar, R.; Raib, A.K. Detection of Minerals in Green Leafy Vegetables Using Laser Induced Breakdown Spectroscopy. *J. Appl. Spectrosc.* **2016**, *83*, 872–877. [CrossRef]
158. Devipriya, S.; Ramesh, N.V.; Vineeth, P.K.; Mohanan, A. A Review on the Inextricable Relation of Ayurveda and Analytical Chemistry. *Mater. Today Proc.* **2020**, *46*, 3089–3095. [CrossRef]
159. Assis, J.V.B.; Ferreira, D.d.S.; Bócoli, D.d.A.; Brait, C.H.H.; Pereira-Filho, E.R. Direct Determination of Ca, K, and Mg in Soy Leaf Samples Using Laser-Induced Breakdown Spectroscopy. *Appl. Spectrosc.* **2024**, *78*, 243–250. [CrossRef]
160. Tripathi, D.K.; Pathak, A.K.; Chauhan, D.K.; Dubey, N.K.; Rai, A.K.; Prasad, R. An Efficient Approach of Laser Induced Breakdown Spectroscopy (LIBS) and ICAP-AES to Detect the Elemental Profile of *Ocimum* L. Species. *Biocatal. Agric. Biotechnol.* **2015**, *4*, 471–479. [CrossRef]
161. Liang, J.; Yan, C.; Zhang, Y.; Zhang, T.; Zheng, X.; Li, H. Rapid Discrimination of Salvia Miltiorrhiza According to Their Geographical Regions by Laser Induced Breakdown Spectroscopy (LIBS) and Particle Swarm Optimization-Kernel Extreme Learning Machine (PSO-KELM). *Chemom. Intell. Lab. Syst.* **2020**, *197*, 103930. [CrossRef]
162. Jabir Mahmood, E.; Muter Mehdy Al-Sultani, M. Detection of Pollutants in Soil Using Laser-Induced Breakdown Spectroscopy (LIBS). *Al-Bahir J. Eng. Pure Sci.* **2024**, *5*, 9. [CrossRef]
163. Rush, T.A.; Wymore, A.M.; Rodríguez, M., Jr.; Jawdy, S.; Vilgalys, R.J.; Martin, M.Z.; Andrews, H.B. Fungal Elemental Profiling Unleashed through Rapid Laser-Induced Breakdown Spectroscopy (LIBS). *mSystems* **2024**, *9*, e0091924. [CrossRef]
164. Limbeck, A.; Brunnbauer, L.; Lohninger, H.; Pořízka, P.; Modlitbová, P.; Kaiser, J.; Janovszky, P.; Kéri, A.; Galbács, G. Methodology and Applications of Elemental Mapping by Laser Induced Breakdown Spectroscopy. *Anal. Chim. Acta* **2021**, *1147*, 72–98. [CrossRef]
165. Piñon, V.; Mateo, M.P.; Nicolas, G. Laser-Induced Breakdown Spectroscopy for Chemical Mapping of Materials. *Appl. Spectrosc. Rev.* **2013**, *48*, 357–383. [CrossRef]
166. Bette, H.; Noll, R. High Speed Laser-Induced Breakdown Spectrometry for Scanning Microanalysis. *J. Phys. D Appl. Phys.* **2004**, *37*, 1281–1288. [CrossRef]
167. Pontes, M.J.C.; Cortez, J.; Galvão, R.K.H.; Pasquini, C.; Araújo, M.C.U.; Coelho, R.M.; Chiba, M.K.; de Abreu, M.F.; Madari, B.E. Classification of Brazilian Soils by Using LIBS and Variable Selection in the Wavelet Domain. *Anal. Chim. Acta* **2009**, *642*, 12–18. [CrossRef]
168. Jolivet, L.; Leprince, M.; Moncayo, S.; Sorbier, L.; Lienemann, C.P.; Motto-Ros, V. Review of the Recent Advances and Applications of LIBS-Based Imaging. *Spectrochim. Acta Part B At. Spectrosc.* **2019**, *151*, 41–53. [CrossRef]
169. Lu, Y.; Tao, Z.; Nie, L.; Guo, X.; Pan, T.; Chen, R.; Li, T.; Kong, W.; Liu, F. Quantitative Elemental Mapping of Heavy Metals Translocation and Accumulation in Hyperaccumulator Plant Using Laser-Induced Breakdown Spectroscopy with Interpretable Deep Learning. *Comput. Electron. Agric.* **2025**, *230*, 109907. [CrossRef]

170. Babos, D.V.; Tadini, A.M.; De Morais, C.P.; Barreto, B.B.; Carvalho, M.A.R.; Bernardi, A.C.C.; Oliveira, P.P.A.; Pezzopane, J.R.M.; Milori, D.M.B.P.; Martin-Neto, L. Laser-Induced Breakdown Spectroscopy (LIBS) as an Analytical Tool in Precision Agriculture: Evaluation of Spatial Variability of Soil Fertility in Integrated Agricultural Production Systems. *Catena* **2024**, *239*, 107914. [CrossRef]
171. Mikkelsen, F.N.; Rieckmann, M.M.; Laursen, K.H. *Advances in Assessing Nutrient Availability in Soils*; Taylor & Francis: Abingdon, UK, 2020.
172. Watchareeruetai, U.; Noinongyao, P.; Wattanapaiboonsuk, C.; Khantiviriya, P.; Duangsrisai, S. Identification of Plant Nutrient Deficiencies Using Convolutional Neural Networks. In Proceedings of the 2018 International Electrical Engineering Congress (iEECON), Krabi, Thailand, 7–9 March 2018. [CrossRef]
173. Hansen, T.H.; De Bang, T.C.; Laursen, K.H.; Pedas, P.; Husted, S.; Schjoerring, J.K. Multielement Plant Tissue Analysis Using ICP Spectrometry. *Methods Mol. Biol.* **2013**, *953*, 121–141. [CrossRef]
174. Van Maarschalkerweerd, M.; Husted, S. Recent Developments in Fast Spectroscopy for Plant Mineral Analysis. *Front. Plant Sci.* **2015**, *6*, 169. [CrossRef]
175. Schmidt, S.B.; Pedas, P.; Laursen, K.H.; Schjoerring, J.K.; Husted, S. Latent Manganese Deficiency in Barley Can Be Diagnosed and Remediated on the Basis of Chlorophyll a Fluorescence Measurements. *Plant Soil.* **2013**, *372*, 417–429. [CrossRef]
176. Le Tougaard, S.; Szameitat, A.; Møs, P.; Husted, S. Leaf Age and Light Stress Affect the Ability to Diagnose P Status in Field Grown Potatoes. *Front. Plant Sci.* **2023**, *14*, 1100318. [CrossRef]
177. Prananto, J.A.; Minasny, B.; Weaver, T. Near Infrared (NIR) Spectroscopy as a Rapid and Cost-Effective Method for Nutrient Analysis of Plant Leaf Tissues. *Adv. Agron.* **2020**, *164*, 1–49. [CrossRef]
178. De Carvalho, G.G.A.; Santos, D.; Da Silva Gomes, M.; Nunes, L.C.; Guerra, M.B.B.; Krug, F.J. Influence of Particle Size Distribution on the Analysis of Pellets of Plant Materials by Laser-Induced Breakdown Spectroscopy. *Spectrochim. Acta Part B At. Spectrosc.* **2015**, *105*, 130–135. [CrossRef]
179. Kunz, J.N.; Voronine, D.V.; Lee, H.W.H.; Sokolov, A.V.; Scully, M.O. Rapid Detection of Drought Stress in Plants Using Femtosecond Laser-Induced Breakdown Spectroscopy. *Opt. Express* **2017**, *25*, 7251–7262. [CrossRef]
180. Bhatt, C.R.; Alfarraj, B.; Ghany, C.T.; Yueh, F.Y.; Singh, J.P. Comparative Study of Elemental Nutrients in Organic and Conventional Vegetables Using Laser-Induced Breakdown Spectroscopy (LIBS). *Appl. Spectrosc.* **2017**, *71*, 686–698. [CrossRef]
181. Jull, H.; Künnemeyer, R.; Schaare, P. Nutrient Quantification in Fresh and Dried Mixtures of Ryegrass and Clover Leaves Using Laser-Induced Breakdown Spectroscopy. *Precis. Agric.* **2018**, *19*, 823–839. [CrossRef]
182. Mukherjee, P.K.; Wahile, A. Integrated Approaches towards Drug Development from Ayurveda and Other Indian System of Medicines. *J. Ethnopharmacol.* **2006**, *103*, 25–35. [CrossRef]
183. Farnsworth, N.R. Ethnopharmacology and Drug Development. *Ciba Found. Symp.* **1994**, *185*, 42–51. [CrossRef]
184. Mahida, Y.; Mohan, J.S.S. Screening of Indian Plant Extracts for Antibacterial Activity. *Pharm. Biol.* **2006**, *44*, 627–631. [CrossRef]
185. Perumal Samy, R.; Ignacimuthu, S. Antibacterial Activity of Some Folklore Medicinal Plants Used by Tribals in Western Ghats of India. *J. Ethnopharmacol.* **2000**, *69*, 63–71. [CrossRef]
186. Pushpangadan, P.; Atal, C.K. Ethno-Medico-Botanical Investigations in Kerala I. Some Primitive Tribals of Western Ghats and Their Herbal Medicine. *J. Ethnopharmacol.* **1984**, *11*, 59–77. [CrossRef]
187. Pushpangadan, P.; Rajasekharan, S.; Ratheshkumar, P.K.; Jawahar, C.R.; Nair, V.V.; Lakshmi, N.; Amma, L.S. 'Arogyappacha' (*Trichopus zeylanicus* Gaerin), the 'Ginseng' of Kani Tribes of Agashyar Hills (Kerala) for Ever Green Healh and Vitality. *Anc. Sci. Life.* **1988**, *8*, 13–16.
188. Sharma, N.; Singh, V.K.; Lee, Y.; Kumar, S.; Rai, P.K.; Pathak, A.K.; Singh, V.K. Analysis of Mineral Elements in Medicinal Plant Samples Using Libs and ICP-OES. *At. Spectrosc.* **2020**, *41*, 234–241. [CrossRef]
189. Nouman Khan, M.; Wang, Q.; Idrees, B.S.; Waheed, R.; Haq, A.U.; Abrar, M.; Jamil, Y. Evaluation of Medicinal Plants Using Laser-Induced Breakdown Spectroscopy (LIBS) Combined with Chemometric Techniques. *Lasers Med. Sci.* **2023**, *38*, 149. [CrossRef] [PubMed]
190. Rai, P.K.; Pathak, A.K.; Ghatak, S.; Watal, G.; Rai, A.K.; Jayasundar, R. LIBS Based Spectroscopic Analysis and Antidiabetic Evaluation of a Polyherbal Formulation. *J. Food Meas. Charact.* **2013**, *7*, 114–121. [CrossRef]
191. Shahbaz, A.; Abbasi, B.A.; Iqbal, J.; Fatima, I.; Anber Zahra, S.; Kanwal, S.; Devkota, H.P.; Capasso, R.; Ahmad, A.; Mahmood, T. Chemical Composition of *Gastrocotyle hispida* (Forssk.) Bunge and Heliotropium Crispum Desf. and Evaluation of Their Multiple In Vitro Biological Potentials. *Saudi J. Biol. Sci.* **2021**, *28*, 6086–6096. [CrossRef] [PubMed]
192. Liang, J.; Li, M.; Du, Y.; Yan, C.; Zhang, Y.; Zhang, T.; Zheng, X.; Li, H. Data Fusion of Laser Induced Breakdown Spectroscopy (LIBS) and Infrared Spectroscopy (IR) Coupled with Random Forest (RF) for the Classification and Discrimination of Compound Salvia Miltiorrhiza. *Chemom. Intell. Lab. Syst.* **2020**, *207*, 104179. [CrossRef]
193. Watal, G.; Dhar, P.; Srivastava, S.K.; Sharma, B. Herbal Medicine as an Alternative Medicine for Treating Diabetes: The Global Burden. *Evid.-Based Complement. Altern. Med.* **2014**, *2014*, 596071. [CrossRef]

194. Zhou, F.; Xie, W.; Lin, M.; Ye, L.; Zhang, C.; Zhao, Z.; Liu, F.; Peng, J.; Kong, W. Rapid Authentication of Geographical Origins of Baishao (*Radix paeoniae alba*) Slices with Laser-Induced Breakdown Spectroscopy Based on Conventional Machine Learning and Deep Learning. *Spectrochim. Acta Part B At. Spectrosc.* **2024**, *212*, 106852. [CrossRef]
195. Fayyaz, A.; Ali, N.; Umar, Z.A.; Asghar, H.; Waqas, M.; Ahmed, R.; Ali, R.; Baig, M.A. CF-LIBS Based Elemental Analysis of Saussurea Simpsoniana Medicinal Plant: A Study on Roots, Seeds, and Leaves. *Anal. Sci.* **2024**, *40*, 413–427. [CrossRef] [PubMed]
196. Aldakheel, R.K.; Gondal, M.A.; Nasr, M.M.; Dastageer, M.A.; Almessiere, M.A. Quantitative Elemental Analysis of Nutritional, Hazardous and Pharmacologically Active Elements in Medicinal Rhatany Root Using Laser Induced Breakdown Spectroscopy. *Arab. J. Chem.* **2021**, *14*, 102919. [CrossRef]
197. Alresawum, Y.; Ghalila, H.; Lahmar, S.; Gholap, A.V.; Mbesse Kongbonga, Y.G.; Feudjio, W.M. Laser Induced Breakdown Spectroscopy (LIBS) for Minerals Analysis and for Monitoring the Change in Elemental Compositions of the Mixtures of Herbal Medicines. *Laser* **2017**, *9*, 68–76.
198. Jabbar, A.; Akhtar, M.; Mehmood, S.; Kurniawan, K.H.; Hedwig, R.; Baig, M.A. Analytical Approach of Laser-Induced Breakdown Spectroscopy to Detect Elemental Profile of Medicinal Plants Leaves. *Indones. J. Chem.* **2019**, *19*, 430–440. [CrossRef]
199. Shukla, S.; Rai, P.K.; Chatterji, S.; Rai, N.K.; Rai, A.K.; Watal, G. LIBS Based Screening of Glycemic Elements of Ficus Religiosa. *Food Biophys.* **2012**, *7*, 43–49. [CrossRef]
200. Aldakheel, R.K.; Rehman, S.; Almessiere, M.A.; Khan, F.A.; Gondal, M.A.; Mostafa, A.; Baykal, A. Bactericidal and In Vitro Cytotoxicity of Moringa Oleifera Seed Extract and Its Elemental Analysis Using Laser-Induced Breakdown Spectroscopy. *Pharmaceuticals* **2020**, *13*, 193. [CrossRef]
201. Watal, G.; Sharma, B.; Rai, P.K.; Jaiswal, D.; Rai, D.K.; Rai, N.K.; Rai, A.K. LIBS-Based Detection of Antioxidant Elements: A New Strategy. *Methods Mol. Biol.* **2010**, *594*, 275–285. [CrossRef]
202. Chen, R.; Li, X.; Li, W.; Yang, R.; Lu, Y.; You, Z.; Liu, F. Crater—Spectrum Feature Fusion Method for Panax Notoginseng Spectroscopy. *Foods* **2024**, *14*, 1083. [CrossRef]
203. Wang, C.; Li, H.; Sun, J.; Lü, H.; Wang, F.; Zhang, R. Study on Enrichment Characteristics of Chinese Herbal Medicine Based on LIBS Technology. *Optoelectron. Lett.* **2023**, *19*, 88–94. [CrossRef]
204. Han, W.; Su, M.; Sun, D.; Yin, Y.; Wang, Y.; Gao, C.; Yang, F.; Fu, Y. Analysis of Metallic Elements Dissolution in the Astragalus at Different Decocting Time by Using LIBS Technique. *Plasma Sci. Technol.* **2020**, *22*, 085501. [CrossRef]
205. Andrews, H.B.; Wymore, A.M.; Wetter, E.E.; Herndon, E.M.; Li, H.; Martin, S.A.; Griffiths, N.A.; Yang, X.; Muchero, W.; Weston, D.J.; et al. Rapid Screening of Wood and Leaf Tissues: Investigating Silicon-Based Phytoliths in Populus Trichocarpa for Carbon Storage Applications Using Laser-Induced Breakdown Spectroscopy and Scanning Electron Microscopy-Energy Dispersive X-Ray Spectroscopy. *J. Anal. At. Spectrom.* **2023**, *38*, 2353–2364. [CrossRef]
206. Zhu, C.; Lv, J.; Liu, K.; Li, Q.; Tang, Z.; Zhou, R.; Zhang, W.; Chen, J.; Liu, K.; Li, X.; et al. Fast Detection of Harmful Trace Elements in Glycyrrhiza Using Standard Addition and Internal Standard Method—Laser-Induced Breakdown Spectroscopy (SAIS-LIBS). *Microchem. J.* **2021**, *168*, 106408. [CrossRef]
207. Wang, Y.; Bu, Y.; Cai, Y.; Wang, X. High-Sensitivity Analysis of Mercury in Medicinal Herbs Using Nanoparticle-Enhanced Laser-Induced Breakdown Spectroscopy Combined with Argon Purging. *J. Anal. At. Spectrom.* **2023**, *38*, 121–130. [CrossRef]
208. Yang, L.; Meng, L.; Gao, H.; Wang, J.; Zhao, C.; Guo, M.; He, Y.; Huang, L. Building a Stable and Accurate Model for Heavy Metal Detection in Mulberry Leaves Based on a Proposed Analysis Framework and Laser-Induced Breakdown Spectroscopy. *Food Chem.* **2021**, *338*, 127886. [CrossRef]
209. Lim, S.H.; Choi, C.I. Pharmacological Properties of *Morus nigra* L. (*Black mulberry*) as a Promising Nutraceutical Resource. *Nutrients* **2019**, *11*, 437. [CrossRef] [PubMed]
210. Mahboubi, M. *Morus alba* (*Mulberry*), a Natural Potent Compound in Management of Obesity. *Pharmacol. Res.* **2019**, *146*, 104341. [CrossRef]
211. Wan, X.; Lei, M.; Chen, T.; Tan, Y.; Yang, J. Safe Utilization of Heavy-Metal-Contaminated Farmland by Mulberry Tree Cultivation and Silk Production. *Sci. Total Environ.* **2017**, *599–600*, 1867–1873. [CrossRef] [PubMed]
212. Zheng, P.C.; Li, X.J.; Wang, J.M.; Zheng, S.; Zhao, H.D. Quantitative Analysis of Cu and Pb in Coptidis by Reheated Double Pulse Laser Induced Breakdown Spectroscopy. *Acta Phys. Sin.* **2019**, *68*, 125202. [CrossRef]
213. Fatima, I.; Hussain, T.; Rafay, M.; Kanwal, S.; Rauf, N.; Malik, T.S.S.; Mahmood, T. Untargeted Elemental and Metabolomic Profiling of Some Poaceae Species Using LIBS and GC-MS Methods. *Commun. Soil. Sci. Plant Anal.* **2021**, *52*, 1037–1050. [CrossRef]
214. Fang, Y.; Ramasamy, R.P. Current and Prospective Methods for Plant Disease Detection. *Biosensors* **2015**, *5*, 537–561. [CrossRef]
215. Picon, A.; Alvarez-Gila, A.; Seitz, M.; Ortiz-Barredo, A.; Echazarra, J.; Johannes, A. Deep Convolutional Neural Networks for Mobile Capture Device-Based Crop Disease Classification in the Wild. *Comput. Electron. Agric.* **2019**, *161*, 280–290. [CrossRef]
216. Sankaran, S.; Ehsani, R.; Morgan, K.T. Detection of Anomalies in Citrus Leaves Using Laser-Induced Breakdown Spectroscopy (LIBS). *Appl. Spectrosc.* **2015**, *69*, 913–919. [CrossRef]

217. Ranulfi, A.C.; Romano, R.A.; Bebeachibuli Magalhães, A.; Ferreira, E.J.; Ribeiro Villas-Boas, P.; Marcondes Bastos Pereira Milori, D. Evaluation of the Nutritional Changes Caused by Huanglongbing (HLB) to Citrus Plants Using Laser-Induced Breakdown Spectroscopy. *Appl. Spectrosc.* **2017**, *71*, 1471–1480. [CrossRef]
218. Sharma, N.; Khajuria, Y.; Singh, V.K.; Kumar, S.; Lee, Y.; Rai, P.K.; Singh, V.K. Study of Molecular and Elemental Changes in Nematode-Infested Roots in Papaya Plant Using FTIR, LIBS and WDXRF Spectroscopy. *At. Spectrosc.* **2020**, *41*, 110–118. [CrossRef]
219. Peng, J.; Song, K.; Zhu, H.; Kong, W.; Liu, F.; Shen, T.; He, Y. Fast Detection of Tobacco Mosaic Virus Infected Tobacco Using Laser-Induced Breakdown Spectroscopy. *Sci. Rep.* **2017**, *7*, 44551. [CrossRef] [PubMed]
220. Liu, F.; Shen, T.; Wang, J.; He, Y.; Zhang, C.; Zhou, W. Detection of Sclerotinia Stem Rot on Oilseed Rape (*Brassica napus* L.) Based on Laser- Induced Breakdown Spectroscopy. *Trans. ASABE* **2019**, *62*, 123–130. [CrossRef]
221. Senesi, G.S.; De Pascale, O.; Marangoni, B.S.; Rodrigues, A.; Caires, L.; Nicolodelli, G.; Pantaleo, V. Chlorophyll Fluorescence Imaging (CFI) and Laser-Induced Breakdown Spectroscopy (LIBS) Applied to Investigate Tomato Plants Infected by the Root Knot Nematode (RKN) Meloidogyne Incognita and Tobacco Plants Infected by Cymbidium Ringspot Virus. *Photonics* **2022**, *9*, 627. [CrossRef]
222. Rehan, I.; Gondal, M.A.; Aldakheel, R.K.; Almessiere, M.A.; Rehan, K.; Khan, S.; Sultana, S.; Khan, M.Z. Determination of Nutritional and Toxic Metals in Black Tea Leaves Using Calibration Free LIBS and ICP: AES Technique. *Arab. J. Sci. Eng.* **2022**, *47*, 7531–7539. [CrossRef]
223. Ranulfi, A.C.; Senesi, G.S.; Caetano, J.B.; Meyer, M.C.; Magalhães, A.B.; Villas-Boas, P.R.; Milori, D.M.B.P. Nutritional Characterization of Healthy and Aphelenchoides Besseyi Infected Soybean Leaves by Laser-Induced Breakdown Spectroscopy (LIBS). *Microchem. J.* **2018**, *141*, 118–126. [CrossRef]
224. Bin, L.; Qiu, W.; Chao-hui, Z.; Zhao-yang, H.; Hai, Y.; Jun, L.; Yan-de, L. Research on Anthracnose Grade of Camellia Oleifera Based on the Combined LIBS and THz Technology. *Plant Methods* **2022**, *18*, 52. [CrossRef]
225. Sharma, N.; Kamni; Singh, V.K.; Kumar, S.; Lee, Y.; Rai, P.K.; Singh, V.K. Investigation of Molecular and Elemental Changes in Rice Grains Infected by False Smut Disease Using FTIR, LIBS and WDXRF Spectroscopic Techniques. *Appl. Phys. B* **2020**, *126*, 122. [CrossRef]
226. Sharma, N.; Kumar, S.; Lee, Y.; Singh, V.K.; Singh, V.K. Spectroscopic Investigations of Healthy and Diseased Ber (*Ziziphus mauritiana*) Fruits Using Laser-Induced Breakdown Spectroscopy in Combination with Partial Least Squares-Discriminant Analysis. *Arab. J. Sci. Eng.* **2022**, *47*, 7519–7529. [CrossRef]
227. Xu, F.; Hao, Z.; Huang, L.; Liu, M.; Chen, T.; Chen, J.; Zhang, L.; Zhou, H.; Yao, M. Comparative Identification of Citrus Huanglongbing by Analyzing Leaves Using Laser-Induced Breakdown Spectroscopy and near-Infrared Spectroscopy. *Appl. Phys. B* **2020**, *126*, 43. [CrossRef]
228. Yang, P.; Nie, Z.; Yao, M. Diagnosis of HLB-Asymptomatic Citrus Fruits by Element Migration and Transformation Using Laser-Induced Breakdown Spectroscopy. *Opt. Express* **2022**, *30*, 18108–18118. [CrossRef] [PubMed]
229. Yao, M.; Fu, G.; Xu, J.; Li, T.; Zhang, L.; Liu, M.; Yang, P. In Situ Diagnosis of Mature HLB-Asymptomatic Citrus Fruits by Laser-Induced Breakdown Spectroscopy. *Appl. Opt.* **2021**, *60*, 5846–5853. [CrossRef]
230. Huang, L.; Chen, J.; Xu, F.; Xu, X.; Liu, M.; Luo, Z.; Chen, T.; Yao, M.; Rao, G. Identification of Huanglongbing-Infected Navel Oranges Based on Laser-Induced Breakdown Spectroscopy Combined with Different Chemometric Methods. *Appl. Opt.* **2018**, *57*, 8738–8742. [CrossRef]
231. Di, W.; Meng, L.; Yang, L.; Wang, J.; Fu, X.; Du, X.; Li, S.; He, Y.; Huang, L. Feasibility of Laser-Induced Breakdown Spectroscopy and Hyperspectral Imaging for Rapid Detection of Thiophanate-Methyl Residue on Mulberry Fruit. *Int. J. Mol. Sci.* **2019**, *20*, 2017. [CrossRef]
232. Gonzalez, P.; Ponce, L.; Flores, T.; Etxeberria, E.; Ponce, A. Rapid Identification of Huanlongbing-Infected Citrus Plants Using Laser-Induced Breakdown Spectroscopy of Phloem Samples. *Appl. Opt.* **2018**, *57*, 8841–8844. [CrossRef]
233. Safi, A.; Tavassoli, S.H.; Cristoforetti, G.; Legnaioli, S.; Palleschi, V.; Rezaei, F.; Tognoni, E. Determination of Excitation Temperature in Laser-Induced Plasmas Using Columnar Density Saha-Boltzmann Plot. *J. Adv. Res.* **2019**, *18*, 1–7. [CrossRef]
234. Tognoni, E.; Cristoforetti, G.; Legnaioli, S.; Palleschi, V.; Salvetti, A.; Mueller, M.; Panne, U.; Gornushkin, I. A Numerical Study of Expected Accuracy and Precision in Calibration-Free Laser-Induced Breakdown Spectroscopy in the Assumption of Ideal Analytical Plasma. *Spectrochim. Acta Part B At. Spectrosc.* **2007**, *62*, 1287–1302. [CrossRef]
235. Cristoforetti, G.; Legnaioli, S.; Palleschi, V.; Tognoni, E.; Cristoforetti, G.; Legnaioli, S.; Palleschi, V. Calibration-Free Laser-Induced Breakdown Spectroscopy: State of the Art. *Spectrochim. Acta Part B At. Spectrosc.* **2010**, *65*, 1–14. [CrossRef]
236. Fayek, N.; Tawfik, W.; KhalafAllah, A.; Fikry, M. Advancing Environmental Monitoring: Unveiling Heavy Metals Contamination with Calibration-Free Picosecond Laser-Induced Breakdown Spectroscopy (CF-PS-LIBS). *J. Opt.* **2025**. [CrossRef]
237. Hu, Z.; Zhang, D.; Wang, W.; Chen, F.; Xu, Y.; Nie, J.; Chu, Y.; Guo, L. A Review of Calibration-Free Laser-Induced Breakdown Spectroscopy. *Trends Anal. Chem.* **2022**, *152*, 116618. [CrossRef]
238. Zhang, N.; Ou, T.; Wang, M.; Lin, Z.; Lv, C.; Qin, Y.; Li, J.; Yang, H.; Zhao, N.; Zhang, Q. A Brief Review of Calibration-Free Laser-Induced Breakdown Spectroscopy. *Front. Phys.* **2022**, *10*, 887171. [CrossRef]

239. Miziolek, A.W.; Palleschi, V.; Schechter, I. *Laser Induced Breakdown Spectroscopy (LIBS)*, 1st ed.; Cambridge University Press: Cambridge, UK, 2008; ISBN 9780521852746.
240. Khoso, M.A.; Shaikh, N.M.; Kalhoro, M.S.; Jamali, S.; Ujan, Z.A.; Ali, R. Comparative Elemental Analysis of Soil of Wheat, Corn, Rice, and Okra Cropped Field Using CF-LIBS. *Optik* **2022**, *261*, 169247. [CrossRef]
241. Borduchi, L.C.L.; Milori, D.M.B.P.; Villas-Boas, P.R. One-Point Calibration of Saha-Boltzmann Plot to Improve Accuracy and Precision of Quantitative Analysis Using Laser-Induced Breakdown Spectroscopy. *Spectrochim. Acta Part B At. Spectrosc.* **2019**, *160*, 105692. [CrossRef]
242. Cavalcanti, G.H.; Teixeira, D.V.; Legnaioli, S.; Lorenzetti, G.; Pardini, L.; Palleschi, V. One-Point Calibration for Calibration-Free Laser-Induced Breakdown Spectroscopy Quantitative Analysis. *Spectrochim. Acta Part B At. Spectrosc.* **2013**, *87*, 51–56. [CrossRef]
243. Khoso, M.A.; Nizamani, A.H.; Saleem, H.; Soomro, A.M.; Bhutto, W.A.; Jamali, S.; Kalhoro, M.S.; Shaikh, N.M. Elemental Composition of the Soils Using Laser Induced Breakdown Spectroscopy. *Int. J. Adv. Res. Eng. Technol. (IJARET)* **2021**, *12*, 389–400.
244. El Sherbini, A.M.; Hegazy, H.; El Sherbini, T.M. Measurement of Electron Density Utilizing the Hα-Line from Laser Produced Plasma in Air. *Spectrochim. Acta Part B At. Spectrosc.* **2006**, *61*, 532–539. [CrossRef]
245. Qasim, M.; Anwar-Ul-haq, M.; Shah, A.; Sher Afgan, M.; Haq, S.U.; Khan, R.A.; Baig, M.A. Compositional Analysis of Silybum Marianum Plant at Reduced Pressure Using Calibration-Free LIBS. *Rom. Rep. Phys.* **2024**, *76*, 605. [CrossRef]
246. Bulajic, D.; Corsi, M.; Cristoforetti, G.; Legnaioli, S.; Palleschi, V.; Salvetti, A.; Tognoni, E. A Procedure for Correcting Self-Absorption in Calibration Free-Laser Induced Breakdown Spectroscopy. *Spectrochim. Acta Part B At. Spectrosc.* **2002**, *57*, 339–353. [CrossRef]
247. Rezaei, F.; Karimi, P.; Tavassoli, S.H. Estimation of Self-Absorption Effect on Aluminum Emission in the Presence of Different Noble Gases: Comparison between Thin and Thick Plasma Emission. *Appl. Opt.* **2013**, *52*, 5088–5096. [CrossRef] [PubMed]
248. Rezaei, F.; Tavassoli, S.H. A New Method for Calculation of Thick Plasma Parameters by Combination of Laser Spectroscopy and Shadowgraphy Techniques. *J. Anal. At. Spectrom.* **2014**, *29*, 2371–2378. [CrossRef]
249. Rezaei, F. Two-Lines Method for Estimation of Plasma Temperature and Characterization of Plasma Parameters in Optically Thick Plasma Conditions. *Appl. Opt.* **2020**, *59*, 3002. [CrossRef]
250. Rezaei, F.; Tavassoli, S.H. Utilizing the Ratio and the Summation of Two Spectral Lines for Estimation of Optical Depth: Focus on Thick Plasmas. *Spectrochim. Acta Part B At. Spectrosc.* **2016**, *125*, 25–30. [CrossRef]
251. Yang, N.; Eash, N.S.; Lee, J.; Martin, M.Z.; Zhang, Y.; Walker, F.R.; Yang, J.E. Multivariate Analysis of Laser-Induced Breakdown Spectroscopy Spectra of Soil Samples. *Soil Sci.* **2010**, *175*, 447–452. [CrossRef]
252. Yang, P.; Li, X.; Nie, Z. Determination of the Nutrient Profile in Plant Materials Using Laser-Induced Breakdown Spectroscopy with Partial Least Squares-Artificial Neural Network Hybrid Models. *Opt. Express* **2021**, *29*, 20687. [CrossRef]
253. Rezaei, F.; Karimi, P.; Tavassoli, S.H. Effect of Self-Absorption Correction on LIBS Measurements by Calibration Curve and Artificial Neural Network. *Appl. Phys. B* **2014**, *114*, 591–600. [CrossRef]
254. Pořízka, P.; Klus, J.; Képeš, E.; Prochazka, D.; Hahn, D.W.; Kaiser, J. On the Utilization of Principal Component Analysis in Laser-Induced Breakdown Spectroscopy Data Analysis, a Review. *Spectrochim. Acta Part B At. Spectrosc.* **2018**, *148*, 65–82. [CrossRef]
255. Dai, B.; Liang, F. Flower Classification Using LIBS Combined with PCA Chemometrics. *Spectroscopy* **2025**. [CrossRef]
256. Rezaei, M.; Rezaei, F.; Karimi, P. Different Hybrid Prediction's Machine Learning Algorithms for Quantitative Analysis in Laser-Induced Breakdown Spectroscopy. *J. Appl. Spectrosc.* **2023**, *90*, 705–716. [CrossRef]
257. Khalilian, P.; Rezaei, F.; Darkhal, N.; Karimi, P.; Safi, A.; Palleschi, V.; Melikechi, N.; Tavassoli, S.H. Jewelry Rock Discrimination as Interpretable Data Using Laser-Induced Breakdown Spectroscopy and a Convolutional LSTM Deep Learning Algorithm. *Sci. Rep.* **2024**, *14*, 5169. [CrossRef]
258. Aiswarya, J.; Mariammal, K.; Sathiesh Kumar, V.; Veerappan, K. Investigation of Nitrogen/Potassium Deficiency in Alternanthera Sessilis Plant Using Deep Learning Model Combined with CF-LIBS Approach. *Optik* **2025**, *321*, 172183.
259. Ji, H.; Ye, Y.; Gao, W.; Liu, Y. Online Detection of Tobacco Combustion Components Based on Laser-Induced Breakdown Spectroscopy. *Spectrosc. Lett.* **2025**, *58*, 453–464. [CrossRef]
260. Palleschi, V. *Chemometrics and Numerical Methods in LIBS*; Wiley Pulishing: Hoboken, NJ, USA, 2023; pp. 1–384.
261. Wang, W.; Kong, W.; Shen, T.; Man, Z.; Zhu, W.; He, Y.; Liu, F.; Liu, Y. Application of Laser-Induced Breakdown Spectroscopy in Detection of Cadmium Content in Rice Stems. *Front. Plant Sci.* **2020**, *11*, 599616. [CrossRef]
262. Rai, D.; Rai, A.K.; Rai, A.K.; Singh, D.B.; Yadav, A.K. Libs—A Promising Technique for Control of Food Quality. *J. Opt.* **2025**. [CrossRef]
263. Cisewski, J.; Snyder, E.; Hannig, J.; Oudejans, L. Support Vector Machine Classification of Suspect Powders Using Laser-Induced Breakdown Spectroscopy (LIBS) Spectral Data. *J. Chemom.* **2012**, *26*, 143–149. [CrossRef]
264. Zhu, S.; Song, G.; Zhang, W.; Zhang, Y.; Wei, Y.; Zhang, Q.; Chen, D.; Li, J.; Sun, T. LIBS Analysis of Elemental Carbon and Fixed Carbon in Coal by Dual-Cycle Regression Based on Matrix-Matched Calibration. *J. Anal. At. Spectrom.* **2024**, *39*, 841–853. [CrossRef]

265. Cai, Y.; Yu, W.; Gao, W.; Zhai, R.; Zhang, X.; Yu, W.; Wang, L.; Liu, Y. Polluted Soil–Plant Interaction Analysis and Soil Classification Based on Laser-Induced Breakdown Spectroscopy and Machine Learning. *Anal. Methods* **2024**, *16*, 6964–6973. [CrossRef]
266. De Giacomo, A.; Gaudiuso, R.; Koral, C.; Dell'Aglio, M.; De Pascale, O. Nanoparticle Enhanced Laser Induced Breakdown Spectroscopy: Effect of Nanoparticles Deposited on Sample Surface on Laser Ablation and Plasma Emission. *Spectrochim. Acta Part B At. Spectrosc.* **2014**, *98*, 19–27. [CrossRef]
267. Jantzi, S.C.; Motto-Ros, V.; Trichard, F.; Markushin, Y.; Melikechi, N.; De Giacomo, A. Sample Treatment and Preparation for Laser-Induced Breakdown Spectroscopy. *Spectrochim. Acta Part B At. Spectrosc.* **2016**, *115*, 52–63. [CrossRef]
268. Ohta, T.; Ito, M.; Kotani, T.; Hattori, T. Emission Enhancement of Laser-Induced Breakdown Spectroscopy by Localized Surface Plasmon Resonance for Analyzing Plant Nutrients. *Appl. Spectrosc.* **2009**, *63*, 555–558. [CrossRef]
269. Cai, J.; Wu, T.; Chen, Y.; Yang, S.; Zhang, Z.; Liu, Y. Rapid Detection and Discrimination of Plant Leaves Using Laser-Induced Breakdown Spectroscopy. *J. Laser Appl.* **2024**, *36*, 032027. [CrossRef]
270. Navarro, D.A.; Bisson, M.A.; Aga, D.S. Investigating Uptake of Water-Dispersible CdSe/ZnS Quantum Dot Nanoparticles by Arabidopsis Thaliana Plants. *J. Hazard. Mater.* **2012**, *211–212*, 427–435. [CrossRef] [PubMed]
271. Kaiser, J.; Novotný, K.; Martin, M.Z.; Hrdlička, A.; Malina, R.; Hartl, M.; Adam, V.; Kizek, R. Trace Elemental Analysis by Laser-Induced Breakdown Spectroscopy—Biological Applications. *Surf. Sci. Rep.* **2012**, *67*, 233–243. [CrossRef]
272. Kadhim, L.A.; Abdel Hussein, A.K.; Zoory, M.J.; Nader, R. Comparison of LIBS and XRF for Accurate Micronutrient Analysis in Dried White Lemon. *J. Opt.* **2025**. [CrossRef]
273. De Oliveira, D.M.; Fontes, L.M.; Pasquini, C. Comparing Laser Induced Breakdown Spectroscopy, near Infrared Spectroscopy, and Their Integration for Simultaneous Multi-Elemental Determination of Micro- and Macronutrients in Vegetable Samples. *Anal. Chim. Acta* **2019**, *1062*, 28–36. [CrossRef] [PubMed]
274. Sapkota, A.; Krachler, M.; Scholz, C.; Cheburkin, A.K.; Shotyk, W. Analytical Procedures for the Determination of Selected Major (Al, Ca, Fe, K, Mg, Na, and Ti) and Trace (Li, Mn, Sr, and Zn) Elements in Peat and Plant Samples Using Inductively Coupled Plasma-Optical Emission Spectrometry. *Anal. Chim. Acta* **2005**, *540*, 247–256. [CrossRef]
275. Clemens, S. Toxic Metal Accumulation, Responses to Exposure and Mechanisms of Tolerance in Plants. *Biochimie* **2006**, *88*, 1707–1719. [CrossRef]
276. Uchida, R. Essential Nutrients for Plant Growth Nutrient Functions and Deficiency Symptoms. *Plant Nutr. Manag. Hawaii's Soils* **2000**, *4*, 31–55.
277. Wu, B.; Becker, J.S. Imaging Techniques for Elements and Element Species in Plant Science. *Metallomics* **2012**, *4*, 403–416. [CrossRef] [PubMed]
278. Zhao, F.J.; Moore, K.L.; Lombi, E.; Zhu, Y.G. Imaging Element Distribution and Speciation in Plant Cells. *Trends Plant Sci.* **2014**, *19*, 183–192. [CrossRef]
279. Van der Ent, A.; Przybyłowicz, W.J.; de Jonge, M.D.; Harris, H.H.; Ryan, C.G.; Tylko, G.; Paterson, D.J.; Barnabas, A.D.; Kopittke, P.M.; Mesjasz-Przybyłowicz, J. X-Ray Elemental Mapping Techniques for Elucidating the Ecophysiology of Hyperaccumulator Plants. *New Phytol.* **2018**, *218*, 432–452. [CrossRef] [PubMed]
280. Peng, J.; Ye, L.; Shen, T.; Liu, F.; Song, K.; He, Y. Fast Determination of Copper Content in Tobacco (*Nicotina tabacum* L.) Leaves Using Laser-Induced Breakdown Spectroscopy with Univariate and Multivariate Analysis. *Trans. ASABE* **2018**, *61*, 821–829. [CrossRef]
281. Castillo-Michel, H.A.; Larue, C.; Pradas del Real, A.E.; Cotte, M.; Sarret, G. Practical Review on the Use of Synchrotron Based Micro- and Nano- X-Ray Fluorescence Mapping and X-Ray Absorption Spectroscopy to Investigate the Interactions between Plants and Engineered Nanomaterials. *Plant Physiol. Biochem.* **2017**, *110*, 13–32. [CrossRef]
282. Jaswal, B.B.S.; Singh, V.K. Analytical Assessments of Gallstones and Urinary Stones: A Comprehensive Review of the Development from Laser to LIBS. *Appl. Spectrosc. Rev.* **2015**, *50*, 473–498. [CrossRef]
283. Fernandes Andrade, D.; Pereira-Filho, E.R.; Amarasiriwardena, D. Current Trends in Laser-Induced Breakdown Spectroscopy: A Tutorial Review. *Appl. Spectrosc. Rev.* **2021**, *56*, 98–114. [CrossRef]
284. Larios, G.S.; Nicolodelli, G.; Senesi, G.S.; Ribeiro, M.C.S.; Xavier, A.A.P.; Milori, D.M.B.P.; Alves, C.Z.; Marangoni, B.S.; Cena, C. Laser-Induced Breakdown Spectroscopy as a Powerful Tool for Distinguishing High- and Low-Vigor Soybean Seed Lots. *Food Anal. Methods* **2020**, *13*, 1691–1698. [CrossRef]
285. Brennecke, T.; Čechová, L.; Horáková, K.; Šimoníková, L.; Buday, J.; Prochazka, D.; Modlitbová, P.; Novotný, K.; Miziolek, A.W.; Pořízka, P.; et al. Imaging the Distribution of Nutrient Elements and the Uptake of Toxic Metals in Industrial Hemp and White Mustard with Laser-Induced Breakdown Spectroscopy. *Spectrochim. Acta Part B At. Spectrosc.* **2023**, *205*, 106684. [CrossRef]

Disclaimer/Publisher's Note: The statements, opinions and data contained in all publications are solely those of the individual author(s) and contributor(s) and not of MDPI and/or the editor(s). MDPI and/or the editor(s) disclaim responsibility for any injury to people or property resulting from any ideas, methods, instructions or products referred to in the content.